REPUBLIC OF TURKEY

YILDIZ TECHNICAL UNIVERSITY

GRADUATE SCHOOL OF NATURAL AND APPLIED SCIENCES

PERFORMANCE INVESTIGATION OF DUAL MILLER CYCLE-ORGANIC RANKINE CYCLE COMBINED PLANT FOR MARINE APPLICATIONS

Merhawi Samuel ZEROM

MASTER OF SCIENCE THESIS

Department of Naval Architecture and Marine Engineering

Naval Architecture and Marine Engineering Program

Advisor

Assoc. Prof. Güven GONCA

July, 2019

REPUBLIC OF TURKEY

YILDIZ TECHNICAL UNIVERSITY

GRADUATE SCHOOL OF NATURAL AND APPLIED SCIENCES

PERFORMANCE INVESTIGATION OF DUAL MILLER CYCLE – ORGANIC CYCLE COMBINED PLANT FOR MARINE APPLICATIONS

A thesis submitted by Merhawi Samuel ZEROM in partial fulfillment of the requirements for the degree of MASTERS OF SCIENCE is approved by the committee on 27.06.2019 in Department of Naval Architecture and Marine Engineering, Naval Architecture and Marine Engineering Program.

Assoc. Prof. Guven GONCA

Yıldız Technical University

Advisor

Approved By the Examining Committee

Assoc. Prof. Guven Gonca, Advisor
Yıldız Technical University _____

Lec. Dr. Aykut Safa,
Yıldız Technical University _____

Prof. Dr. Oğuz Salim SÖĞÜT,
Istanbul Technical University _____

I hereby declare that I have obtained the required legal permissions during data collection and exploitation procedures, that I have made the in-text citations and cited the references properly, that I haven't falsified and/or fabricated research data and results of the study and that I have abided by the principles of the scientific research and ethics during my Thesis Study under the title of Performance Investigation of Dual Miller Cycle – Organic Rankine Cycle Combined Plant for Marine Applications supervised by my supervisor, Assoc. Prof. Guven Gonca. In the case of a discovery of false statement, I am to acknowledge any legal consequence.

Merhawi Samuel ZEROM

Signature

Dedicated to my family

ACKNOWLEDGEMENTS

I feel contented and glad to sincerely and greatly thank my supervisor Assoc. Prof. Guven GONCA for his guidance and thorough supervision towards the successful completion of this thesis. Working with my supervisor has improved my knowledge in this field tremendously. I would also like to extend my thanks to Mr. Vehsi Sahin a research assistant of the department, for his support in the research format and ethics areas.

I would like to deliver my debt immense of endless appreciation to my father and mother, Mr. Lebasi Samuel Zerom and Mrs. Senait Brhane for their indispensable love and support. I hereby commend you for standing by me through my entire journey.

Also, my appreciation goes to my brothers and sisters: I appreciate the motivation, affection and the consideration you have offered me.

Moreover, I can't be more delighted to thank and appreciate friends of mine: Mr. Muhyedin Mohammed and Mr. Ermias Debesay, for their great support and encouragement.

Merhawi Samuel ZEROM

TABLE OF CONTENTS

LIST OF SYMBOLS VII

LIST OF ABBREVIATIONS IX

LIST OF FIGURES XI

LIST OF TABLES XIII

ABSTRACT XIV

ÖZET XVI

1 Introduction 1

1.1 Literature Review 1

1.2 Objective of the Thesis 6

1.3 Hypothesis 6

2 Marine Diesel Engines 7

2.1 Internal Combustion Engines 7

2.2 Marine Diesel Engine 7

2.3 Air Standard Dual Cycle 12

2.4 Marine Diesel Engines Exhaust Emissions 15

3 Miller Cycle and Dual Miller Cycle 20

3.1 Miller Cycle 20

3.2 Thermodynamic Analysis of Miller Cycle 21

3.3 Thermodynamic Analysis of Dual Miller Cycle 23

4 Waste Heat Recovery Technologies and Organic Rankine Cycles 27

4.1 Waste Heat Recovery Technologies for Marine Use 27

4.2 Organic Rankine Cycle 37

5 Design and Methodology 48

5.1 Dual Miller Cycle - Organic Rankine Cycle Combination 48

5.2 Theoretical Model of Dual Miller cycle Combined with Organic Rankin Cycle 49

6 Results and Discussions 62

6.1 Analysis of and Synthesis of Combined Dual Miller Cycle – Organic Rankine Cycle 62

7 Conclusion and Recommendations 80

References 82

Publications from the Thesis 90

LIST OF SYMBOLS

A	Heat Transfer Area
C_v	Constant Volume Specific Heat (kJ/kg.K)
C_p	Constant Pressure Specific Heat(kJ/kg.K)
d	bore(m)
F	Fuel Air Ratio
F_{st}	Stoichiometric Fuel Air Ratio
h	Enthalpy (kJ/kg)
htr	Heat Transfer Coefficient
Hu	Lower Heat Value of the Fuel
l	Loss
L	Stroke length (m), Energy Loss Percentage(%)
m	Mass(Kg)
$\dot{m}$	Time Dependent Mass Rate
N	Engine Speed (rpm)
P	Pressure (bar), Power(kW)
P_{de}	Power Density
P_{ef}	Effective Power
$\dot{Q}$	Rate of Heat Transfer (kW)
r	Compression Ratio

r_M	Miller Cycle Ratio
r_0	Cut - off Ratio
R	Ideal Gas Constant (Kj/Kg K)
s	Entropy(Kj/kg K)
S	Stroke (m)
$\overline{SP}$	Mean Piston Speed (m/s)
T	Temperature (K), Total
T_0 , T_1	Ambient temperature, starting temperature
ν	Specific Volume (kg/m^3)
V_s	Displacement Volume (m^3)
$Xdest_{tot}$	Exergy Destruction
α	Cycle Temperature Ratio, Atomic Number of Carbon
β	Pressure Ratio, Atomic Number of Hydrogen
Φ	Equivalence Ratio
Δ	Atomic Number of Nitrogen
λ	Cycle Pressure Ratio
ε	Exergetic Efficiency, Cut off Ratio
ξ	Molar Fuel-Air Ratio
ρ	Density (kg/m^3)
η	Efficiency
μ	Coefficient of Friction

LIST OF ABBREVIATIONS

BDC	Bottom Dead Center
CA	Crank Angl
CC	Combustion Chamber
CFC	Chloro Fluoro Carbon
CI	Compression Ignition
dB	decibel
DMC	Dual Miller Cycle
ECA	Emission Control Area
ECOP	Ecological Coefficient of Performance
EES	Engineering Equations Solver
EFECPOD	Effective Ecological Power Density
EIPP	Engine International Air Pollution Prevention
GWP	Global Warming Potential
HC	Hydro Carbon
HCFC	Hydro Chloro Fluoro Carbon
ICE	Internal Combustion Engines
IMO	International Maritime Organization

ISO	International Standards Organization
KC	Kalina Cycle
LNG	Liquid Natural Gas
LPG	Liquid Petroleum Gas
MARPOL	Marine Pollution
MDE	Marine Diesel Engine
M/V	Marine Vessel
ODP	Ozone Depletion Layer
ORC	Organic Rankine Cycle
PM	Particulate Matter
RC	Rankine Cycle
RGF	Residual Gas Fraction
SCR	Steam Conventional Rankine Cycle
SI	Spark Ignition
TDC	Top Dead Center
TEG	Thermo Electric Generator
TT	Total Temperature
WHR	Waste Heat Technology

LIST OF FIGURES

Figure 2.1 4-Stroke Marine Diesel Engine; (a) Suction (b) compression (c) expansion d) Exhaust [33] 10

Figure 2.2 Two-Stroke Marine Diesel Engine; (a) exhaust and suction (b) compression (c) expansion [33] 11

Figure 2.3 Scavenging system kinds for 2 stroke Marine Diesel Engines; (a) cross flow (b) loop and (c) Unit flow. [35] 12

Figure 2.4 (a) P-v Diagram; (b) T-s Diagram for Air Standard Dual Cycle [36] ...13

Figure 2.5 Main exhaust emissions from today's low speed diesel engine [32] 15

Figure 2.6 Propositions of the exhaust gas emissions of a medium speed diesel engine [32]. 17

Figure 2.7 Maximum permissible NOX emissions for marine diesel engines (IMO) [39].....18

Figure 3.1 P-V diagrams for the Miller cycle [47]……..22

Figure 3.2 T-s diagrams for Miller cycle [48] 22

Figure 3.3 P-V and T-s schematic diagrams for Dual Miller Cycle [49] 24

Figure 4.1 Heat balance for MAN 12K98ME/MC marine diesel engine [71]……28

Figure 4.2 Schematic of a simple Rankine cycle plant [21].....30

Figure 4.3 Temperature–entropy (T–s) diagram for a Rankine Cycle [21].....31

Figure 4.4 Supercritical Rankine Cycle [76] 32

Figure 4.5 Schematic of a simple Kalina cycle plant [77].....33

Figure 4.6 A simple thermo-electric generator (TEG) module [21].....33

Figure 4.7 Suitable Waste Heat Temperature Range for Each Technology [21] ..35

Figure 4.8 Appropriate efficiency distribution for various WHRs [21] 35

Figure 4.9 Schematic diagram of an ORC system for waste heat recovery [49]. .39

Figure 4.10 T-s diagram of a particular ORC having R245fa as medium [11] 40

Figure 4.11 T-s diagram of the three main categories of working fluids [93] 42

Figure 5.1 Schematic diagram of DMC – ORC combination……...48

Figure 5.2 T-s diagram of DMC that delivers exhaust to the ORC 50

Figure 5.3 T- s diagram of ORC (heat source is DMC engine's exhaust).....51

Figure 6.1 Dual Miller Cycle – Organic Rankine Cycle parameters performance at variable equivalence ratio 62

Figure 6.2 Comparison of Dual Miller Cycle versus Dual Miller Cycle – Organic Rankin Cycle parameters performance at variable equivalence ratio (ϕ).....63

Figure 6.3 Influence of pressure ratio (β) on ecological performance (ECOP).....65

Figure 6.4 Comparison of DMC against DMC- ORC at a variable pressure ratio (β).....66

Figure 6.5 Influence of crank angle (θr) on performance parameters with Steam as a working fluid.....68

Figure 6.6 Influence of θr on performance parameters with RC318 as a working fluid in a DMC and DMC- ORC.....69

Figure 6.7 Influence of θ_r on performance parameters with R245fa as a working fluid in a DMC and DMC – ORC 70

Figure 6.8 Influence of "Z (rpm)" on performance parameters with R245fa as a working fluid.....73

Figure 6.9 Influence of cycle temperature ratio (α) on engine performance parameters with RC318 as a working fluid.....74

Figure 6.10 Influence of bore to stroke length ratio, on engine performance parameters with R245fa as a working fluid 77

Figure 6.11 Influence of stroke length (l), on engine performance parameters. ...77

Figure 6.12 Influence of bore diameter (d) of cylinder on engine performance parameters 78

LIST OF TABLES

Table 2.1 Exhaust waste products proportion of CI engines [39] 17

Table 4.1 Grading of Heat Energy Based on Temperature Distribution [72]……. .28

Table 4.2 Temperature distribution of majority marine waste heat sources [21, 40, 73, 74 and 75] 29

Table 4.3 Overview of Fluids Characteristics Observation in Steam and Organic Rankine Cycles [81] 37

Table 4.4 Safety categorization of working fluids [74].....43

Table 4.5 Working fluid candidates for the engine exhaust gas waste heat recovery [95] 45

Table 4.6 Properties of working fluids used in the current investigation [96] 47

Table 5.1 Dual Miller Cycle Engine Parameters [96]……...49

Table 6.1 Comparison of Maximum Values Achieved in DMC and DMC-ORC…….71

ABSTRACT

Performance Investigation of Dual Miller Cycle – Organic Rankine Cycle Combined Plant for Marine Applications

Merhawi Samuel ZEROM

Department of Naval Architecture and Marine Engineering

Master of Science Thesis

Advisor: Assoc. Prof. Güven GONCA

Shipping is an essential part of current world economy as almost 90% of world trade commodities are transported by sea transport system. It has unparalleled significance on our daily life. Shipping provides the cheapest and reliable mode of transport. However, the unstable and ever-increasing fuel prices and the restrictions put on hazardous ship emissions by IMO are creating pressure on the shipping industry, so as to increase the main engine's thermal efficiency and to limit the ecologically hazardous ship's exhaust emissions.

Therefore, in this thesis, a step is taken to examine a way of optimum conditions for both efficiency and exhaust emissions by introducing a combined plant of Dual Miller Cycle engine and Organic Rankine Cycle type waste heat recovery focused on marine applications. This thesis has examined a way of optimizing the thermo-ecologic effectiveness of Dual Miller – Organic Rankine Cycle combinations. A recently developed performance analysis criterion called

effective ecological power density (EFECPOD) is applied for the Dual Miller Cycle – Organic Rankine Cycle combinations. Three different types of working fluids with appropriate characters are used in the Organic Rankine Cycle. Effective efficiency, effective power, exergy destruction, effective power density, ecological coefficient of performance and exergetic efficiency are investigated for both Dual Miller Cycle and Dual Miller Cycle – Organic Rankine Cycle configuration. Emission's configurations and engine's physical orientation are associated with cycle temperature and combustion chamber volume (swept volume) respectively. In addition, the swept volume is associated to the monetary value of the engine, for this reason the system under this investigation has importance for multipurpose optimizations. Performance investigation of Dual Miller Cycle Engine – Organic Rankine Cycle combined plant is carried out using the Engineering Equations Solver (EES). The impacts of engine design and working parameters such as cycle temperature ratio, cycle pressure ratio, engine speed, cylinder dimensions and equivalence ratio on the effective ecological power density (EFECPOD), effective efficiency, effective power density, ecological coefficient of performance, exergy destruction and exergetic efficiency are investigated. The results of this examination have shown optimum values of the engine design and operating parameters in terms of thermo-ecological feasibility which also reduces harmful ship emissions like nitrous oxides.

Key words: Dual Miller Cycle, Organic Rankine Cycle, optimization, marine engine, emission

ÖZET

Denizcilik Uygulamaları İçin Dual Miller Çevrimi – Organik Rankine Çevrimi Kombine Tesisinin Performans İncelemesi

Merhawi Samuel ZEROM

Gemi İnşaat ve Gemi Makineleri Mühandisliği Anabilim Dalı

Yüksek Lisans Tezi

Tez Danışmanı: Doç. Dr. Güven GONCA

Dünya ticaret mallarının yaklaşık % 90' ı deniz ulaştırma sistemi ile taşındığı için, deniz taşımacılığı, mevcut dünya ekonomisinin önemli bir parçasıdır. Bu günlük yaşamımızda eşsiz bir öneme sahiptir. Deniz taşımacılığı sistemi en ucuz ve güvenilir olduğu taşıma sistemidir. Fakat, sürekli artan petrol fiyatları ve IMO tarafından gemi egzoz emisyonlarına getirilen kısıtlamalar, ana makinenin termal verimliliğini ve doğaya zararlı egzoz gazlarının sınırlandırılması konusunda gemi endüstrisi üzerinde baskı oluşturmaktadır.

Bu tezde, bu nedenle deniz uygulamalarına odaklanmış kombine Dual- Miller Çevrimi ve Organik Rankine çevrimi ile atık ısı geri kazanılarak hem egzoz emisyonları hem verimlilik için uygun koşulların incelenmesi için bir adım atılacaktır. Bu tez, Dual Mıller- Organik Rankine Çevrimi kombinasyonlarının termo- ekolojık etkinliğini optimize etmenin bir yolunu incelemiştir. Dual Miller çevrimi - Organik Rankin Çevrimi kombinasyonları için etkili ekolojik güç

yoğunluğu (EFECPOD) adı verilen yeni geliştirilen bir performans analizi kriteri uygulanmiştir.Organik Rankine Çevrimi'nde uygun karakterlere sahip üç farklı tipte iş akışkanı kullanılmıştır. Dual Miller Çevrimi ve Dual Miller Çevrimi - Organik Rankine Çevrimi konfigürasyonları için etkin verim, etkin güç, , exerji yıkımı, etkin güç yoğunluğu, ekolojik performans katsayısı ve ekserjetik verim incelenmiştir. Emisyon konfigürasyonları ve Motorun fiziksel yönü, sırasıyla çevrim sıcaklığı ve yanma odası hacmi (süpürme hacmi) ile ilişkilidir.

Ek olarak, süpürme hacmi motorun parasal değeri ile de ilişkilidir, bu nedenle bu araştırma altındaki sistem çok amaçlı optimizasyonlar için önem taşımaktadır. Dual Miller çevrimi - Organik Rankine çevrimi kombine tesisinin performans incelemesi Engineering Equations Solver (EES) kullanılarak gerçekleştirilmiştir. çevrim sıcak oranı, çevrim basınç oranı, motor hızı, silindir boyutları, eşdeğerlik oranı gibi motor işletme ve tasarım parametrelerinin etkili ekolojik güç yoğunluğu (EFECPOD), etkin güç, etkin güç yoğunluğu, ekolojik performans katsayısı, exerji yıkımı ve ekserjetik verim üzerindeki etkileri araştırılmıştır. Bu incelemenin sonuçları, termo-ekolojik fizibilite bakımından motor tasarım ve işletme parametrelerinin optimum değerlerini göstermiştir, bu da azot oksitler gibi zararlı gemi emisyonlarını azaltır.

Anahtar Kelimeler: Dual Miller Çevrimi, Organik Rankine Çevrimi, optimizasyon, gemi motoru, emisyon.

1

Introduction

1.1 Literature Review

The recently emerging strict regulations and limitations put on vessel's emissions plus the international inclination to produce greener vessels has bolstered the researches undergoing to enhance the overall efficiency of vessels. An increment of ships efficiency is able to be obtained by utilizing various energy efficiency approaches which the most commonly used ones are like increasing thrust efficiency, enhancing the auxiliary machinery and prime mover efficiencies, reducing aerodynamic and hydrodynamic resistances of the vessel [1]. The ships overall efficiency will to a greater amount rely on the implementation of the so said energy efficiency approaches. The JOULES project cofounded by the European Union concentrates to integrate the energy conserving approaches so as to get advanced power grid that directs towards a crucial improvement of ships efficiency [2].

In a vessel the most significant origin of power loss is the prime mover (engine) [3]. So, enhancement of prime mover's effectiveness might bring a sound decrement in fuel consumption of a vessel. Approximately one half of the aggregate energy loss is emitted via the exhaust gases [4]. Moreover, from the various energy loss sources of the vessel, the prime mover's exhaust gases possess a significant importance because of the grade of energy they carry. The demand of waste heat recovery in vessels emerged as a response to the world oil crisis that occurred in the 1970's in USA and Europe [5]. In recent decades a lot of approaches have been implemented to utilize the energy that has been escaping to the atmosphere.

The Miller process is one of the few options that engine builders have for simultaneously reducing emissions and improving engine efficiency. Since all

engine builders strive to meet engine emissions limits without any loss of efficiency practically every modern engine works these days with at least moderate Miller timing. The Miller cycle is derived from Otto cycle having shorter compression stroke than expansion stroke [6]. Recent improvements in VVT [7] and the probability of compression ratio change [8], permits the Miller cycle serve in an effective way. Numerous equations have emerged letting the explanation of Miller cycle and defining the main parameters that helps for its progress.

Ibrahim [9] made an investigative study focused on influences of the engine speed and altering medium's specific heat ratio utilized over Miller cycle. Achieved works showed that as compression ratio gets lower than a specified amount, the power developed gets diminished with rising engine speed, whereas if the rate of compressing air surpasses the specified amount, the power output first rises and soon declines with the increment of engine speed. And in another work in [10], an analysis regarding the significance of air - fuel ratio and stroke length over Miller cycle level of effectiveness in which the outcomes implied that when compression ratio is above a specific amount the power output initially shows growth and afterwards declines. Bello et al. [11] have investigated on a performance to recover waste heat using ORC and the outcome showed an increment in ship efficiency and deduction of pollutant emissions. Sprouse III et al. [12] deduced from a review focused on waste heat recoveries that ORC is the top used cycle to generate energy, from a poor to a moderate quality waste heat. In a thermodynamic analysis study that straightly contrasts engines functioning with Otto, Miller and Diesel cycles done by Ribeiro and Martins [13], the results of computer model simulation averred that the Miller cycle engine with VCR was best engine in overall working ranges, when compared to Otto cycle engine and Diesel cycle engine, especially in part load conditions. Similarly from a study of an eco- friendly Dual Miller Cycle for marine vessels delivered by Gonca [14], it was found that the P_{out}, P_{de} and η_{ef} increase up to a set amount and then start to decline in parallel to increment in equivalence ratio and compression ratio. Moreover, it was also found that the heat transfer energy losses increase, as

insufficient burning and exhaust output destructions lowers as compression ratio increases for a stable α situation [14]. In a theoretical performance optimization of I.C.E conducted by Ust et al. [15], they have delivered a thermodynamic optimization for defining optimum working conditions and design parameters, and in parallel to this , it is analyzed that the power output (P_{out}) and thermal efficiency (η_{ef}) conditions for the Diesel Miller Cycle is usually higher than the Dual Miller and Otto Miller Cycles. In an attempt to increase thermal efficiency of an optimization study done by Mo et al. [16] on a Gas Engine by applying Miller cycle, the results of the simulations displayed that the inlet valves closing 40^0CA earlier (EIVC40) with increment of compression ratio to 13 happened to be the best way to enhance efficiency. Moreover, the experimental outcomes of the same study have assured the method employed has its maximum fuel consumption rate at maximum speed whereas gets lowered at moderate and lower speeds. The engine knocking tendency increased at the same time.

Chunlan et al. [17] made a contrasting investigation of variable cycle Diesel engine relying on three dimensional simulations and on this study Dual and LIVC Miller cycles were contrasted by simulation and the result showed that, though the performance of EIVC Miller Cycle resembles LIVC Miller Cycle, highest cylinder temperature was found lesser than that of LIVC Miller cycle that led to a reduced NO_x emission, however greater soot emission for EIVC Miller cycle. In a work by Song et al. [18], that aimed to regenerate energy loss from a marine diesel engine, utilizing ORC technology. Investigation outcomes averred that optimized system is workable and financially advantageous, by increasing efficiency up to 10.2% for the main engine [18]. In a study of design and optimization of Organic Rankin Cycles for WHR in marine fields applying the basics of natural selection done by Ulrik et al. [19], it was recommended that there is no a typical or just one type of fluid that can be utilized in ORC system fulfilling the desired necessities of system unsophistication, lower pressure, adequate efficiency, minimum detriment and lesser ecological influence. So, as a result very few alternatives are left from the investigated fluids. Moreover, R245fa and R236ea look affordable possessing trivial detriment and close to

optimal efficiency at acceptable pressures. Linke et al. [20] made a review study about methodical approaches for working fluid selection and the devising, assimilation as well as regulation of Organic Rankine Cycles, and it was found in the review study that design of ORC systems as a difficult work. It was also described that a lot of options are available at every stage of the plan from working fluid isolation through cycle improvement to the productive assimilation of the cycle with main plant systems. In a study of WHRs for marine fields made by Singh and Pedersen [21], an in-depth review was done on the most significant technologies for waste heat recovery. From their review it was revealed that Engine exhaust gas contains the biggest portion of WHR, and KC showed good WHRs for average quality sources with great effectiveness, while ORC revealed bigger efficiency to regain energy for low to medium heat sources. Therefore, as most of marine applications operate at part loads, ORC is more practically advantageous for marine operations. On a study by Martins et al. [22], Miller cycle has the best efficiency under minimum and part load conditions, especially for lower loads (0.3 to 0.4) where it may reach up to 73% theoretical efficiency.

These days, the development of marine diesel engines equipped with variable valve actuation (VVA) and advanced turbocharging systems have permitted the usage of Miller cycle for decreasing NO_x emissions [23]. Investigations done before have put Miller cycle by early inlet valve closure (EIVC) implementing boosted air pressure through two-stage turbocharging. These studies revealed that highest values of EIVC in conjunction with increased boost pressure resulted in a remarkable reduction of engine-emitted NO_x up to 50% without deterioration of brake specific fuel consumption (BSFC) compared to conventional Diesel engine operation. Though various methods have been proposed in the literature to materialize Miller cycle in diesel engines, it has not been clarified up to now, which is the best combination of methods for simultaneous reduction of diesel-emitted specific CO_2 and NO_x emissions. In a numerical analysis for improving power and efficiency of Miller cycle by Shimogata et al. [24], the outcomes revealed that Miller cycle ameliorates both

efficiency and energy rate by optimizing the compression and expansion ratios. In an experimental emission test done on a turbocharged diesel engine changed to Miller cycle engine, especially nitrous oxide, carbon di oxide , hydrocarbon , smoke and brake specific fuel consumption data was collected for investigation, and results of the insulated Miller cycle engine depicted reduction in emissions and improvement in BSFC, in comparison to standard Diesel engine [25]. On the other hand, according to an experimental and numerical investigation done about lowering of NO_X emissions of DI Diesel engines transformed into Miller cycle by Stebeler et al. [26], for an average sized Diesel engine, outcomes affirmed that the power produced as well as SFC are enhanced to some degree, while NO_X emissions are able to be diminished by around 20%. Another way of theoretical investigation of working of Miller cycle for lowering NO_x in two versions [23], with first version of Miller cycle showing NO_x emissions reduction up to 8% and making an engine energy wastage of 1%, while for the second version of Miller cycle NO_x emission was reduced up to 46% while making an engine energy wastage of 13%, at full rating. A study using Miller cycle to minimize nitrous oxides emissions from an engine was done by Wang et al. [27], hence according to outcomes of the investigation; it is shown that the utilization of Miller cycle is capable of decreasing the combustion temperature and NO_x emissions. Moreover, these outcomes illustrate that Miller cycle ratio has a significant role on combustion temperature and emissions. Lowering Miller cycle ratio leads to a low burning and low exhaust temperatures and the deduction of exhaust emissions. Ecological interests emphasize the requirement for minimizing the greenhouse gases emissions and pollutant [28]. Abramovic et al. [29] made analysis of variable inlet valve control of 4 stroke diesel engines using Miller cycle.

This study utilizes the recently developed performance analysis by Gonca and Sahin [30] called Effective Ecological Power Density (EFECPOD. From the available Literature it is evident that a lot of work has been done to put a light on optimization of heat engines or Diesel engines in particular. This thesis intends to put more light on this subject, by combining the optimized part of

Dual Miller Cycle with the optimized part of ORC and investigates the increments in efficiency or useful work and the reduction of specific fuel consumption as well as the reduction of NO_x or other hazardous emissions.

1.2 Objective of the Thesis

It has been lucidly understood to energy engineers that renewable energy sources like solar power plants or geothermal power plants do not compare economically to the conventional thermal power plants, if the environmental aspects are put aside. Hence if conventional thermal energy sources are to be utilized the fuel consumption, energy efficiency and the environmental viabilities should be considered and optimized, which leads to the use of waste heat recoveries like ORC. Moreover, efficient engines like Miller cycle engine has been investigated and put in operation. To sum up this thesis combines DMC engine with ORC type waste heat recovery. Therefore the objectives of this thesis are; to develop a combination of DMC-ORC and investigate this combination by seeking optimal operating conditions that enhance the power output or overall efficiency of the system, and also to find optimum operating values of the performance parameters employed that may reduce the SFC and lessens the hazardous emissions like NO_x and SO_x.

1.3 Hypothesis

DMC and ORC have never been combined togethere, so this work is unique in the way it would combine these two significant alternatives and is expected to get an enhanced performance. The result may also bolster the presumption as true. The result of the work probably would clearly show that there is an increase in efficiency by using the DMC – ORC combined plant as oppossed to DMC individual performance. The EFECPOD, effective power and other performnance parameters of the combined plant are also expected to show a significant improvement.

2

Marine Diesel Engines

2.1 Internal Combustion Engines

An internal combustion engine (I.C.E) is an engine that generates energy or power due to the combustion of fuel and air in the cylinder of an engine. Literally it is the chemical reaction of fuel with air that produces the work done. The fuels that are being used in internal combustion engines today contains diesel, petrol, naphtha, octane, and acetone and liquefied gases. The I.C.E shall comply with the requirements listed below to be considered as a worthy engine and to function at a standard level [31].

- Fuel and air have to be admitted to the engine at a convenient ratio.
- Fuel and air have to get compressed before or after the mixture is formed.
- Air fuel charge has to be combusted and as a result engine component will reciprocate to the next stages.
- The exhaust gas shall be discharged from the combustion chamber to ensure that the suction of fresh air or fuel air mixture into the combustion chamber follows.

2.2 Marine Diesel Engine

The I.C.E. has been into operation since 1888. Dr. Rudolf Diesel invented the diesel engine within 10 years. After this, Sulzer invented the first marine diesel engine with a power output of 20hp at 60 rpm. Diesel engines are also called as Compression Ignition (CI) engines. CI engines burn a fuel oil that is injected into the combustion space, once the charge air is fully compressed. Combustion commences when the compression temperature of the charge air become able to ignite the atomized liquid fuel. According to speed the marine diesel engines are

classified into three major classifications; low speed (< 200 rpm), medium speed (200- 1000 rpm) and high speed (> 1000 rpm) [31].

2.2.1 Marine Diesel Engine 4-Stroke and 2-Stroke

The MDE propulsion system is overshadowed by low speed two strokes cross head engines and higher or medium speed four stroke engines [32]. The four-stroke diesel engine is frequently used in applications that require compact size of plant. Vessels demand enormous amount of power to propel them through the water. For this reason, bigger ships possess a two stroke MDE. The height is the main problem for many coastal ferries though [31].

2.2.1.1 Four Stroke Marine Diesel Engines

Engines of this type perform one cycle in two crank shaft revolutions. In other ways the piston bounces up and down four times to perform one cycle as shown in Figure 2.1. The four strokes are [31];

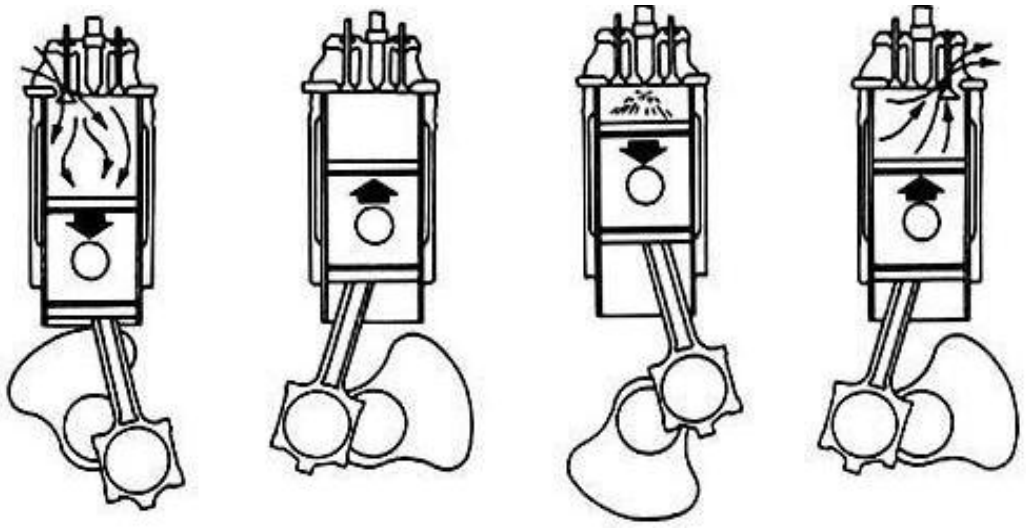
- Suction stroke; fresh air is sucked as the inlet valve opens, while the exhaust valve is closed. The piston bounces towards BDC, creating a vacuum pressure that sucks air at atmospheric pressure to enter.
- Compression stroke; when the piston reaches the BDC, together the inlet and exhaust valves get covered. So, the air charge in the combustion space will be compressed as the piston goes up towards the TDC.
- Power stroke; at compression stroke's final stage the temperature and pressure of the compressed air increases. At this incident finely atomized fuel oil is injected into the combustion space and combustion commences and produces high pressure gas. This combusting gas expands pushing the piston towards BDC and rotates the crank shaft.
- Exhaust stroke; as the combustion is about to finish, the piston reaches BDC, and the exhaust valve opens. The piston then changes its way and goes up to the TDC. The opening of exhaust valve at the last of expansion stroke will discharge the combusting exhaust gases to the surrounding.

2.2.1.2 Two Stroke Marine Diesel Engines

In 1879 Sir Dugald Clerk designed the two-stroke diesel engine. In these engines intake and exhaust phases occur with compression and expansion stroke respectively. Therefore, the two-stroke cycle is performed in one crankshaft revolution or two piston strokes. There are not inlet valves; instead there are air inlet ports. A blower pumps air into the cylinder to discharge the exhaust gases and refill up the cylinder with fresh air for burning. According to [33] the two phases are;

- Scavenging (suction and exhaust) phase; the piston bounces down in opposite to cylinder head and as it reaches about half of its displacement the exhaust valve opens and the exhaust gases are emitted into the atmosphere. Towards the finishing of exhaust stroke inlet airports are opened as the piston landing moves away. These ports allow pressurized air from the blower into the cylinder. The space above the piston head gets filled with fresh air that pushes the remnants of exhaust gases into the exhaust manifold. This process is called scavenging.
- Compression; inlet ports are uncovered at the end of power stroke. The piston reaches the outer most position, and then it changes its direction of motion. As the piston goes up wards, the piston seals the inlet airports, followed by exhaust gas closure and within a short span of time the upward movement of the piston compresses the charge air leading to a maximum cylinder pressure. Now high-pressure fuel is injected and ignited. So, the expansion of the combustion gases does the useful work by pushing the piston outwards as shown in figure 2.2.

The comparison in the design of 2-stroke and 4-stroke marine diesel engines holds a great focus, as both of them are inclined to make engines of large power production, light in weight, compact size and minimum brake specific fuel consumption. The necessary criteria's that are ought to have preference in the selection of marine diesel engines are specified below [31]:

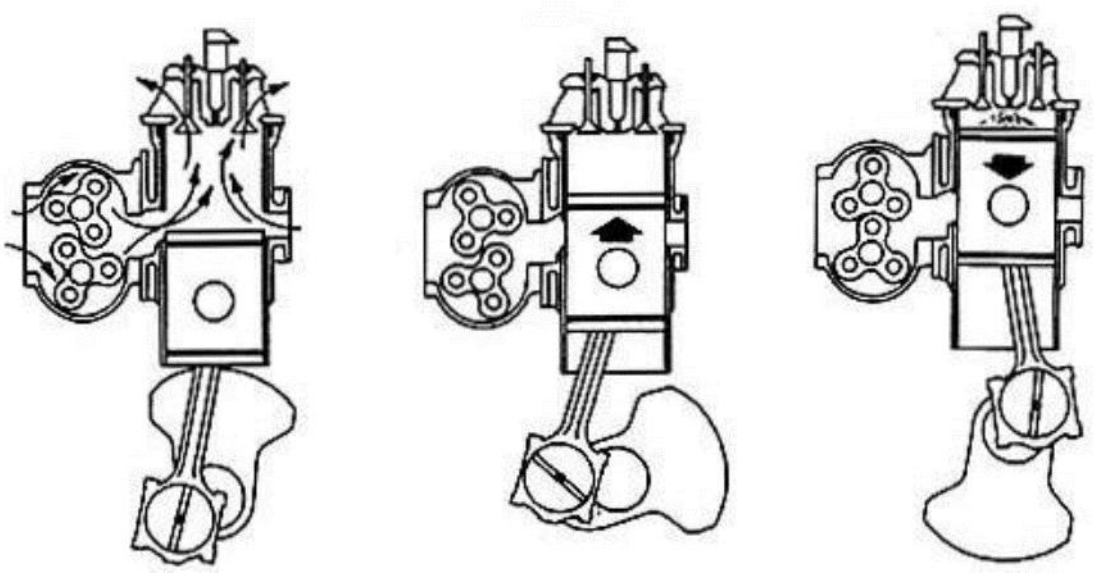


Stroke 1 Stroke 2 Stroke 3 Stroke 4

Suction COMPRESSION Expansion EXHAUST

Figure 2.1 4-Stroke Marine Diesel Engine; (a) Suction (b) compression (c) expansion d) Exhaust [33]

- Engine capability to sustain functioning under unexpected hull of the vessel positions, when the ship is in rolling or tilting position
- Marine diesel engine systems have to be devised to make the engine overcome water temperatures of minimum 35ºC and 40ºC and surrounding temperatures around -45°C.
- Marine engine should have the endurance to erosion brought by sodium reacting with moisturized air and vanadium elements present in the fuel.
- The machinery space especially the prime mover's noise has to be in compliance with the values permissible by the International Standards Organization (ISO).
- Marine engines should endure vibration that comes by way of propeller shaft spinning, transmission shaft and faulty mechanical parts.



a) b) c)

Figure 2.2 Two-Stroke Marine Diesel Engine; (a) exhaust and suction (b) compression (c) expansion [33]

Diesel engine where fuel is ignited by higher compressions (CI), functions at compression ratios beyond that of spark ignition (S.I) engines. Majority of 2-stroke and 4-stroke marine diesel engines functions on modern Diesel cycle or dual combustion cycle these days. Dual-combustion cycle undergoes heat addition at both constant volume and constant pressure representing Otto cycle and Diesel cycle respectively. Dual-combustion cycle commences fuel atomization and combustion ahead, that is at about 20^{o} before top dead center (TDC) [34]. Diesel engine that formerly worked with diesel cycle is modified to work with a Dual Cycle. Dual cycle engine has highest efficiency when compared with Diesel cycle and Otto cycles.

Variations exist among 4-stroke and 2-stroke marine Diesel engines in the way they admit air charge into the engine. 4-stroke Diesel engine uses the inlet valve to suck air into the combustion space, whereas the 2-stroke Diesel engines uses inlet airports to deliver fresh air into the cylinder. Scavenging system on 2-stroke marine diesel engine is classified into three kinds, they are i) cross flow, ii) loops and iii) uni – flow as illustrated in figure 2.3. Each of these three kinds of scavenging systems has merits and demerits. Cross flow system needs piston

skirt for avoiding air and waste products exit as the piston reaches TDC. Similarly, the loop system is meant for reduced air temperatures and higher temperature exhaust gas via ports in close proximity. It is of great importance to prevent temperature variations for liner wall. Lastly scavenge uni-flow is a system that is highly effective as well as vastly utilized in marine diesel engines.

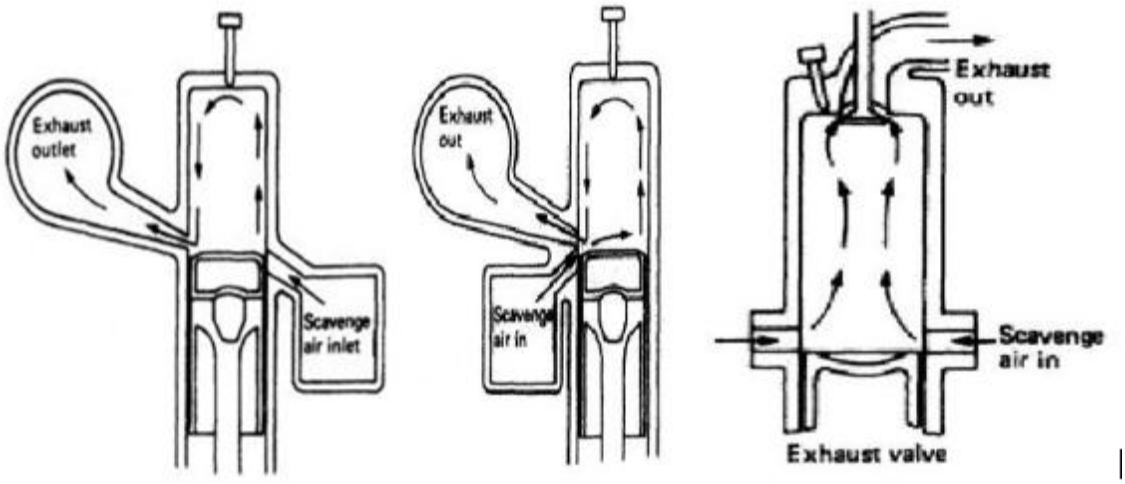
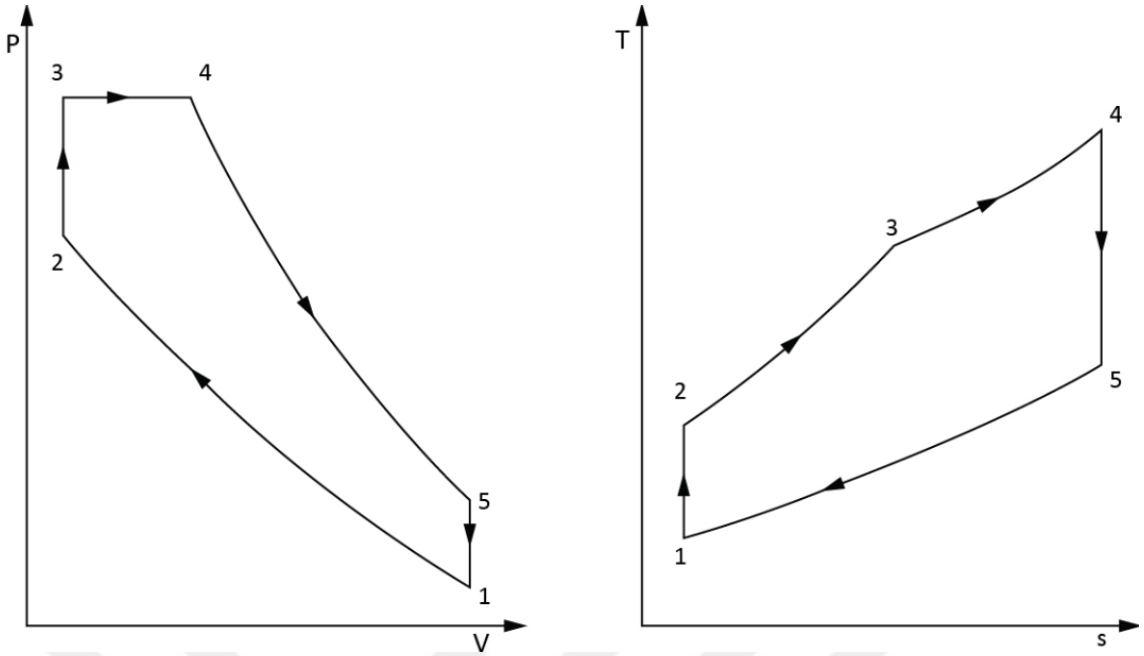


Figure 2.3 Scavenging system kinds for 2 stroke Marine Diesel Engines; (a) cross flow (b) loop and (c) Unit flow. [35]

2.3 Air Standard Dual Cycle

In air standard cycle the gas mixture is regarded as air for the whole cycle and the thermodynamic measurements of air are used for the process.

The I.C.E working on this cycle undergoes compression and expansion strokes that are regarded as adiabatic process. The whole cycle is referred as a reversible process. Even though the compression of air and expansion process is reversible, it is natural for friction to exist between the mating parts of the cylinder. However, the friction loss is negligible because of the smoothness of the mating (sliding) surfaces and adequate lubrication [36]. Figure 2.4 below demonstrates (a) Specific volume versus pressure or P-V diagram and (b) Entropy versus temperature, T-s diagram, for the cycle described above.



(a) (b)

Figure 2.4 (a) P-v Diagram; (b) T-s Diagram for Air Standard Dual Cycle [36]

From the P-V and T-s plots portrayed in here, stage 1-2 is a reversible adiabatic compression process displacing from BDC to TDC; stage 2-3 is a stroke of fixed volume heat supply ; 3-4 is a process of heat supply at a constant pressure; 4-5 is a reversible adiabatic expansion activity and stroke 5-1 is a constant volume heat rejection. Heat is added into the engine by burning of the finely atomized, injected fuel oil with the adequately compressed charge air. Cycle temperature is the highest temperature obtained in the cycle at a constant pressure. Work per unit of mass is developed by this one complete cycle [36].

$$W = C_v\left(T_3 - T_2\right) + C_p\left(T_4 - T_3\right) - C_v\left(T_5 - T_1\right) \tag{2.1}$$

W stands for work per unit of mass; C_v represents specific heat at constant volume; C_p is the specific heat at constant pressure;T_1, T_2, T_3, T_4 and T_5 are cycle temperatures of processes 1 through 5. Processes 1-2 and 4-5 are adiabatic processes. Let

$$\frac{P_3}{P_2} = \beta\,, \quad \frac{V_4}{V_3} = r_0\,, \quad \frac{V_1}{V_2} = r \tag{2.2}$$

$$T_2 = T_1 \cdot r^{k-1} \tag{2.3}$$

$$T_3 = T_2\beta = T_1 \cdot \beta r^{k-1} \tag{2.4}$$

$$T_4 = T_1 \cdot \beta r^{k-1} r_0 \tag{2.5}$$

And

$$T_5 = T_4\left(\frac{\beta}{r}\right)^{k-1} = T_1 \cdot \beta r_0^k \tag{2.6}$$

k represents ratio of the specific heats $\left(C_p/C_v\right)$; r stands for compression ratio $\left(V_1/V_2\right)$; β stands for pressure ratio $\left(\frac{P_3}{P_2}\right)$ and r_0 stands for cut of ratio $\left(V_4/V_3\right)$.

Moreover, heat per unit mass is delivered into the system both at constant volume – process 2- 3($\dot{Q}_1$) and at constant pressure – process 3 - 4 ($\dot{Q}_2$) as is given below.

$$\dot{Q}_1 = C_v\left(T_3 - T_2\right) \quad and \quad \dot{Q}_2 = C_p\left(T_4 - T_3\right) \tag{2.7}$$

Thus, the total heat added per unit mass into the system ($\dot{Q}_{in}$) is,

$$\dot{Q}_{in} = C_v\left(T_3 - T_2\right) + C_p\left(T_4 - T_3\right) \tag{2.8}$$

Heat per unit mass rejected to the surrounding,

$$\dot{Q}_3 = C_v\left(T_5 - T_1\right) \tag{2.9}$$

Then the thermal efficiency for the dual cycle is given as;

$$\eta_{Dual} = \frac{Net\ work\ done}{Total\ heat\ added\ to\ the\ system},$$

$$\eta_{Dual} = \frac{\dot{Q}_1 + \dot{Q}_2 - \dot{Q}_3}{\dot{Q}_1 + \dot{Q}_2} = 1 - \frac{\dot{Q}_3}{\dot{Q}_1 + \dot{Q}_2} = 1 - \frac{C_v\left(T_5 - T_1\right)}{C_v\left(T_3 - T_2\right) + C_p\left(T_4 - T_3\right)} = 1 - \frac{\left(T_5 - T_1\right)}{\left(T_3 - T_2\right) + k\left(T_4 - T_3\right)}$$

$$\eta_{Dual} = 1 - \frac{\left(T_1 \cdot \beta r_0^{\,k} - T_1\right)}{\left(T_1 \cdot \beta r^{k-1} - T_1 \cdot r^{k-1}\right) + k\left(T_1 \cdot \beta r^{k-1} r_0 - T_1 \cdot \beta r^{k-1}\right)}$$

$$\eta_{Dual} = 1 - \frac{1}{r^{k-1}} \frac{\left(\beta r_0^{\,k} - 1\right)}{\left(\beta - 1\right) + k\beta\left(r_0 - 1\right)} \tag{2.10}$$

2.4 Marine Diesel Engines Exhaust Emissions

Marine vessels recently have been obliged to comply with tight restrictions enacted on hazardous exhaust gas emissions set by international and local responsible bodies in adherence to concerns regarding air pollution. The main constituents of noxious exhaust products out of ships diesel engines are nitrogen, oxygen, carbon di oxide and water vapor including lesser amounts of sulfates, nitrates, particulate matter and unburned hydrocarbons as is shown in figure 2.5. From these various emissions NO_X is one of the most hazardous emissions. It assists in the production of Ozone (O_3) and other irritating parts, that tends to bring the urban summer eye and nose etc. [37].

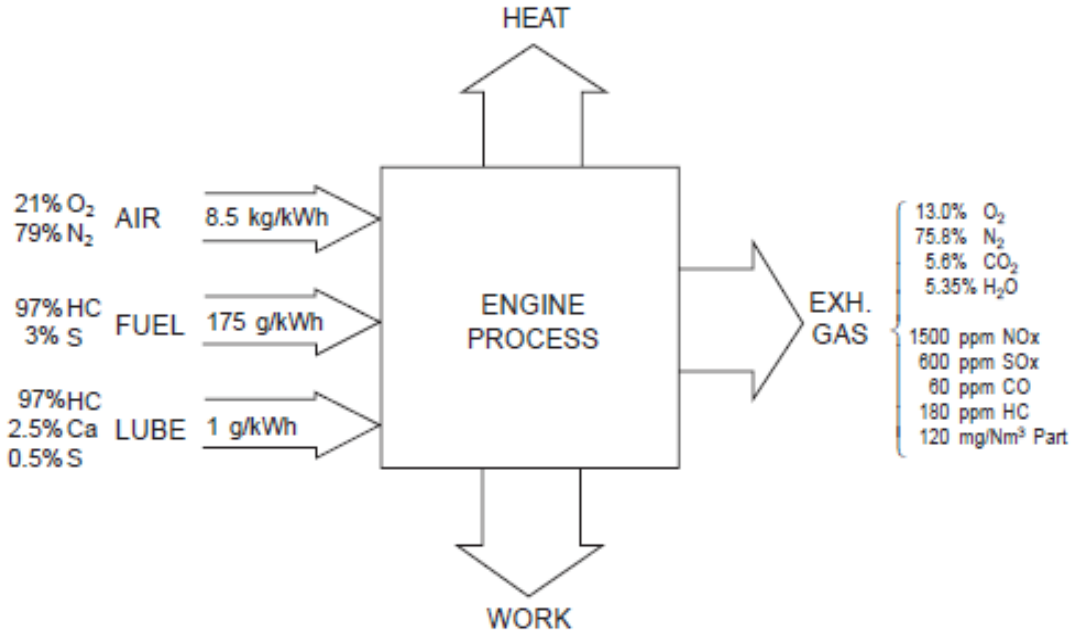


Figure 2.5 Main exhaust emissions from today's low speed diesel engine [32]

Emitted exhaust gases constitute the following main emissions described successively [32]:

a) Nitrogen Oxides (NO_x): Produced while combusting at peak temperatures in the combustion chamber. They have got much attention for being considered as carcinogenic and lead to photochemical smog production over urban areas plus a rainfall that is acidic in nature.
b) Sulfur Oxides (SO_x): generated during combustion from oxygen and sulfur. Its formation takes place at lower temperatures in opposite to the NO_x formation.

SO_x Can be transported more than 100's kms in the atmosphere and then gets accumulated in many lakes and rivers, minimizing the alkalinity. Ground water acidification and corrosion of water supply systems are other problems of SO_x.

c) Hydrocarbons (HC): Formed by combustion of fuel oil and lubrication oil that is not complete and by evaporating fuel.
d) Carbon Monoxide (CO): Is a product of a combustion process that is not complete, because of scarcity of air charge (oxygen) and improper way of mixing. CO is an extremely poisonous gas, but if available in great proportions.
e) Particulate Matter (PM): Is an intricate composition of inorganic and organic compounds as a consequence of a combustion that is not complete, partially unburned lubricant oil, ash in fuel, sulfur compounds and water.

Greater than 50% of PM is soot. Soot's are not deleterious; however, they can contribute to the formation of aqueous hydrocarbons, which may be carcinogen. Particulates don't contain more than 0.003% of engine exhaust emissions.

f) Noxious emissions: make 0.25 – 0.4% by volume of exhaust gas, based at the extent of sulfur present in the fuel, its lower heating value and the engine type, speed and efficiency.

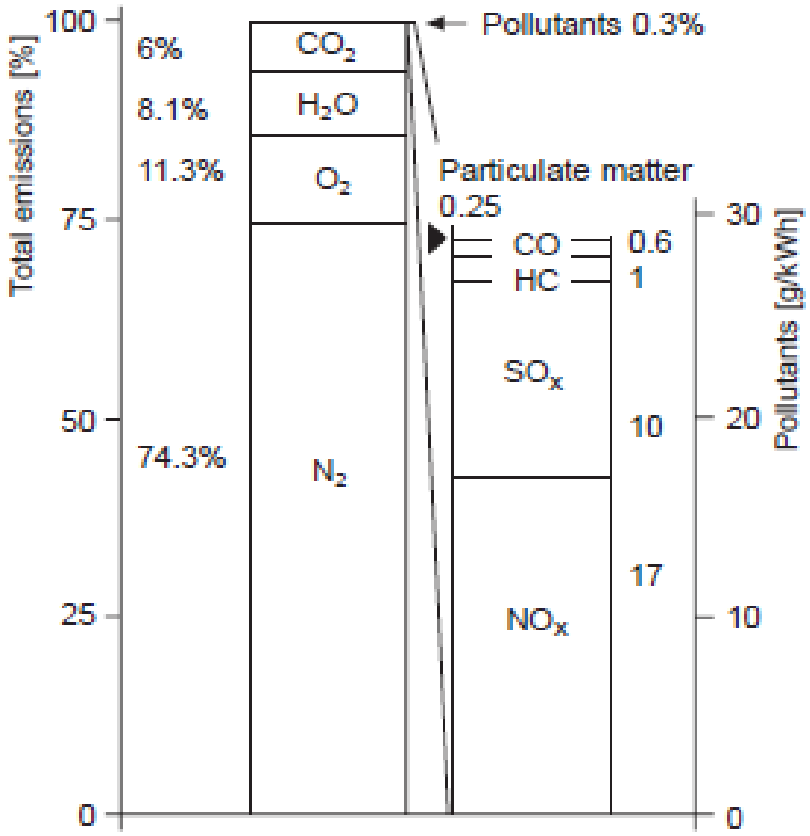


Figure 2.6 Propositions of the exhaust gas emissions of a medium speed diesel engine [32].

Table 2.1 Exhaust waste products proportion of CI engines [38]

Composition	Content(g/kWh)	Molecular Weight (g/mol)	Fraction (%)
O_2	13.66	32.00	14.83
CO_2	552	44.00	4.36
H_2O	321	18.01	6.20
CO	0.28	28.01	–
SO_2	0.46	64.06	–
NO_x (NO_2)	11.17	46.01	–
HC (CH_4)	0.19	16.04	–
N_2	687	28.01	74.61

2.4.1 Control of NO_X Emissions

The international perspective to NO_X emissions controls can be demonstrated by IMO Annex VI (regulation for prevention of air pollution from ships), under MARPOL 73/78 which was adopted in 1997 conference. Engines have to comply with the IMO curve that is associated to engine speed. For this purpose, an engine needs to be certified in compliant to the NO_x technical code and given an EIPP (Engine International Air Pollution Prevention) certificate. IMO's today's maximum permissible NO_X emission level on engine speed for Tier I, spreads from 17g/kWh for N< 130 rpm to 9.84g/kWh for N> 2000 rpm. Look at figure 2.7 below for more illustration [39]. Moreover, there are Tier II and Tier III limits applied for special and more strictly controlled areas.

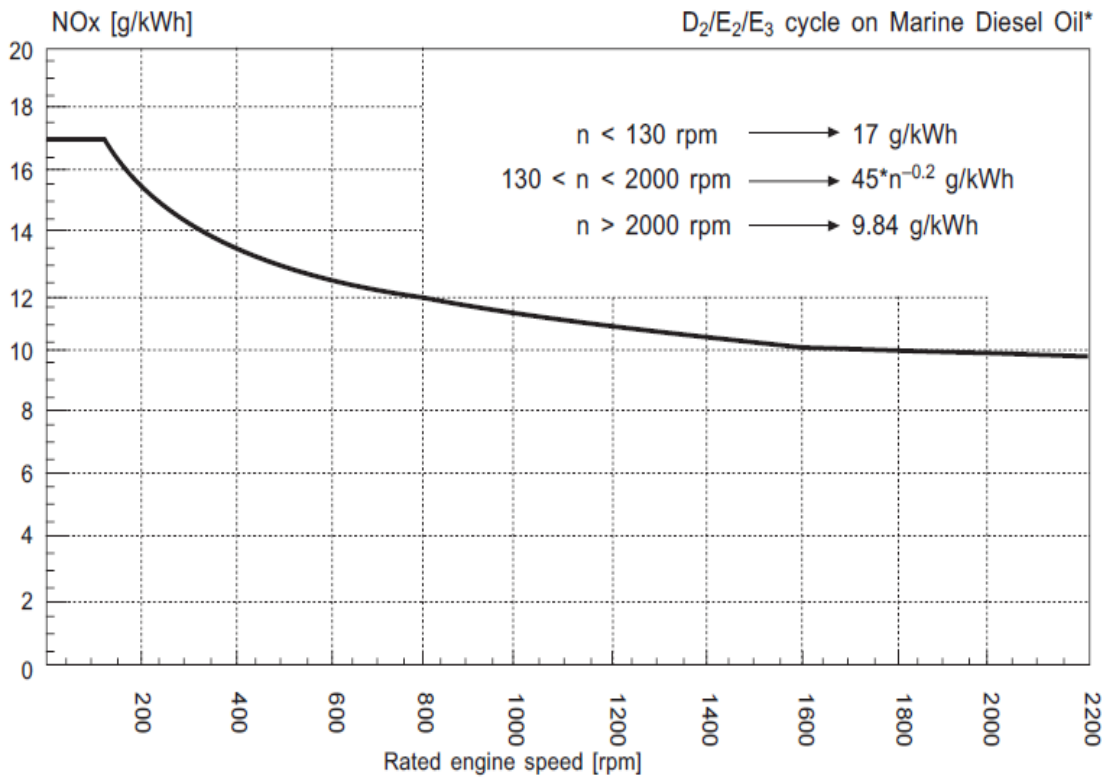


Figure 2.7 Maximum permissible NO_X emissions for marine diesel engines (IMO) [39]

Traditionally thermal efficiency increment has resulted to an increase in NO_X emissions. So, engine designers seek to reduce NO_X waste products without compromising efficiency and engine fuel economy.

Major factors for the production of NO_X are high thermal energy and presence of excess oxygen; the higher the temperature with a longer combustion span, the larger extent of NO_X will be generated. This partly reveals that low speed 2 – S engines create more NO_X emissions than medium and high speed 4-S engines of similar power developed.

There are two main methods for reducing NO_X emission levels as mentioned below [32];

a) Primary methods with a task of minimizing NO_X emissions generated in the act of combustion process by improving engine variables that influence emissions, such as valve timing, fuel injection and turbocharging. This part might account up to 30 – 60% reduction of NO_X emission.
b) Secondary methods aimed to extricate NO_X out of the exhaust gases using downstream cleaning strategies. This process can account up to 95% decrease in NO_X.

Under IMO, an Annex VI of MARPOL convention entered into force 19 May 2005, determines restrictions on sulfur di oxide and nitrogen oxide emissions and forbids intentional emissions of ozone depleting materials [40]. Designated emission control areas (ECAs) present highly strict standards for SO_X , NO_X and PM. A chapter adopted in 2011 provides compulsory technical and operational energy efficiency regulations emphasizing at minimizing greenhouse gas emissions from ships.

3

Miller Cycle and Dual Miller Cycle

3.1 Miller Cycle

Engine cycles possessing effective expansion ratio than the effective compression ratio can be regarded as over expanded cycles [41]. Over expanded cycles may be in the form of early intake valve closing (EIVC) or late intake valve closing (LIVC). EIVC and LIVC minimize the maximum temperature of the compression. Miller cycle is a cycle of combustion practiced in four stroke internal combustion engines. An American engineer Ralph Miller developed this cycle in 1940's. It was early used in vessels and power generators, in 1990's it was adopted by Mazda. Majority of the input energy wasted from an engine is because of the work demanded to compress the air in the compression phase. To make Miller cycle the intake valve should be open for longer than what normally should happen [42]. During the compression stroke, some charge is pushed way back through the normally closed inlet valve. To assist this, the combustion chamber is fed with more charge by a supercharger. The compression stoke covers just 70 to 80% of the physical displacement of the piston. The Miller cycle functions when the supercharger is able to compress the charge with a lower power than the piston does, for example at higher compressions the piston does better.

Miller cycle is being used in diesel engines as well as petrol engines [43]. Miller cycle's ultimate goal in diesel engines is to minimize NO_X emissions. Mazda's 2.3 KJ – ZEM brought into use in 1993, was the gasoline engine type car application that applied Miller cycle [44]. Niigata power delivered a medium speed diesel engine with Miller cycle application, the 32FX [45]. The importance of using Miller cycle for minimizing NO_X emissions from diesel engines commenced in the 1990's for IMO Tier 1 marine engines [45].

3.2 Thermodynamic Analysis of Miller Cycle

As is illustrated in figure 3.1 the significant behavior of Miller cycle has been the minimizing the compression stroke length. It can be illustrated from the figure that while the piston reciprocates downward during the intake stroke, the engine pressure maintains a constant pressure line, 6–1. The net work done of the paths 1-7 and 7-1 is zero, resulting to a lower effective compression ratio,

$$r = \frac{v_1}{v_2} \tag{3.1}$$

And the expansion ratio,

$$r_e = \frac{v_4}{v_3} \tag{3.2}$$

Figure 3.2 illustrates T-s diagram for the Miller cycle. Compression stroke 1-2 is isentropic process. The heat addition Q_{in}, 2–3 is also isochoric process and heat rejection of 4–5 is isochoric process. The formula for the thermal efficiency of the Miller cycle is given as [46];

Ratio of expansion ratio to compression ratio,

$$\lambda = \frac{r_e}{r} \tag{3.3}$$

Heat rejected from 4 – 5 and 5 – 1,

$$Q_{out} = mC_v\left(T_4 - T_5\right) + mC_p\left(T_5 - T_1\right) \tag{3.4}$$

Heat added into the system,

$$Q_{in} = mC_v\left(T_3 - T_2\right) \tag{3.5}$$

Thermal efficiency of Miller Cycle $= \frac{Q_{in} - Q_{out}}{Q_{in}} = 1 - \frac{Q_{out}}{Q_{in}}$,

$$\eta_{Miller} = 1 - \frac{mC_v\left(T_4 - T_5\right) + mC_p\left(T_5 - T_1\right)}{mC_v\left(T_3 - T_2\right)},$$

$$\eta_{Miller} = 1 - \left(\lambda r_c\right)^{1-\gamma} - \frac{\lambda^{1-\gamma} - \lambda\left(1-\gamma\right) - \gamma}{\gamma - 1} \cdot \frac{P_1 V_1}{Q_{in}} \tag{3.6}$$

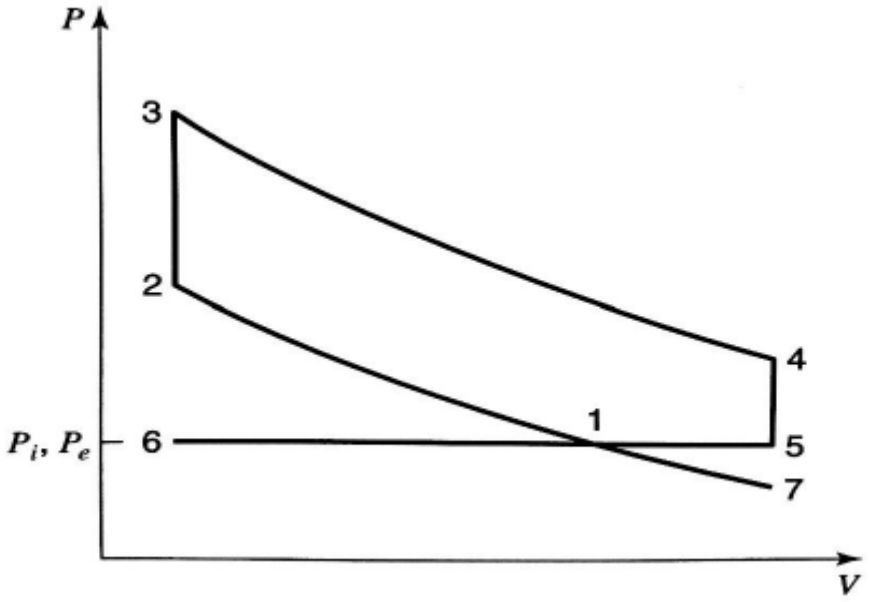


Figure 3.1 P-V diagrams for the Miller cycle [47]

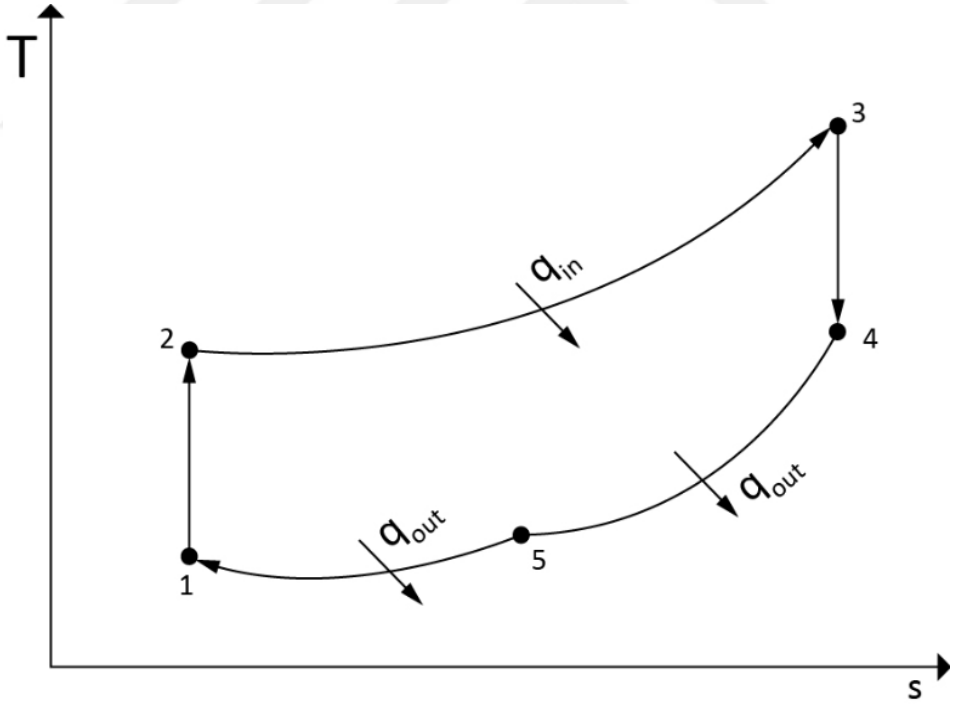


Figure 3.2 T-s diagrams for Miller cycle [48]

3.3 Thermodynamic Analysis of Dual Miller Cycle

Figure 3.3 demonstrates the P-V and T-s graphs for an air standard DMC. From the figure, stage 1-2s represents a compression at constant entropy, whereas stage 1-2 takes irreversibility into account. Energy is supplied in two stages; at stage 2-3 at a fixed volume and at stage 3-4 at a fixed pressure. Stage 4-5s represents an expansion at constant entropy while process 4-5 projects irreversibility. Energy is rejected at two stages; at an invariable volume, stage

5-6 and at a fixed pressure stage 6-1. The working fluid considered here is air at STD. It is assumed as an ideal gas. The aggregate amount of heat added Q_{in} and aggregate heat rejected Q_{out} can be calculated as follows [49]:

$$\dot{Q}_{in} = \dot{Q}_{23} + \dot{Q}_{34} = \dot{m}\left[C_v\left(T_3 - T_2\right) + C_p\left(T_4 - T_3\right)\right] \tag{3.7}$$

$$\dot{Q}_{out} = \dot{Q}_{56} + \dot{Q}_{61} = \dot{m}\left[C_v\left(T_5 - T_6\right) + C_p\left(T_6 - T_1\right)\right] \tag{3.8}$$

Where T_1, T_2, T_3, T_4, T_5, and T_6 represent temperatures from positions 1 to 6 consecutively and $\dot{m}$ represents mass per unit time, C_V and C_P stand for specific heat capacities of the ideal gas at a fixed volume and fixed pressure. Cycle power output according to first law of thermodynamics is given by;

$$\dot{W} = \dot{Q}_{in} - \dot{Q}_{out} = \dot{m}C_v\left[\left(T_3 - T_2\right) + k\left(T_4 - T_3\right) - \left(T_5 - T_6\right) - k\left(T_6 - T_1\right)\right] \tag{3.9}$$

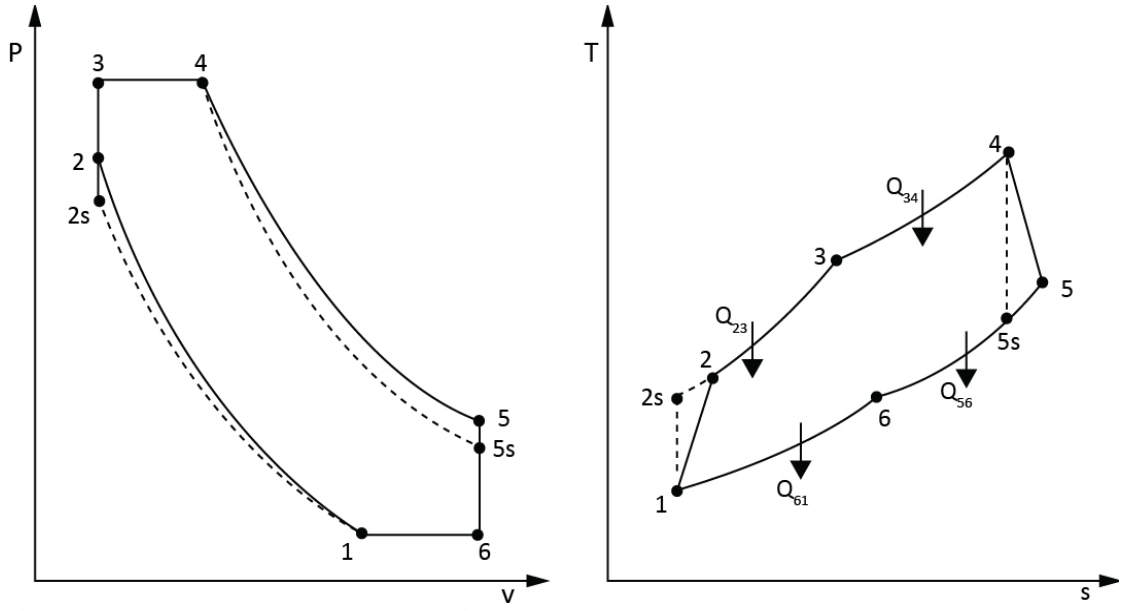


Figure 3.3 P-V and T-s schematic diagrams for Dual Miller Cycle [49]

And the thermal efficiency is given as:

$$\eta = \frac{\dot{W}}{\dot{Q}_{in}} = 1 - \frac{\dot{Q}_{out}}{\dot{Q}_{in}} = 1 - \frac{\left[\left(T_5 - T_6\right) + k\left(T_6 - T_1\right)\right]}{\left[\left(T_3 - T_2\right) + k\left(T_4 - T_3\right)\right]} \tag{3.10}$$

Where k is the rate of the specific heats at fixed pressure to the value at a fixed volume $\left(C_v/C_p\right)$. Isentropic Efficiencies of the compression and expansion stages are [50]:

$$\eta_C = \frac{T_{2s} - T_1}{T_2 - T_1} \tag{3.11}$$

$$\eta_E = \frac{T_4 - T_5}{T_2 - T_{5s}} \tag{3.12}$$

η_C and η_E explain the degree of irreversibility of the adiabatic mechanism. Rearranging Equations (3.11) and (3.12), it can be calculated as:

$$T_2/T_1 = \eta_C + \left(r^{k-1} - 1\right) \tag{3.13}$$

$$T_5/T_4 = \left\{1 - \eta_E\left[1 - \left(1/\delta^{k-1}\right)\right]\right\} \tag{3.14}$$

While compression ratio (r) may be described as:

$$r = v_1 / v_2 \tag{3.15}$$

Engine plan coefficients such as pressure ratio (β), cut-off ratio (r_o), cycle temperature ratio (α) and cycle pressure ratio (λ) might be written one by one as follows:

$$\beta = P_3 / P_2 = T_3 / T_2 \tag{3.16}$$

$$r_0 = V_4 / V_3 = T_4 / T_3 \tag{3.17}$$

$$\alpha = T_{\max} / T_{\min} = T_4 / T_1 \tag{3.18}$$

$$\lambda = P_{\max} / P_{\min} = P_3 / P_1 = P_4 / P_1 \tag{3.19}$$

For comparing Dual cycles, Miller cycle ratio (r_M) [51] is applied for describing the variation between DMC and Dual-Diesel cycle. Both r_M and stroke ratios are described below:

$$r_M = V_6 / V_1 = T_6 / T_1 \tag{3.20}$$

$$\varepsilon = V_6 / V_2 \tag{3.21}$$

DMC occurs DDC when $r_M = 1$, Where DDC is dual diesel cycle.

From second law of thermodynamics:

$$T_1^k \cdot T_3^{1-k} \cdot T_4^k = T_{2s} \cdot T_{5s} \cdot T_6^{k-1} \tag{3.22}$$

Inserting Eqns. (3.11) - (3.22), into equations (3.3) and (3.4) we get new relations among the coefficients as given below;

$$\delta = \frac{r_M * r}{\rho} \tag{3.23}$$

$$\alpha = \rho \frac{\lambda}{r} = \rho \frac{\lambda r_M}{\varepsilon} = \rho\beta \left(1 + \frac{r^{k+1} - 1}{\eta} \right) \tag{3.24}$$

The dimensionless power output [$\bar{W} = \dot{W} / (\dot{m} C_v T_1)$] and thermal efficiency (η) are obtained by putting Eqns. (3.11) - (3.24) into the Eqns. (3.9) and (3.10) by getting use of the dimensionless coefficients as presented below:

$$\overline{\dot{W}} = \left(\beta\left(1-k\right)-1\right)\left(\frac{\lambda r_M}{\varepsilon\beta}\right)+k\left[\rho\beta\left(1+\frac{\left(\frac{\varepsilon}{r_M}\right)^{k-1}-1}{\eta_C}\right)\right]+r_M\left(1-k\right)+k-\left[\rho\beta\left(1+\frac{\left(\frac{\varepsilon}{r_M}\right)^{k-1}-1}{\eta_C}\right)\right]+$$

$$\eta_E\left[\rho\beta\left(1+\frac{\left(\frac{\varepsilon}{r_M}\right)^{k-1}-1}{\eta_C}\right)\right]-\left[\rho\beta\left(1+\frac{\left(\frac{\varepsilon}{r_M}\right)^{k-1}-1}{\eta_C}\right)\right]\eta_E\left(\frac{1}{\lambda r_M}\left[\rho\beta\left(1+\frac{\left(\frac{\varepsilon}{r_M}\right)^{k-1}-1}{\eta_C}\right)\right]\right)^{1-k} \tag{3.25}$$

Based on the above equations,

$$\eta = \frac{\overline{\dot{W}}}{\left(\beta\left(1-k\right)-1\right)\left(\frac{\lambda r_M}{\varepsilon\beta}\right)+k\left[\rho\beta\left(1+\frac{\left(\frac{\varepsilon}{r_M}\right)^{k-1}-1}{\eta_C}\right)\right]} \tag{3.26}$$

4
Waste Heat Recovery Technologies and Organic Rankine Cycles

4.1 Waste Heat Recovery Technologies for Marine Use

I.C engines are vastly utilized in small to medium size applications such as vehicles, industries, marine vessels and electrical power plants. In I.C engines approximately 30 – 40% of fuel energy content changes into useful energy output, while the rest part is emitted through the exhaust wastes, EGR, and heat losses [52 - 54]. The waste heat on marine vessels is basically fuel energy that is emitted into the surrounding (atmosphere) from different ongoing operations. A vessel fitted with Diesel engine has the prime mover as the biggest source of waste heat.

It is estimated that around 28% of the heat supplied is emitted to the atmosphere via exhaust manifold of a CI engine [55]. In an experiment by Wang et al. [56] done on a CI engine, the power wasted via exhaust to the atmosphere was found to be around 19% of combustion energy. Similarly, it was described that approximately 26% of heat supplied is lost via exhaust waste of a C.I engine [57]. Moreover, considerable portion of (nearly 42%) energy is lost via cooling system with water as a medium fluid [57].

The power loss might be regained utilizing numerous strategies like Kalina and Rankine cycles [57 – 61], ORC [58, 62- 64], Brayton cycle [65] and thermoelectric generator [55, 64]. From all these heat recovery systems ORC is the most productive, particularly in applications of medium and low thermal energy sources [50, 55, 56, 63, 66, 67].

When compared against steam the organic fluids circulated in ORC's possesses bigger molecular masses leading to effective designs, adequate mass flow rates, and enhanced turbine efficiencies approximating 80 – 85% [68 - 70].

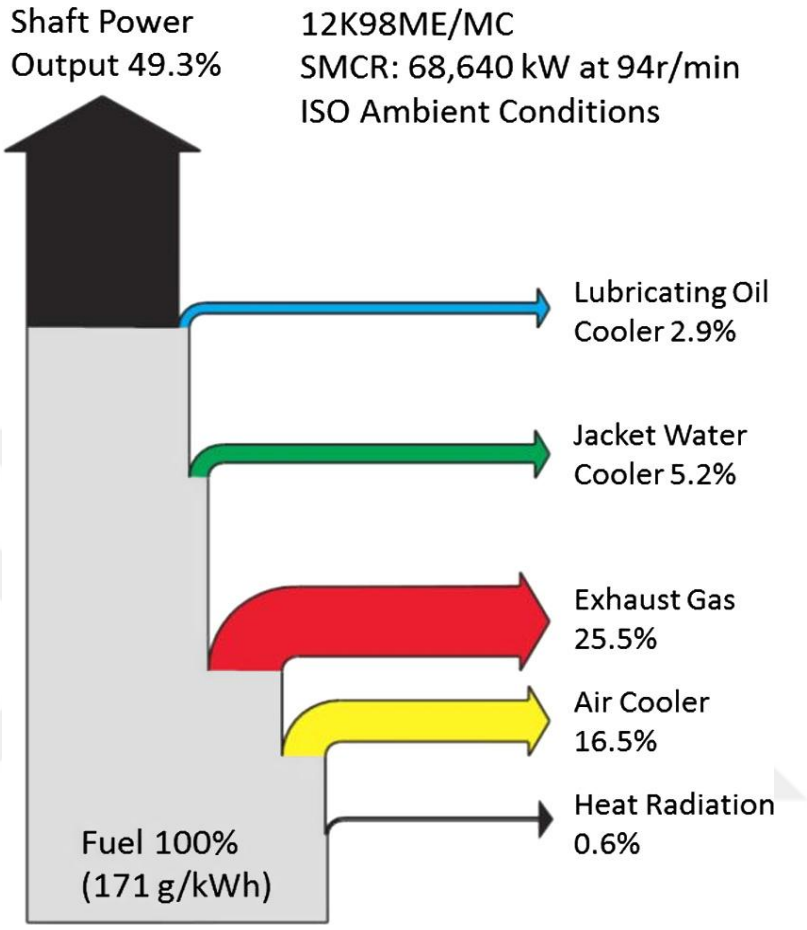


Figure 4.1 Heat balance for MAN 12K98ME/MC marine diesel engine [71].

Table 4. 1 Grading of Heat Energy Based on Temperature Distribution [72].

Grade	**Temperature distribution (°C)**
High	650 and higher
Medium	232 – 649
Low	232 and lower

Heat can be graded according to thermal energy content as in Table 4.1. Moreover Table 4.2 illustrates majority of marine waste heat sources with their possible temperature distributions.

Table 4.2 Temperature distribution of majority marine waste heat sources [21, 40, 73, 74 and 75]

Source	Temperature range
Waste incinerator	850 – 1200 °C [40]
Engine exhaust gas	200 – 500 °C [75]
Scavenger air (compressor outlet)	100 – 160 °C [73,74]
Engine cooling water	70 – 125 °C [73, 74]

An occasion of a latest implementation in India, shows that the incorporated ORC plant regains energy loss with an exhaust gas temp of 320 ^{0}c. The ORC installation can recover 4MW of electrical power, thus minimizing CO_2 emissions approximately 16871 tons annually [68].

4.1.1 Types of Waste Heat Recoveries

Various kinds of waste heat recoveries exist today depending on their application and the source of waste heat. The most commonly applicable types of waste heat recoveries are described below [21].

4.1.1.1 Rankine Cycle (RC)

It is one that transforms thermal power into mechanical energy. A working fluid regularly evaporates and condenses in the process. Physically a basic Rankine cycle constitutes four major compartments; evaporator, expansion device (turbine), condenser and feed pump. The illustration of compartments of the cycle is delivered in fig 4.2 and T – s diagram is presented in Fig. 4.3.

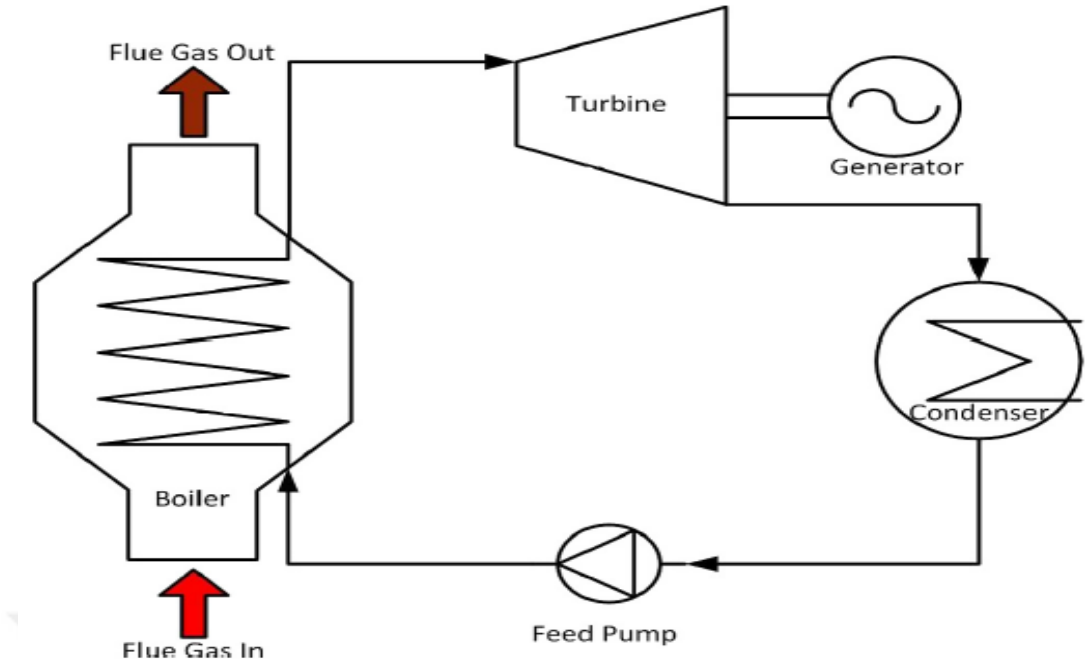


Figure 4.2 Schematic of a simple Rankine cycle plant [21]

4.1.1.2 Steam /Conventional Rankine Cycle (SCR)

The Steam Rankine Cycle is very important to change bigger thermal energy into power output. To specify some, Nuclear power plant, coal fired steam power plant. The steam plant is made up of a condenser, pump, vaporizer, turbine and water (medium).

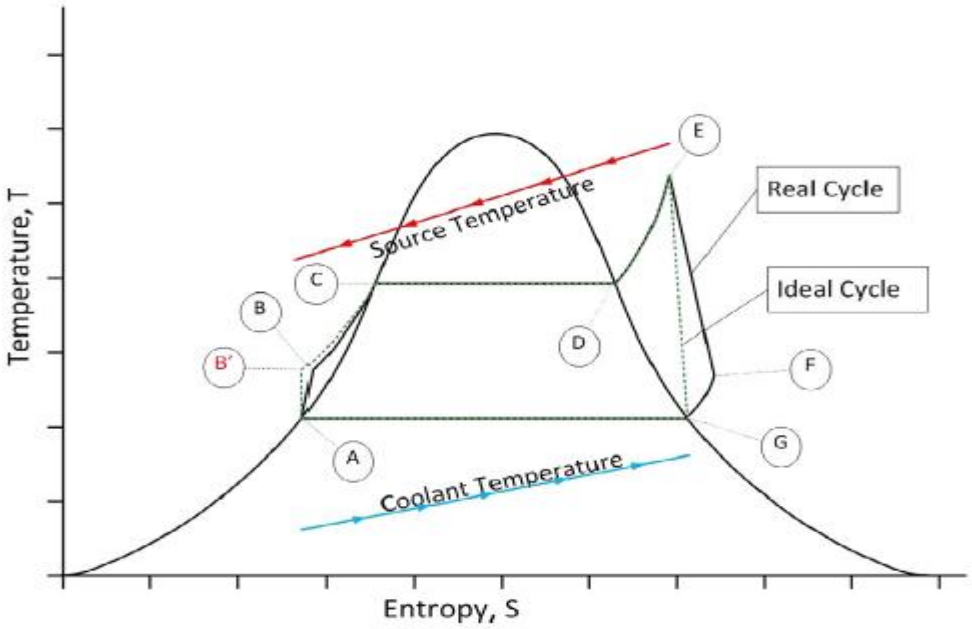


Figure 4.3 Temperature–entropy (T–s) diagram for a Rankine Cycle [21]

4.1.1.3 Organic Rankine Cycle (ORC)

An ORC is a modified form of a SRC, in which the working fluid of steam Rankine cycle (steam) is substituted by an organic fluid such as hydrocarbon gases and organic refrigerants like hydroflouro carbons (HCFC's). An ORC configuration resembles as that of a Rankine cycle plant, both of them having the same fundamental components [21].

4.1.1.4 Super Critical Rankine Cycle (SCRC)

The thermal power plant being designed to operate on a cycle with steam pressures exceeding the critical pressure of water (22.1MPa) and turbine inlet temperatures exceeding 600^0C is called Supercritical Rankine Cycle (SCRC). Supercritical Rankine cycle with multistage reheat may reach up to 48% efficiency (see figure 4.4) [76].

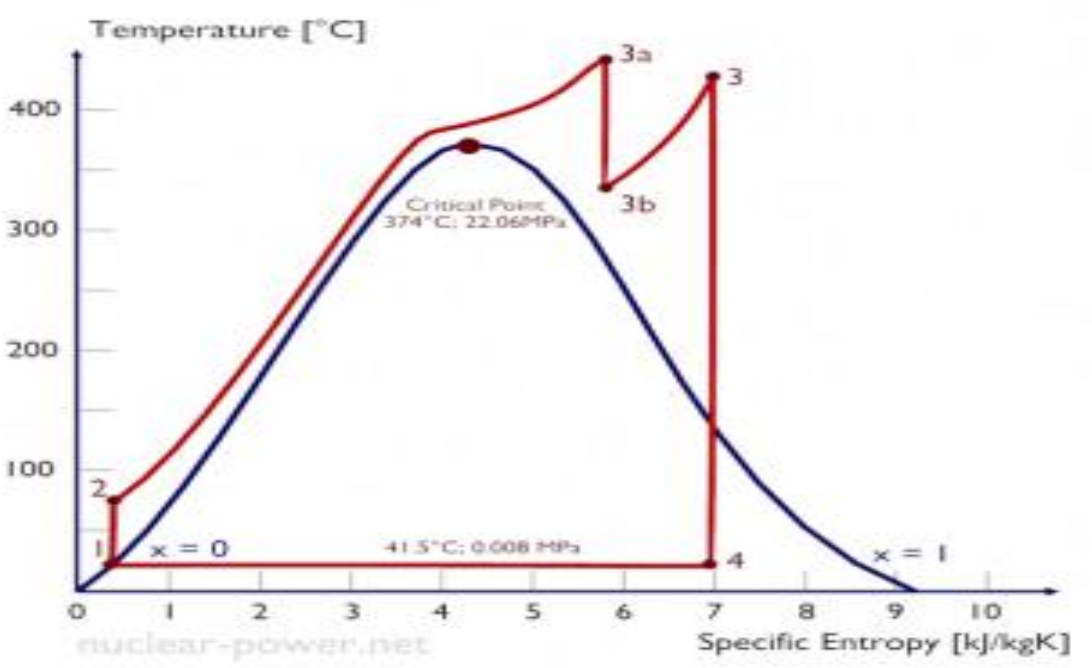


Figure 4.4 Supercritical Rankine Cycle [76]

4.1.1.5 Kalina Cycle

Energy conversion cycle utilizing ammonia – water mixture suggested by Dr. Alex Kalina and afterwards it is known as Kalina Cycle [77]. It is an enhanced version of RC possessing improved effectiveness for numerous applications. The KC as a waste heat recovery apparatus has got significant advantages ranging from lower to moderate temperature heat sources. KC utilizes ammonia mixed with water to function in alternate proportions at different boiling and condensation temperature distributions. KC plant layout resembles much to a RC plant, but possesses some extra compartments. Main KC components consist of recuperate, separator, some blenders and valves added to the basic components of a RC system as is depicted in figure 4.5.

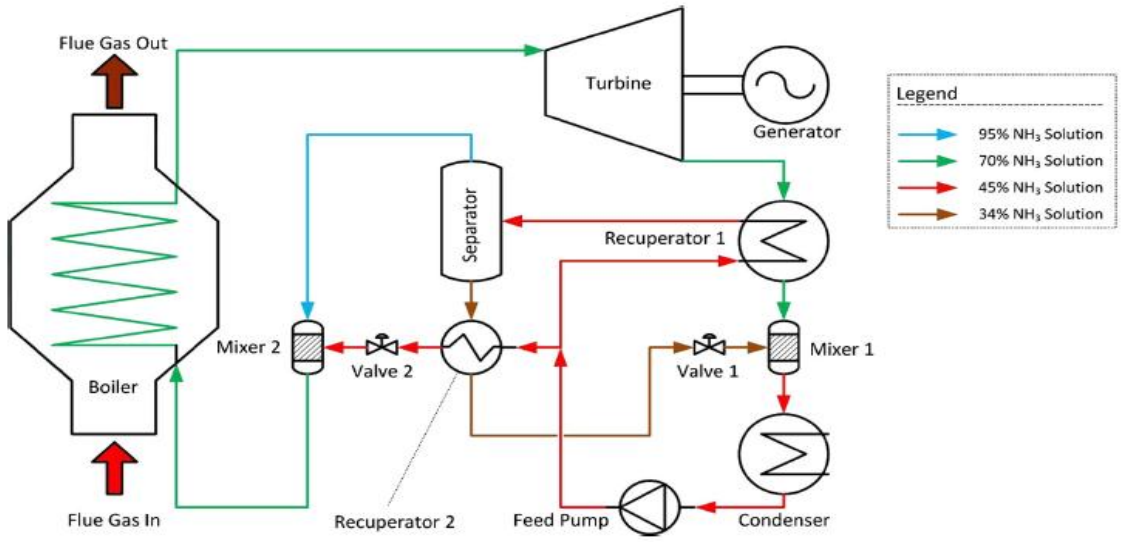


Figure 4.5 Schematic of a simple Kalina cycle plant [77].

4.1.1.6 Thermoelectric Generator (TEG)

In a thermoelectric generator (TEG), a voltage in the semi-conductors is generated due to variance in temperature of heat source and heat sink (see beck effect) [78]. Thermoelectric modules generate electrical energy from thermal energy. A thermocouple has N and P type bars joined electrically in series arrangement [21] as is depicted in figure 4.6.

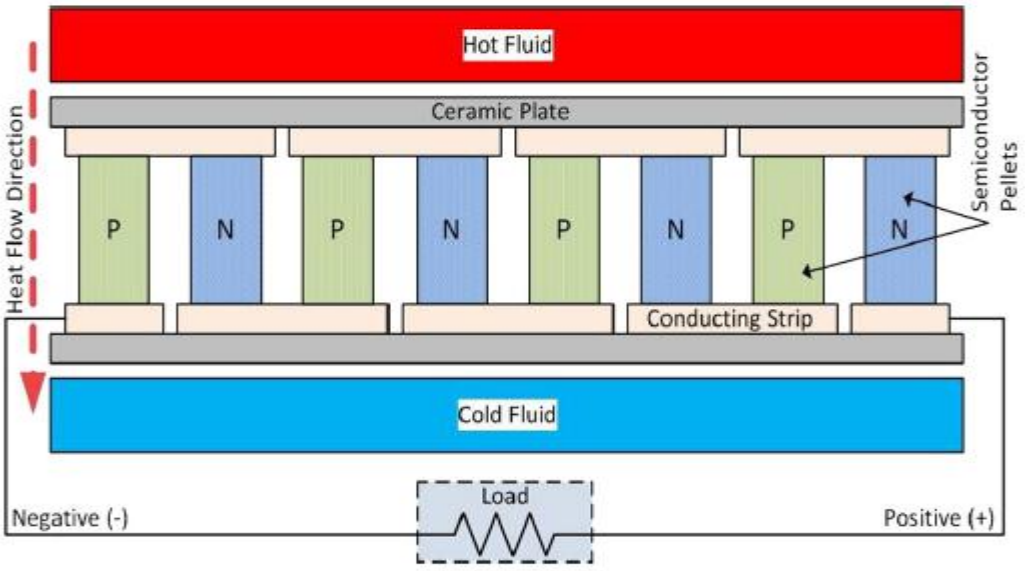


Figure 4.6 A simple thermo-electric generator (TEG) module [21]

Various types of energy loss sources have different amount of temperature or strategies specifically. So, the type of waste heat source or the amount of heat capacity carried in the waste heat from that source may determine the type of heat capacity that can be recovered by appropriate waste heat recovery and waste heat regeneration system to be applied.

4.1.2 Comparison of Waste heat Recoveries

4.1.2.1 General Overview

It is not beneficiary business wise to work with conventional Rankine cycles (i.e. like steam cycle) to generate mechanical or electrical energies from lower grade heat sources. Therefore, comparison and identification of better opportunities to get the best possible efficiency out of the available heat source is very crucial. The choice of waste heat recovery system for a vessel might be case specific which is dependent of machinery onboard including the extent and grade of waste heat energy present. Additional factors like size and space restrictions, extra intricate technologies, shipping routes and commercial patterns of ship may influence in selection [21].

KC provides a satisfactory WHR for medium quality heat source with the best recovery efficiency. KC has got flexibility to function under various working conditions. Similarly, technologies such as ORC and SCRC provide higher recovery efficiency values, RC being safe and reliable. TEG's recovery efficiency is lower but this technology holds a great interest for the future. The working temperature and energy loss recovery productivity of some of the main waste heat recoveries are illustrated in figures 4.7 and 4.8 consecutively.

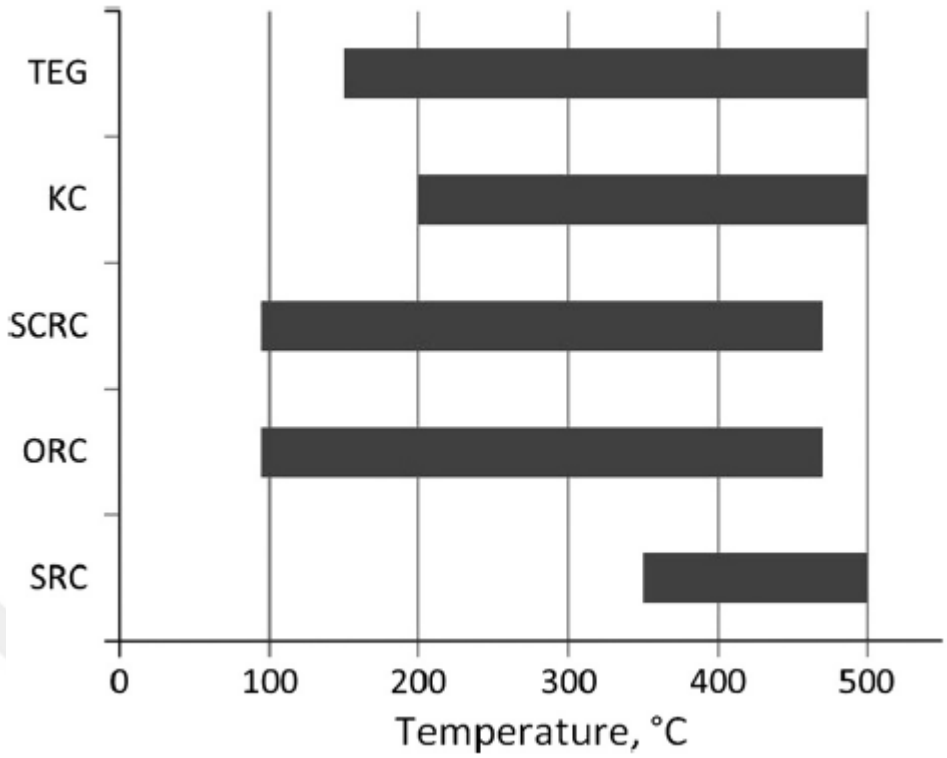


Figure 4.7 Suitable Waste Heat Temperature Range for Each Technology [21]

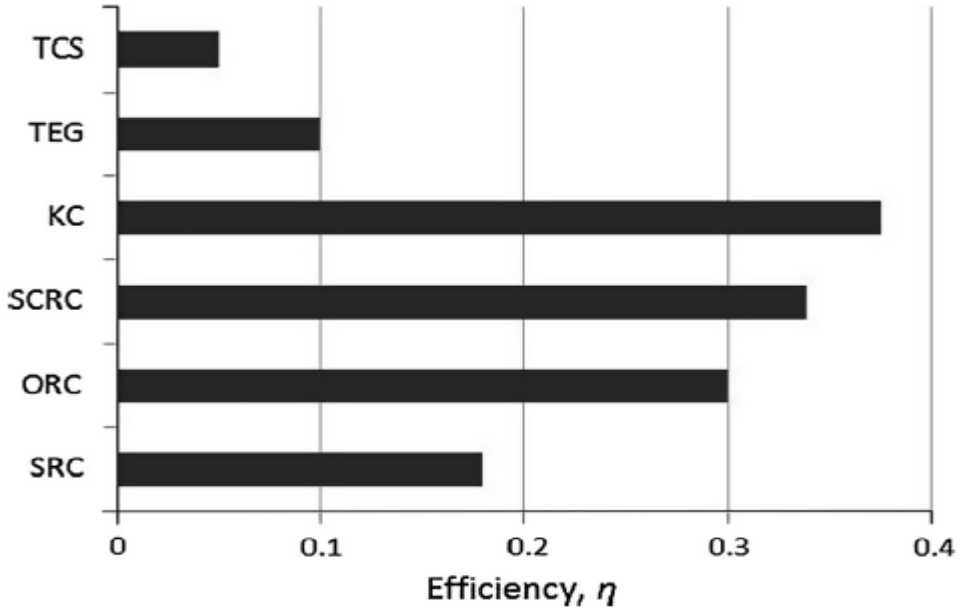


Figure 4.8 Appropriate efficiency distribution for various WHRs [21]

A substantially chosen WHR can ameliorate aggregate plant effectiveness, minimize the running capital, and lowers ship's exhaust gases products conducive to the eco – friendly performance of ships. Moreover, the reason

behind why steam turbines are overtaken by other technologies has to be analyzed with in this context. Some important points regarding the merits and demerits of steam as a working fluid are demonstrated below.

4.1.2.2 Advantages of Water as a Working Fluid

The advantages of steam as a working medium can be briefly summarized as follows [79]:

- Adequate thermal/chemical stability
- Minimum viscosity
- Satisfactory power carrying capacity
- Nontoxic, Nonflammable and environmentally friendly (zero ODP, zero GWP)
- Not expensive and easily available

4.1.2.3 Disadvantages of steam as a working fluid

Some disadvantages of using steam as a working medium are listed below [80]:

- Demand to superheat so as to avoid moisture formation in turbines
- Threat of corrosion of turbine parts
- Over pressure in the evaporator
- Intricate and costly components

Therefore, steam is suitable for high temperature applications. The obstacles to use steam can be appeased in part by choosing convenient working fluid. Organic compounds containing high molecular mass as well as low critical temperature as opposed to water have been recommended for an ORC. Observation of fluid's characteristics in steam and organic Rankine cycles is demonstrated in Table 4.4 below.

Table 4.3 Overview of Fluids Characteristics Observation in Steam and Organic Rankine Cycles [81]

	Steam cycle	**Organic Rankine Cycle**
Fluid	Water	Organic Compound
Critical pressure	High	Low
Critical temperature	High	Low
Boiling point	High	Low
Condensing pressure	Low	Acceptable
Specific heat	High	Low
Viscosity	Low	Relatively high
Flammability	No	Yes, and depends on fluid
Toxicity	No	Yes
Environmental impact	No	High and depends on fluid
Availability	Available	Supply problem
Cost	Cheap	Expensive

4.2 Organic Rankine Cycle

Organic Rankine cycle is one of the most important waste heat recovery technologies used both on and off shores.

4.2.1 Introduction

A Scottish physicist and engineer William John Macquorn Rankine founded the RC. ORC started to be studied as early as 1880's, however ORCs haven't been popular until these days of developing threats regarding consuming of underground fossil fuel reserves and ecological issues have led innovation of low grade lost heat recoveries[79]. Because of its lowered operating temperature, an

ORC has the ability to regain energy from sources with lower thermal energy content. The progress of ORC was enhancing due to the need to utilize various working fluids that are more versatile than water. Power transformation of these low heat sources is feasible by harnessing organic fluids such as Chloro – Flouro-Carbons (CFC), Hydro- Chloro- Fluoro – Carbons (HCFC), and Hydro – Fluoro-Carbons (HFC).

Naturally an ORC applies identical principles with Steam Rankine cycles, however, employs organic working fluids. They possess reduced boiling points making them able to regenerate energy out of low temperature energy sources. The ORC is a reversible cycle, consisting, working fluid compression, heat admission (from exhaust gases in case of ships), expansion and condensation as shown in figure 4.9. A particular ORC utilizing R245fa as a medium is demonstrated in the T-s diagram of figure 4.10 [11]. The energy regenerated out of the waste heat i.e. exhaust gases or jacket cooling water, is converted in to mechanical or electrical energy by the ORC, which in one or the other way helps to cover the ships energy demand. Therefore, as partially the energy requirement of the ship is met by the ORC, specific fuel consumption of the vessel is minimized significantly, leading to deduction of emissions (more importantly the harmful emissions) of the ship. For example, OPCON marine has implemented the first ORC – WHR plant aboard M/V Figago and is estimated to obtain approximately 4 – 5% fuel savings for that occasion, with a further prediction of a saving possibility of 5 – 10% for other installations [78].

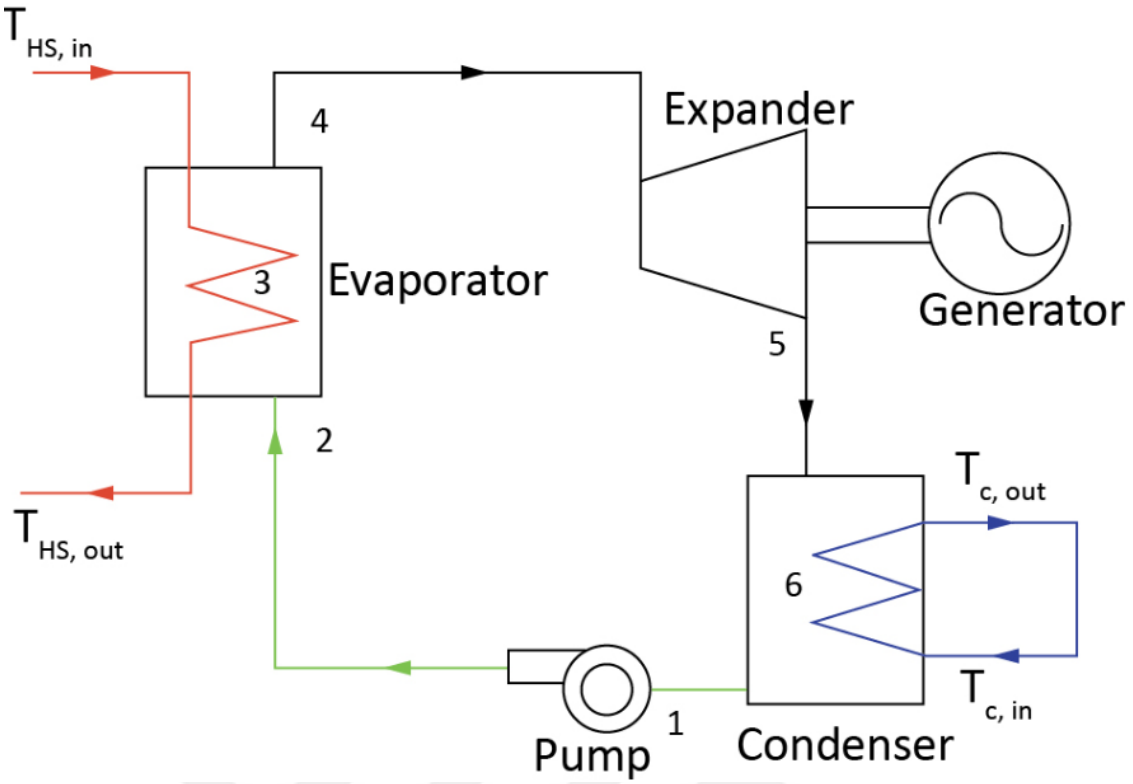


Figure 4.9 Schematic diagram of an ORC system for waste heat recovery [49].

4.2.2 Selection of Working Fluids for Organic Rankine Cycles

The ORC is vastly applied innovation owing to various implementations transforming variety of heat sources to mechanical power distributed from KWs to MWs [81]. The achievement of this technology goes to its unsophisticated and adaptable nature. ORCs are modifiable and might be implemented for a vast distribution of heat source temperature, beginning with 80 °c to 400 °c [82].

The key challenges are isolation of significant working fluids and the alternative suitable design principles, working features of the cycle as well as the desired implementation of the ORCs to the heat source considered. The fluids utilized in ORC's may be drawn out of discrete compounds like Siloxanes, alcohols, hydrocarbons, and so on. Appropriate working fluids have lower latent heat so that lower energy is demanded to vaporize the working fluid [11]. Moreover organic fluids are more adaptable to heat sources, minimizing the irreversibility which comes during heat admission stage. The reduced latent heat of the medium enables higher mass flow rate as opposed to a steam Rankine cycles.

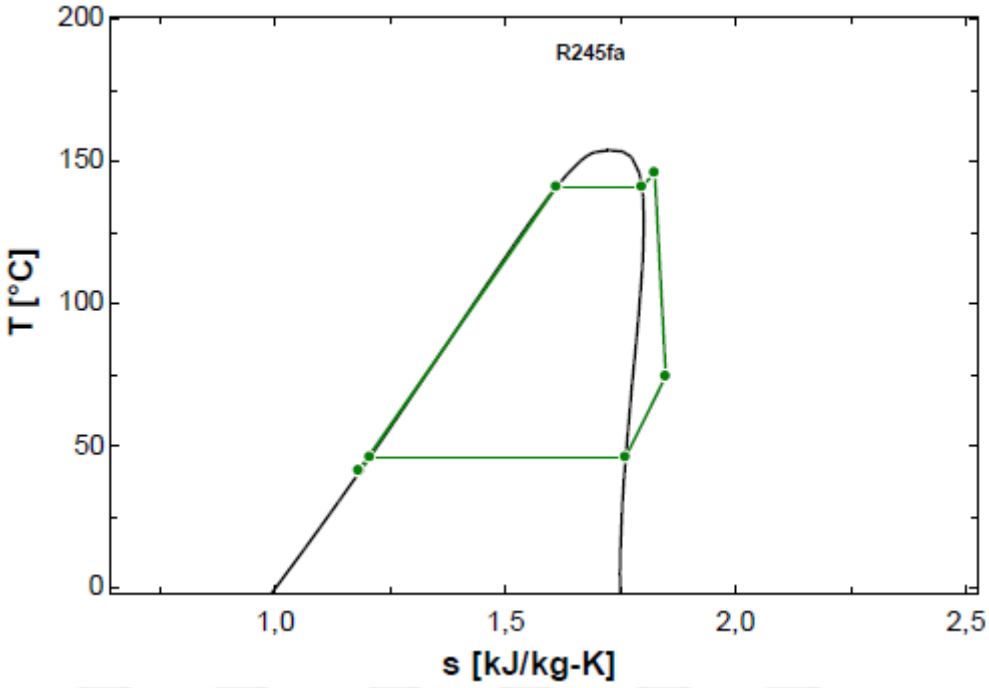


Figure 4.10 T-s diagram of a particular ORC having R245fa as medium [11]

It is essential that a working medium possesses satisfactory thermodynamic properties to acquire higher efficiencies, as well as acceptable energy to be generated from a particular heat source.

The system productivity, safety, ecological influences as well as commercial adequacy of the system rely to a greater amount on the choice of the fluid. However, no single medium is recognized to be the best alternative, thus the choice of the working fluid is more of searching a selective accommodation of characteristics. The possibility of a few alternate mediums to circulate inside an ORC was analyzed in [5].

Working fluid selection has got a mass significance on the effectiveness of ORCs with varying heat sources [83]. Numerous researches have been done on working fluid selection for various ORC technologies. Mago et al. [84] made an evaluation of system performance by taking various dry and wet fluids depending on variable energy sources, and the outcomes signaled that dry fluids were more worthy. The outcomes of an ORC technology that used waste heat of gasoline engine as a source were investigated by comparing discrete working fluids and altering cycle parameters [85]. It was illustrated that the main

characteristics influencing the ORC cycle performance contains latent heat, specific heat and vapor [86]. Similarly, it was recommended by Chen et al. [87] that fluids possessing higher latent heat and lower specific heat were advisable. In contrast to this Yamamato et al [88] implied that fluids with lower latent heats were preferable.

The properties of better alternative fluids can be justifiably identified from the available literature devoted for choosing a working fluid for various heat recovery systems [37, 89, 90, 91 - 94]:

- High density
- high specific heat
- Isentropic or dry fluids
- average critical temperatures and pressures
- Satisfactory condensing and evaporating pressures
- Adequate heat transfer behaviors
- Reliable thermal and chemical stability that makes no deterioration at higher temperatures
- Friendly with other substances.
- Very great thermodynamic outcomes.

Organic mediums are differentiated into three classes according to the saturated vapor line slope in the T-s diagram [92]. So accordingly, an isentropic fluid has got an infinite slope; a dry fluid possesses a positive slope whereas a wet fluid possesses a negative slope.

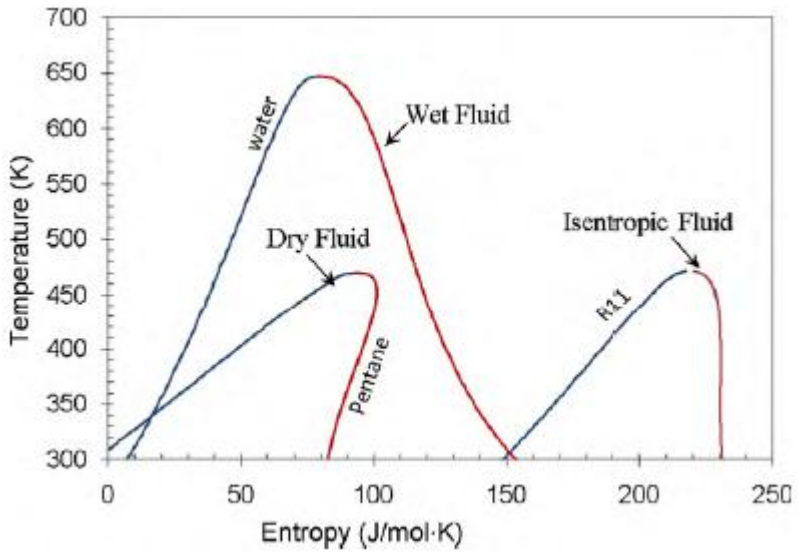


Figure 4.11 T-s diagram of the three main categories of working fluids [93]

Isentropic or dry fluids can be recommended for ORC to prevent vapor condensation in the turbine blades while in expansion phase. Moreover, the fluid also shouldn't be too dry. Dry fluids are emitted out of the turbine with larger superheat that demands an additional processing in the condenser. Wet fluids demand higher inlet temperature to avoid two phase regions. Moreover, according to a data found on screening of working fluids as in [92] examples for the three categories of working fluids are given below.

a) Wet fluids; R-170, R-744, R-41, R-23, R-116
b) Isentropic fluids; R-141b, R-123, R- 123, R-21, R-25ca, R-245fa, R-236ea.
c) Dry fluids; R-601, R-600, R-600a, R-C318 etc.

4.2.3 Working Fluids Properties

4.2.3.1. Thermodynamic properties

These include heat transfer capability, specific heat, latent heat, critical point and fluid density. Working fluids that possess satisfactory density; reduced liquid specific heat and so on can be presumed to offer greater outcomes.

4.2.3.2 Safety and Environmental Criteria's

Water as a working fluid doesn't create any threat to the environment being non-poisonous, non - flammable, chemically stable, possesses zero ODP and zero

GWP. However, more organic working fluids aren't environment friendly as they have got a considerable ODP and GWP. Certain organic working fluids possess a tendency of high toxicity as well as high flammability.

Safety: The ASHRAE (American Society of Heating Refrigerating and Air conditioning Engineers) refrigerant safety categorization demonstrates the fluids extent of hazardousness. The safety status of an organic working fluid can be analyzed by three main criteria's; toxicity, flammability and chemical stability. Properties such as non-corrosively, non – flammability, and non – toxicity are desirable. ASHRAE 34 Classification is used for gauging the safety level of a working fluid. The table below illustrates the safety categorization of working fluids.

Table 4.4 Safety categorization of working fluids [74]

Flammability	Low toxicity	High toxicity
High	A3	B3
Low	A2	B2
Non- flammable	A1	B1

Table 4.5 demonstrates the safety classification of organic fluids as per ASHRAE [74]. From this table the letter A represents when the working fluid possesses lower toxicity, whereas the letter B represents when the working fluid has higher toxicity. The flame propagation of the working fluid is represented by the numbers from 1 to 3. If the flame propagation reaches 3, it determines that the working fluid is of a higher flammability potential and if the number is 2 it shows lower flammability potential, whereas if the flame propagation number becomes 1, it refers to a working fluid with zero flammability potential.

Environmental aspects: The basic issues worth mentioning of environmental aspects are Global warming potential (GWP) and Ozone depletion potential (ODP). The ODP as well as GWP reflect the medium's tendency of influencing

the Ozone layer depletion and global warming. For these reasons fault many working fluids the likes of R-11, R-12, R-113 and so on are currently getting expelled from consideration. Moreover, some mediums like R-21, R-22, and R-123 etc. will be phased out in the coming years.

GWP: indicates to the global warming that is induced by a specific working fluid relative to CO_2 for a 100-year time reference. It contrasts the capability of a various gases that are assumed to be contributing to accumulate heat in the atmosphere.

ODP: is a technical amount indicating to the capability of a material to deplete the ozone gas layer in relative to chloro fluorocarbon-11, R-11(CF –11). R11 has an ODP value of one, whereas various CFCs and HCFCs obtain an ODP value spreading from 0.01 to 1. For screening working fluids, ODP is a crucial criterion deserving a required attention. So, a working fluid need to have a very low ODP to be chosen or used.

Higher molecular weight of a working fluid makes the ORC system compact in size. The organic working fluid R245fa has got high molecular weight with low GWP and zero ODP, which makes the working fluid convenient for ORC application.

Table 4.5 Working fluid candidates for the engine exhaust gas waste heat recovery [95]

Working fluid	Molecular weight (g/mol)	Normal boiling point(K)	Critical Temperature(K)	Critical Pressure(Kpa)	GWP	ODP	ASHRAE 34[a]
Cyclohexane	84.16	353.9	553.6	4075.0	Low	0	A3
Benzene	78.11	353.2	562.1	4894.0	Low	0	B2
Toluene	92.14	383.8	591.8	4126.0	Low	0	A3
Nonane	128.26	423.9	594.6	2281.0	Low	0	A3
Decane	142.28	447.3	617.7	2103.0	Low	0	A3

4.2.4 Theoretical Analysis of ORC System

An ORC has components not much different from the conventional Rankine Cycle. These include, pump, evaporator, condenser and turbine for expansion (see figure 4.3). Both of these cycles have got the same working principles, the main variance being the working fluid utilized in the operation. The four main operations of an ideal ORC, to perform one cycle are presented as follows;

a) Compression process; in this stage the fluid that has been saturated into liquid phase in the condenser is pumped isentropically as shown in fig 4.3 to the evaporator.

b) Heat addition; this action is performed in the evaporator. The heat transformation from the exhaust gases of the engine to the working fluid makes

the working fluid to gain (accumulate) thermal energy that is enough to evaporate the working fluid from liquid state into vapor state.

C) Expansion; expansion of the evaporated fluid that has attained a certain amount of energy takes place in the turbine of the ORC. The kinetic energy developed by the expansion of the fluid is transformed into mechanical energy by the turbine blades. From this the energy can be carried in different forms for various applications.

d) Heat rejection; in the ORC as in many other WHRs, heat is rejected in the condenser. The working fluid after expansion has lost its energy and quality. So it has to be condensed to liquid state before it goes into the evaporator.

4.2.5 Properties of Working Fluids Applied in the Current Investigation

It is very imperative to understand the unique properties of the working fluids that are selected in this thesis.

4.2.5.1 Steam (R718)

In water the critical point occurs at around 647k and 22.064 MPa. In the vicinity of the critical point the physical properties of the liquids and the vapor change dramatically, with both phases becoming even more similar. According to information taken from NASA [96] water vapor (steam) is the most abundant and powerful greenhouse gas in Earth's atmosphere, yet the GWP has not been quantified in the literature.

4.2.5.2 R245fa ($C_3H_3F_5$ 1, 1, 1, 3, 3- Penta flouro propane)

R245fa is one of HFCs, which is utilized for various technologies, one of which is as a working fluid for ORCs. Its normal boiling point is 288.05 K and its critical temperature is 427 K. This fluid has a GWP value of 950 [96]. Its value of ODP is zero. This fluid is non-flammable as well as approximately non-toxic. Chemically it has a property of non- biodegradability.

4.2.5.3 RC318: (C_4H_4 Octaflouro cyclobutane)

This fluid has lower critical temperature of 388.38 K as compared to R245fa and has a GWP value of 10250.

The property of the working fluids selected for this thesis is summarized in table 4.8 below.

Table 4.6 Properties of working fluids used in the current investigation [97]

Working fluid	Molecular weight (g/mol)	Normal boiling point(K)	Critical temperature (K)	Critical pressure (Kpa)	GWP	ODP	ASHARE 34[a]
Steam	18.05	373.2	647	22.064	<1	0	A1
RC318	200.03	266.18	388.38	2.77	10250	0	A1
R245fa	134.05	288.05	427.2	3.64	950	0	B1

5
Design and Methodology

5.1 Dual Miller Cycle - Organic Rankine Cycle Combination

Figure 5.1 below represents Dual Miller Cycle coupled with Organic Rankine Cycle that is fed waste heat from the DMC's exhaust products.

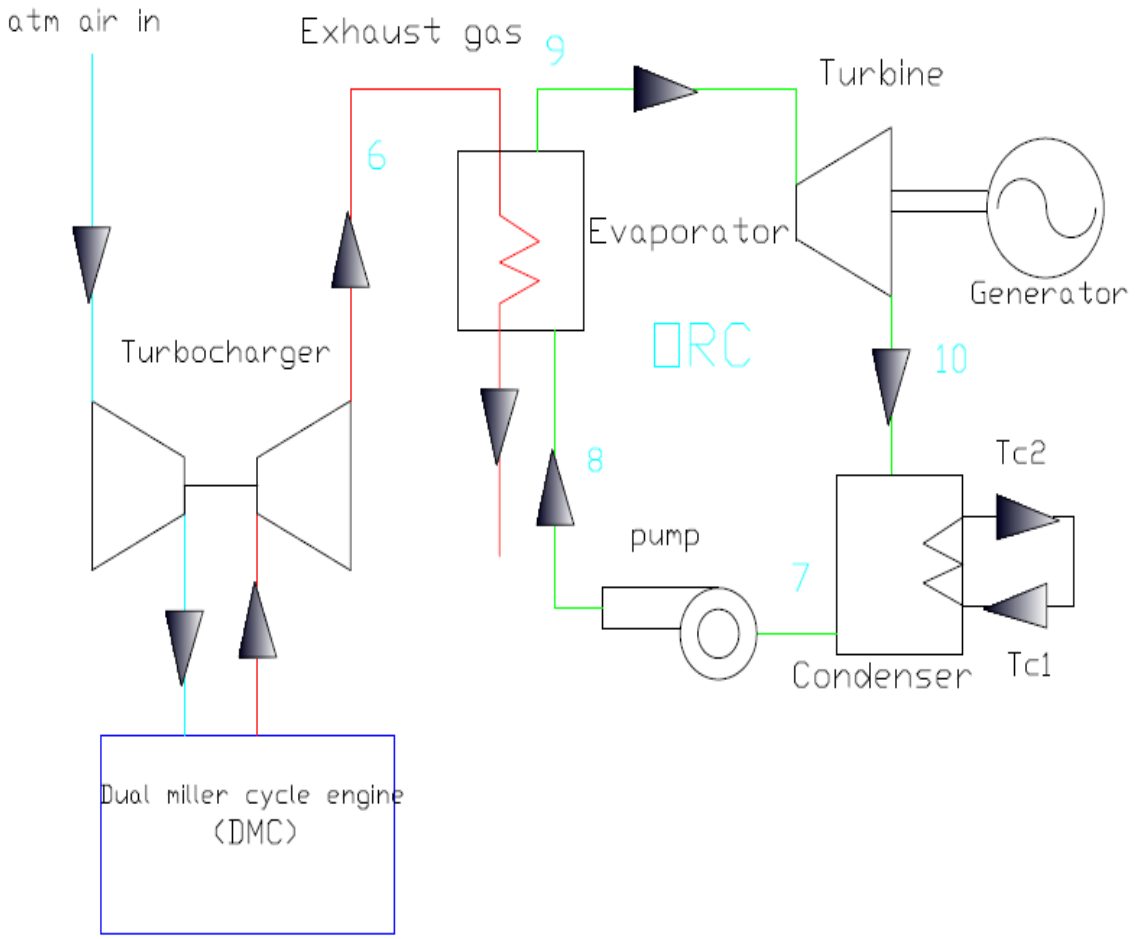


Figure 5.1 Schematic diagram of DMC – ORC combination

5.2 Theoretical Model of Dual Miller cycle Combined with Organic Rankin Cycle

A theoretical thermodynamic model using Engineering Equations Solver (EES) software is implemented to analyze the optimization of Dual Muller - ORC combination. This study presents a comprehensive analysis of DMC with an ORC incorporated to recover a portion of the waste heat. The parameters are analyzed based on the standard dimensions and parameters taken from REFROP 9.0, for a dual cycle marine diesel engine and then converted or modified into Dual Miller cycle as can be referred in table 1. Two organic working fluids used RC318 and R245fa selected based on their appropriateness for the task, plus steam are used. A numerical simulation of effective efficiency, power density, EFECPOD, ECOP, exergetic efficiency and exergy destruction is carried out based on Engineering Equations Solver (EES) software, for the theoretical model.

Table 5. 1 Dual Miller Cycle Engine Parameters [97]

Specification	Value	Unit
Residual gas fraction RGF	5 – 20	%
Engine speed	1000 - 3500	Rpm
Cylinder bore (d)	0.05 – 0.08	m
Stroke length (L)	0.05 – 0.11	m
Intake temperature (T1)	275 – 375	K
Intake pressure (P1)	100 – 200	Kpa
Wall temperature (T.W)	400 – 800	K
Air mass flow rate ($\dot{m}$)	0.01– 0.02	Kg/s
Heat transfer Coefficient (h_{tr})	0.2 – 1	KW/m^2k

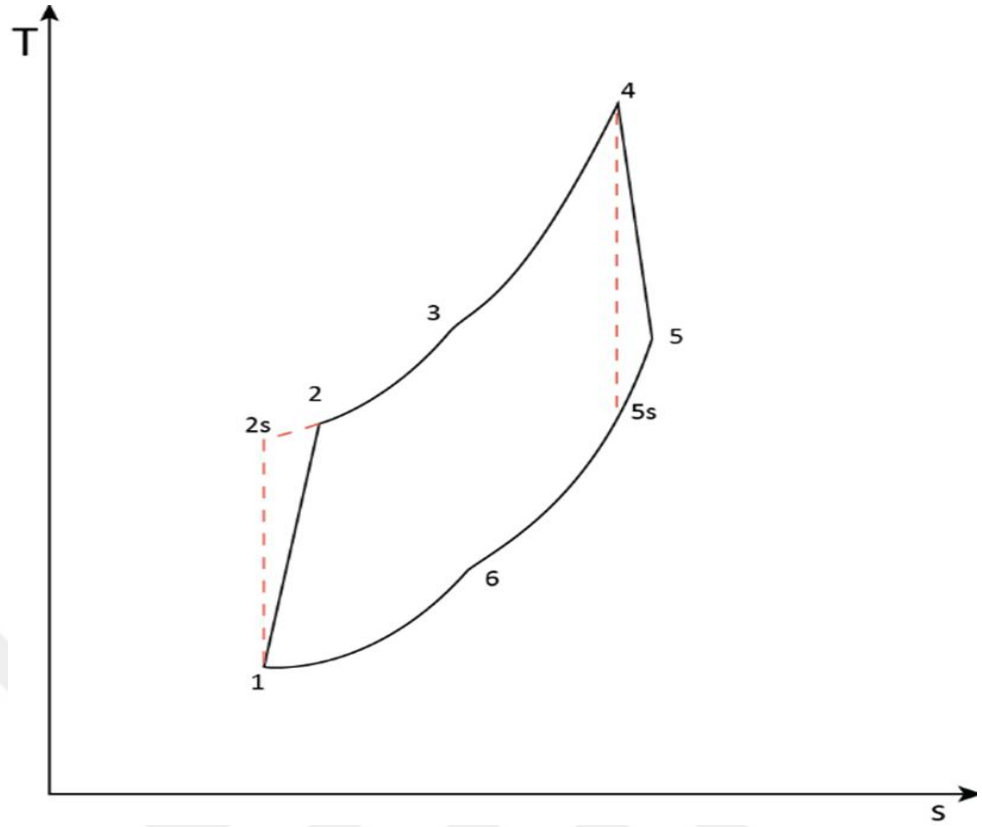


Figure 5.2 T-s diagram of DMC that delivers exhaust to the ORC

In this thesis, necessary criteria's such as EFECPOD,P_{ef}, P_{de}, effective efficiency and energy destruction may be expressed as given below[30]:

$$EFECPOD = \frac{\eta_{ef} P_{ef}}{\frac{T_1}{T_0} \alpha V_T},\ \eta_{ef} = \frac{P_{ef}}{Q_f},\quad P_{ef} = Q_{in} - Q_{out},\ P_d = P_{ef} / V_T \qquad (5.1)$$

Where Q_{in} represents total heat addition, added at two stages namely Q_{in1} the heat supplied at fixed volume (stage 2-3) and Q_{in2} the heat supplied at fixed pressure (3–4) and the aggregate heat rejected Q_{out} is the sum of Q_{out1} the heat rejected at a fixed volume (5–6) and Q_{out2} the heat rejected at a fixed pressure (6-1) could be given as follows:

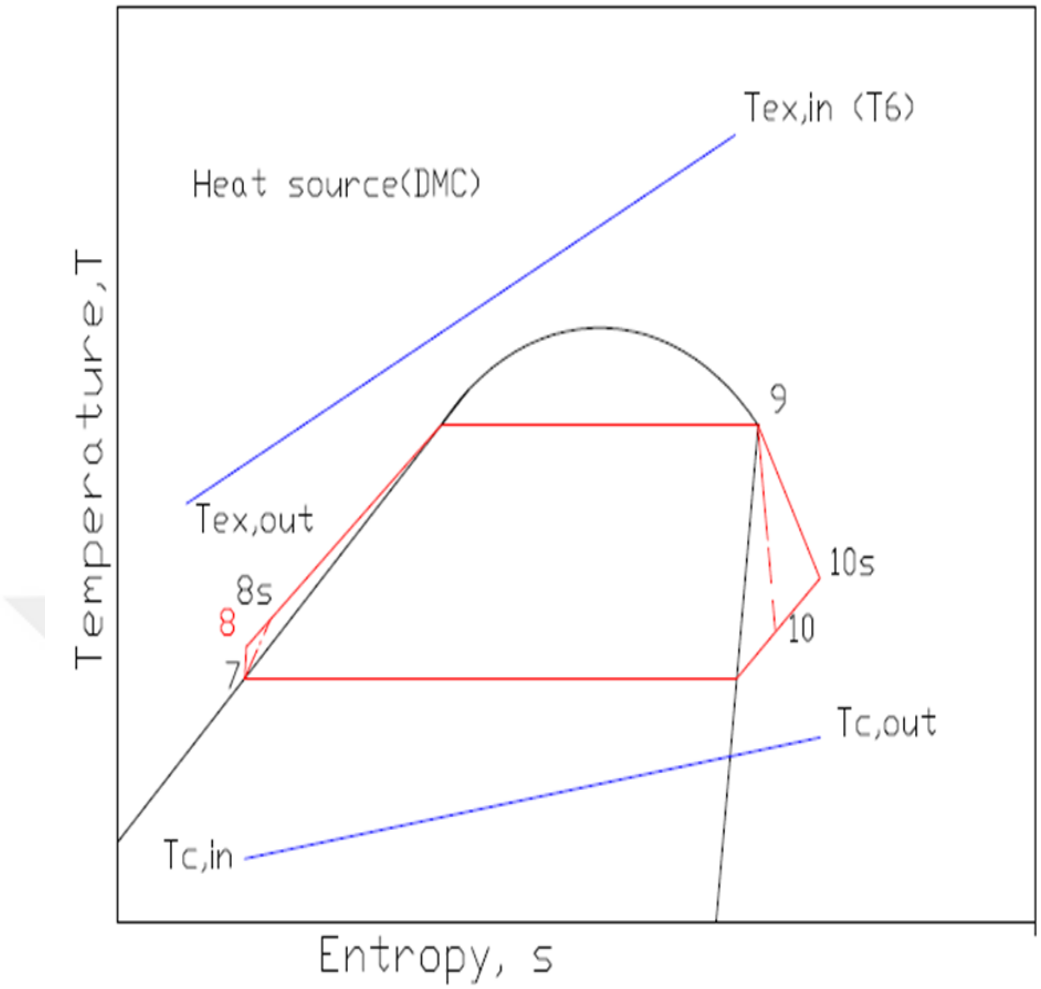


Figure 5.3 T- s diagram of ORC (heat source is DMC engine's exhaust)

$$Q_{in1,DMC} = \dot{m}_T \left[\int_2^3 C_p dT\right] = \dot{m}_T * \left[\left(2.506 * 10^{-11} * \frac{{T_3}^3}{3} + 1.454 * 10^{-7} * \frac{{T_3}^{2.5}}{2.5} - 4.246 * 10^{-7} * \frac{{T_3}^2}{2} + 3.162 * 10^{-5} * \frac{{T_3}^{1.5}}{1.5} + 1.0433 * T_3 - 1.512 * 10^4 * \left(-\frac{{T_3}^{-0.5}}{0.5}\right) + 3.063 * 10^5 * \left(-{T_3}^{-1}\right) - 2.212 * 10^5 * \left(-\frac{{T_3}^{-2}}{2}\right)\right) - \left(2.506 * 10^{-11} * \frac{{T_2}^3}{3} + 1.454 * 10^{-7} * \frac{{T_2}^{2.5}}{2.5} - 4.246 * 10^{-7} * \frac{{T_2}^2}{2} + 3.162 * 10^{-5} * \frac{{T_2}^{1.5}}{1.5} + 1.0433 * T_2 - 1.512 * 10^4 * \left(-\frac{{T_2}^{-0.5}}{0.5}\right) + 3.063 * 10^5 * \left(-{T_2}^{-1}\right) - 2.212 * 10^7 * \left(-\frac{{T_2}^{-2}}{2}\right)\right)\right] \quad (5.2)$$

$$Q_{in2,DMC} = \dot{m}_T \left[\int_3^4 C_p dT\right] = \dot{m}_T \left[\left(2.506 * 10^{-11} * \frac{{T_4}^3}{3} + 1.454 * 10^{-7} * \frac{{T_4}^{2.5}}{2.5} - 4.246 * 10^{-7} * \frac{{T_4}^2}{2} + 3.162 * 10^{-5} * \frac{{T_4}^{1.5}}{1.5} + 1.0433 * T_4 - 1.512 * 10^4 * \left(-\frac{{T_4}^{-0.5}}{0.5}\right) + 3.063 * 10^5 * \left(-{T_4}^{-1}\right) - 2.212 * 10^5 * \left(-\frac{{T_4}^{-2}}{2}\right)\right) - \left(2.506 * 10^{-11} * \frac{{T_3}^3}{3} + 1.454 * 10^{-7} * \frac{{T_3}^{2.5}}{2.5} - 4.246 * 10^{-7} * \frac{{T_3}^2}{2} + 3.162 * 10^{-5} * \frac{{T_3}^{1.5}}{1.5} + 1.0433 * T_3 - 1.512 * 10^4 * \left(-\frac{{T_3}^{-0.5}}{0.5}\right) + 3.063 * 10^5 * \left(-{T_3}^{-1}\right) - 2.212 * 10^7 * \left(-\frac{{T_3}^{-2}}{2}\right)\right)\right] \quad (5.3)$$

$$Q_{in,\,DMC} = Q_{in1,\,DMC} + Q_{in2,\,DMC} \quad (5.4)$$

$$Q_{out1,\ DMC} = \dot{m}_T \left[\int_6^5 C_p dT\right] = \dot{m}_T \left[\left(2.506 * 10^{-11} * \frac{{T_5}^3}{3} + 1.454 * 10^{-7} * \frac{{T_5}^{2.5}}{2.5} - 4.246 * 10^{-7} * \frac{{T_5}^2}{2} + 3.162 * 10^{-5} * \frac{{T_5}^{1.5}}{1.5} + 1.0433 * T_5 - 1.512 * 10^4 * \left(-\frac{{T_5}^{-0.5}}{0.5}\right) + 3.063 * 10^5 * \left(-{T_5}^{-1}\right) - 2.212 * 10^5 * \left(-\frac{{T_5}^{-2}}{2}\right)\right) - \left(2.506 * 10^{-11} * \frac{{T_6}^3}{3} + 1.454 * 10^{-7} * \frac{{T_6}^{2.5}}{2.5} - 4.246 * 10^{-7} * \frac{{T_6}^2}{2} + 3.162 * 10^{-5} * \frac{{T_6}^{1.5}}{1.5} + 1.0433 * T_6 - 1.512 * 10^4 * \left(-\frac{{T_6}^{-0.5}}{0.5}\right) + 3.063 * 10^5 * \left(-{T_6}^{-1}\right) - 2.212 * 10^7 * \left(-\frac{{T_6}^{-2}}{2}\right)\right)\right] \quad (5.5)$$

$$Q_{out2,\ DMC} = \dot{m}_T \left[\int_1^6 C_p dT\right] = \dot{m}_T \left[\left[2.506 * 10^{-11} * \frac{{T_6}^3}{3} + 1.454 * 10^{-7} * \frac{{T_6}^{2.5}}{2.5} - 4.246 * 10^{-7} * \frac{{T_6}^2}{2} + 3.162 * 10^{-5} * \frac{{T_6}^{1.5}}{1.5} + 1.0433 * T_6 - 1.512 * 10^4 * \left(-\frac{{T_6}^{-0.5}}{0.5}\right) + 3.063 * 10^5 * \left(-{T_6}^{-1}\right) - 2.212 * 10^7 * \left(-\frac{{T_6}^{-2}}{2}\right)\right] - \left[2.506 * 10^{-11} * \frac{{T_1}^3}{3} + 1.454 * 10^{-7} * \frac{{T_1}^{2.5}}{2.5} - 4.246 * 10^{-7} * \frac{{T_1}^2}{2} + 3.162 * 10^{-5} * \frac{{T_1}^{1.5}}{1.5} + 1.0433 * T_1 - 1.512 * 10^4 * \left(-\frac{{T_1}^{-0.5}}{0.5}\right) + 3.063 * 10^5 * \left(-{T_1}^{-1}\right) - 2.212 * 10^7 * \left(-\frac{{T_1}^{-2}}{2}\right)\right]\right] \quad (5.6)$$

$$Q_{out,\ DMC} = Q_{out1,\ DMC} + Q_{out2,\ DMC} \quad (5.7)$$

Where T_0 represents ambient temperature, T_1 stands for a temperature at the start of compression and 'α' stands for cycle temperature ratio which can be calculated as follows:

$$\alpha = \frac{T_{\max}}{T_{\min}} = \frac{T_4}{T_1} \tag{5.8}$$

Compression ratio (r), pressure ratio (β), cut-off ratio (r_o), cycle pressure ratio (λ), stroke ratio (ε) and miller ratio (r_M) are used in the analysis and they could be described as:

$$r = \frac{V_1}{V_2} \tag{5.9}$$

$$\beta = \frac{P_3}{P_2} = \frac{T_3}{T_2} \tag{5.10}$$

$$r_0 = \frac{V_4}{V_3} = \frac{T_4}{T_3} \tag{5.11}$$

$$\lambda = P_{\max} / P_{\min} = P_4 / P_1 \tag{5.12}$$

$$\varepsilon = V_6 / V_2 \tag{5.13}$$

$$r_M = V_6 / V_1 = T_6 / T_1 \tag{5.14}$$

and in terms of crank angle (θ_r)

$$r_M = \frac{180}{180 - \theta_r} \tag{5.15}$$

Where $\dot{Q}_f$ represents sum of heat potential of the supplied fuel and is given as below:

$$\dot{Q}_f = \dot{m}_f H_u \tag{5.16}$$

H_u being lower heat value (LHV). $\dot{m}_f$ the rate of mass (kg/s) and it can be expressed as follows:

$$\dot{m}_f = \frac{m_f z}{60} \tag{5.17}$$

Where Z is the engine angular speed in rpm, m_f, represents fuel mass per cycle (kg) where as A_{sur}, the heat transfer surface area are calculated as below:

$$m_f = m_a \phi F_{st} \tag{5.18}$$

$$A_{sur} = \pi * d * L\left[\frac{r}{r-1}\right] + \frac{\pi d^2}{2} \tag{5.19}$$

As d stands for cylinder bore and ϕ is equivalence ratio. m_a and F_{st} are air mass per cycle and stoichiometric fuel - air ratio. Their formulas can be presented as below.

$$F_{st} = \frac{\xi \cdot (12.01 * \alpha + 1.008 * \beta + 16 * \gamma + 14.01 * \delta)}{28.85} \tag{5.20}$$

Where α,β,γ and δ represent atomic numbers of carbon, hydrogen, oxygen and nitrogen in the fuel used respectively. ξ is a molar fuel – air ratio and is given as follows[98]:

$$\xi = \frac{0.21}{\alpha - \frac{\gamma}{2} + \frac{\beta}{4}} \tag{5.21}$$

$$Vol_T = Vol_s + Vol_0 = \pi \frac{d^2}{4} * L + \frac{\pi \frac{d^2}{4} * L}{r-1} = \pi \frac{d^2}{4} * L\left(\frac{r}{r-1}\right) \tag{5.22}$$

Where Vol_T is the total volume of the combustion space, Vol_s is the displacemnt volume or stroke volume and Vol_o is the volume of the clearance space above the the piston when the piston is at TDC.

$$Vol_T = r * Vol_0 \tag{5.23}$$

$$Vol_s = (r-1) * Vol_0 \tag{5.24}$$

$$Vol = \frac{\pi \frac{d^2}{4} L}{r_M} \tag{5.25}$$

Vol_s is the displacement volume or stroke volume.

$$m_a = \pi \frac{d^2}{4} L \rho_a = \rho_a V_a = \rho_a \left(Vol + Vol_0 \right) = \rho_a \left(Vol_T - V_{rg} \right) \tag{5.26}$$

Or

$$m_a = m_{mix} * \left(1 - RGF\right) = \rho_a * Vol * \left(1 - RGF\right) \tag{5.27}$$

Where Vol and V_{rg} are actual displaced volume during operation and residual gas volume in the engine respectively

$$m_{mix} = m_a + m_f \tag{5.28}$$

$$m_{rg} = \left(m_a + m_f \right) * RGF = m_{mix} * RGF \tag{5.29}$$

$$m_{rg} = \rho_{rg} * V_{rg} \tag{5.30}$$

$$\dot{m}_{rg} = \frac{m_{rg} z}{60} \tag{5.31}$$

$$T_{TM} = \frac{\dot{m}_a T_1 R_a + \dot{m}_a T_1 R_{rg}}{\dot{m}_a R_a + \dot{m}_{rg} R_{rg}} \tag{5.32}$$

Where T_{TM} is the temperature of the total mixture including the residual gas, m_{rg} and $\dot{m}_{rg}$ are mass of residual gas per cycle(kg) and rate of mass of residual gas(kg/s). ρ_a and ρ_{rg} represent densities of air and residual gas respectively and may be described by the following functions.

R_a and R_{rg} are the ideal gas constants of air and residual gas respectively. The value of these constants is 0.287 $^{kJ}/_{kg}$. RGF is residual gas fraction. ρ_a may be described by the following function:

$$\rho_a = \text{f}\ (T_1,\ P_1\ )$$

$$\rho_{rg} = \text{f}\,(T_{TM}, P_1)$$

Where T_1 *and* P_1 are intake temperature and pressures. The alphabet f denotes for a function and the fucntional values are determined from EES software [99].

$$\dot{m}_a = m_a * \frac{z}{120} \tag{5.33}$$

where $\dot{m}_a$ is the rate of air suction in to the cylinder and z is the crankshaft rotational speed in rpm. $\dot{m}_T$ stands for total mass rate of the mixture charge in the cylinder ready for combustion that is calculated as follows:

$$\dot{m}_T = \dot{m}_a + \dot{m}_f + \dot{m}_{rg} = \dot{m}_f \left(1 + F_s/\phi\right) + \dot{m}_{rg} \tag{5.34}$$

The input rate of total heat energy in the heat addition process is given below

$$Q_T = \dot{m}_f\, Q_{LHV} \tag{5.35}$$

$$Qfuel_c = \eta_{com} * \dot{m}_f * Q_{LHV} \tag{5.36}$$

Where η_{com} is the combustion efficiency and $Qfuel_C$ is the actual heat produced during the combustion process.

$$\eta_{com} = \text{-}1.44738 + 4.18581/\phi \text{ - } 1.86876/\phi^2 \tag{5.37}$$

ϕ is an equivalence ratio calculated as follows

$$\phi = \frac{m_f/m_a}{F_s} \tag{5.38}$$

where m_a is air mass per cycle(kg)

$$Qht_c = h_{tr2} A * \left[\frac{\frac{T_2 + T_4}{2} - T_w}{1000} \right] \tag{5.39}$$

$$h_{tr2} = 130 Vol_T^{-0.05} \cdot \left[\frac{P_1}{100}\right]^{0.8} \cdot T_1^{-0.4} \cdot \left(v + 1.4\right)^{0.8} \tag{5.40}$$

Where $\frac{T_2+T_4}{2}$, is in cylinder mean temperature, h_{tr2} is heat transfer coefficient and T_w is cylinder wall temperature.

$$Q_{in} = Qfuel_c - Qht_c \tag{5.41}$$

Where Qht_c is the heat transfer to into the cylinder wall, P_{out} is the actaul power output and can bcalculated from the system as follows:

$$P_{out,\ DMC} = Qfuel_c - Qht_c - Q_{out,DMC} - \text{Pu} \tag{5.42}$$

Pu is the energy lost due to friction and is calculated as

Pu = $\mu * \bar{s}^2$, where μ coefficient of friction of the mating parts and $\bar{s}$ is the mean piston speeed of the DMC engine.

$$\bar{s} = 4*L*N \tag{5.43}$$

$$N = \frac{z}{120} \tag{5.44}$$

$$\eta_{ef,\ DMC} = \frac{P_{out,\ DMC}}{Qfuel} 100 \tag{5.45}$$

$$DL = \frac{d}{L} \tag{5.46}$$

Where "DL" is the bore to stroke ratio of a cylinder dimensions, d and L standing for bore and stroke length of the cylinder.

$$T_{2S1} = \frac{T_{2S} - T_1}{\ln\left(\frac{T_{2S}}{T_1}\right)} \tag{5.47}$$

$$T_{5S4} = \frac{T_4 - T_{5S}}{\ln\left(\frac{T_4}{T_{5S}}\right)} \tag{5.48}$$

C_p and C_v are specific heat at constant pressure and specific heat at constant volume respectively. They varie with temperature variation. From a temperature of 300 K – 3500 K, they may be calculated as follows [98]:

$$C_p = 2.506^{*}\ 10^{-11} * T^2 + 1.454^{*}10^{-7}{*}\ T^{1.5} - 4.246^{*}10^{-7}{*}\mathrm{T} + 3.162^{*}10^{-5} {*}T^{0.5} + 1.3303\text{-}1.512^{*}\ 10^4\ *\ T^{-1.5} + 3.063^{*}10^5{*}\ T^{-2} - 2.212^{*}10^7\ T^{-3} \quad (5.49)$$

$$C_v = C_p - \mathrm{R} \quad (5.50)$$

$$C_{p6} = 2.506^{*}\ 10^{-11} * T_6^{\,2} + 1.454^{*}10^{-7}{*}\ T_6^{\,1.5} - 4.246^{*}10^{-7}{*}T_6 + 3.162^{*}10^{-5} {*}T_6^{\,0.5} + 1.3303\text{-}1.512^{*}\ 10^4\ *\ T_6^{\,-1.5} + 3.063^{*}10^5{*}\ T_6^{\,-2} - 2.212^{*}10^7\ T_6^{\,-3} \quad (3.51)$$

The equations for reversible adiabatic processes (1 – 2s) and (5 – 6s) are descirbed below:

$$C_{v1} = 2.506^{*}\ 10^{-11} * T_{2s1}^{\,2} + 1.454^{*}10^{-7}{*}\ T_{2s1}^{\,1.5} - 4.246^{*}10^{-7}{*}T_{2s1} + 3.162^{*}10^{-5} {*}T_{2s1}^{\,0.5} + 1.3303\text{-}1.512^{*}\ 10^4\ *\ T_{2s1}^{\,-1.5} + 3.063^{*}10^5{*}\ T_{2s1}^{\,-2} - 2.212^{*}10^7\ T_{2s1}^{\,-3} \quad (5.52)$$

$$C_{v2} = 2.506^{*}\ 10^{-11} * T_{5s4}^{\,2} + 1.454^{*}10^{-7}{*}\ T_{5s4}^{\,1.5} - 4.246^{*}10^{-7}{*}T_{5s4} + 3.162^{*}10^{-5} {*}T_{5s4}^{\,0.5} + 1.3303\text{-}1.512^{*}\ 10^4\ *\ T_5^{\,-1.5} + 3.063^{*}10^5{*}\ T_{5s4}^{\,-2} - 2.212^{*}10^7\ T_{5s4}^{\,-3} \quad (5.53)$$

$$C_{v1} \ln\frac{T_{2S}}{T_1} = RR * \ln(r) \quad (5.54)$$

$$C_{v2} \ln\frac{T_{5S}}{T_4} = RR * \ln\left(\frac{\rho}{r * r_M}\right) \quad (5.55)$$

for irreversible conditions T_2 and T_5 can be found from the relations below:

$$\eta_c = \frac{T_{2S} - T_1}{T_2 - T_1} \quad (5.56)$$

$$\eta_e = \frac{T_4 - T_5}{T_4 - T_{5S}} \quad (5.57)$$

Where η_C and η_e are compression efficiency and expansion stroke efficiency of the DMC respectively.

$$V_2 = \frac{V_1}{r} \quad (5.58)$$

$$v_5 = v_6 \tag{5.59}$$

$$\eta_{ef\,,\,DMC} = \frac{P_{out,\,DMC}}{Qfuel} 100 \tag{5.60}$$

$$P_{de,\,DMC} = \frac{P_{out,\,DMC}}{V_T} \tag{5.61}$$

$$Xdest_{tot,\,DMC} = \left(Ex_{tot,\,DMC} - P_{out,\,DMC} \right) \tag{5.62}$$

$$ECOP_{DMC} = 100 \left(\frac{P_{out,\,DMC}}{Xdest_{tot,\,DMC}} \right) \tag{5.63}$$

$$EFECPOD_{DMC} = \left(\frac{\eta_{ef\,,\,DMC} * P_{de,\,DMC}}{\alpha * \frac{T_1}{T_0}} \right) \tag{5.64}$$

Exergic efficiency for the DMC engine is given as :

$$\varepsilon_{DMC} = \frac{Qfuel_{ex,\,DMC} - Xdest_{tot,\,DMC}}{Qfuel_{ex,\,DMC}} 100 \tag{5.65}$$

$$\varepsilon_{DMC} = 100 \left(\frac{P_{out,\,DMC}}{Qfuel_{ex,\,DMC}} \right) \tag{5.66}$$

$$Qfuel_{ex,\,DMC} = \psi * m_f \tag{5.67}$$

Where ψ is the specific energy of the fuel (octane) and $Qfuel_{ex,DMC}$ is the total energy input delivered to the engine.

$$V_T = v_6 * m_T \tag{5.68}$$

Where v_7 is the maximum specific volume at point 7.

When the effect of ORC is combined with DMC , the performance parameters can be described as follows:

$$m_{Turb} = \left(\frac{60 * \dot{m}_{Turb}}{N_{Turb}} \right) \tag{5.69}$$

$$W_p = v_7 * \left(P_8 - P_7\right) \tag{5.70}$$

Where W_p is work done by the pump of the ORC, and v_8 is specific volume of working fluid of the ORC at point 8 represents enthalpy and the enthalpies of the ORC are given as follows.

$$h_8 = h_7 + W_p \tag{5.71}$$

$$P_8 = P_9 \tag{5.72}$$

$$P_6 = P_9 \tag{5.73}$$

$$T_8 = T_6 - dT_B \tag{5.74}$$

$$T_9 = T_6 - dT_A \tag{5.75}$$

Where dT_A and dT_B are change in temperatures as shown in the formulas

$$Q_{in,ORC} = \dot{m}_{Turb} \cdot (h_9 - h_8) \tag{5.76}$$

$$Q_{in,ORC,s} = \dot{m}_{Turb} * (h_9 - h_{8s}) \tag{5.77}$$

Where $Q_{in,ORC}$ is the heat added to the ORC system from the exhaust gases of DMC engine.

$$W_{Turb} = h_9 - h_{10} \tag{5.78}$$

Where W_{Turb} is work done by the turbine of the ORC, h_9 and h_{10} are enthalpies at points 9 and 10 respectively. Power developed by the Turbine of the ORC can be derived from the work done as follows:

$$P_{Turb} = \dot{m}_{Turb} \cdot W_{Turb} \tag{5.79}$$

η_{ORC} is thermal efficiency of the ORC.

$$\eta_{T,ORC} = \frac{h_9 - h_{10s}}{h_9 - h_{10}} \tag{5.80}$$

$$\eta_{C,ORC} = \frac{h_8 - h_7}{h_{8s} - h_7} \tag{5.81}$$

Where $\eta_{C,ORC}$ and $\eta_{T,ORC}$ are thermal efficiencies of the compressor and turbine of the ORC.

$$W_{Turb,s} = h_9 - h_{10s} \tag{5.82}$$

$$P_{Turb,s} = \dot{m}_{Turb} \cdot W_{Turb,s} \tag{5.83}$$

Thermal efficiency of the ORC, $\eta_{th,ORC}$ can be determined from equations (5.77) and (5.83) as follows

$$\eta_{th,\,ORC} = \frac{P_{Turb,s}}{Q_{in,\,ORC}} = \left(\frac{h_9 - h_{10s}}{h_9 - h_{8s}} \right) \tag{5.84}$$

$$P_{ef\,,\,DMC-ORC} = P_{out,\,DMC} + P_{Turb,\,s} \tag{5.85}$$

$$P_{de,\,DMC-ORC} = \frac{P_{ef\,,\,DMC-ORC}}{V_T} \tag{5.86}$$

$$Xdest_{tot,DMC-ORC} = Ex_{tot} - P_{ef\,,DMC-ORC} \tag{5.87}$$

$$\varepsilon_{\,DMC-ORC} = \frac{P_{ef\,,\,DMC-ORC}}{Qfuel_{ex}} \cdot 100 \tag{5.88}$$

$$\eta_{ef\,,\,DMC-ORC} = \frac{P_{ef\,,\,DMC-ORC}}{Qfuel} \cdot 100 \tag{5.89}$$

$$ECOP_{DMC-ORC} = \frac{P_{ef\,,\,DMC-ORC}}{Xdest_{tot,\,DMC-ORC}} \cdot 100 \tag{5.90}$$

$$EFECPOD_{DMC-ORC} = \frac{\eta_{ef\,,DMC-ORC} * P_{de,DMC-ORC}}{\frac{T_1}{T_0} * \alpha} \tag{5.91}$$

6
Results and Discussions

6.1 Analysis of and Synthesis of Combined Dual Miller Cycle – Organic Rankine Cycle

In this chapter the results and discussions of the theoretical model are presented supported by the plotted figures of various parameters.

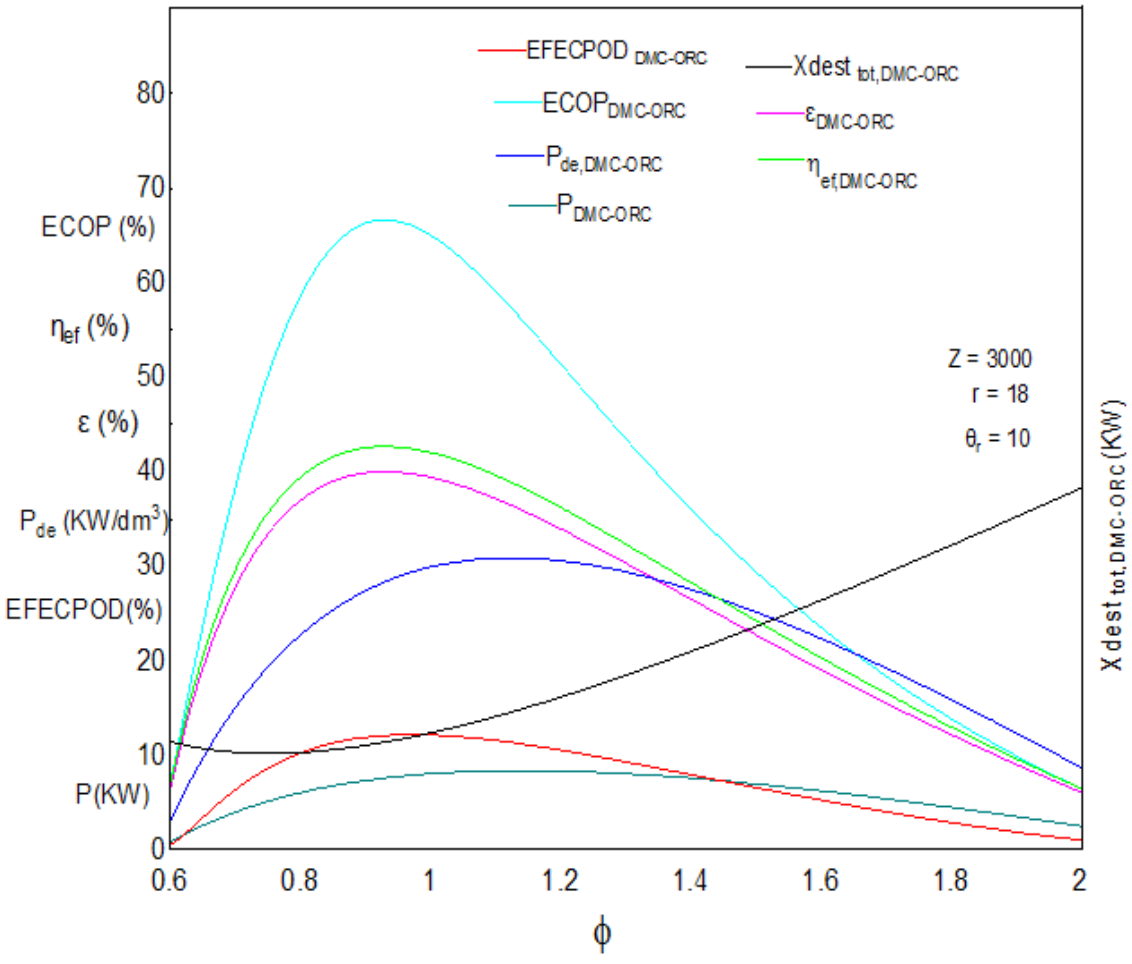


Figure 6.1 DMC – ORC parameters performance at variable equivalence ratio

Figure 6.1 indicates just the general figurative overview of performances recorded by a DMC-ORC plant. However, these values will be further discussed in terms of comparison with the values of DMC plant viewed in the same figure

from the respective parameters lines running side by side as is shown in figure 6.2.

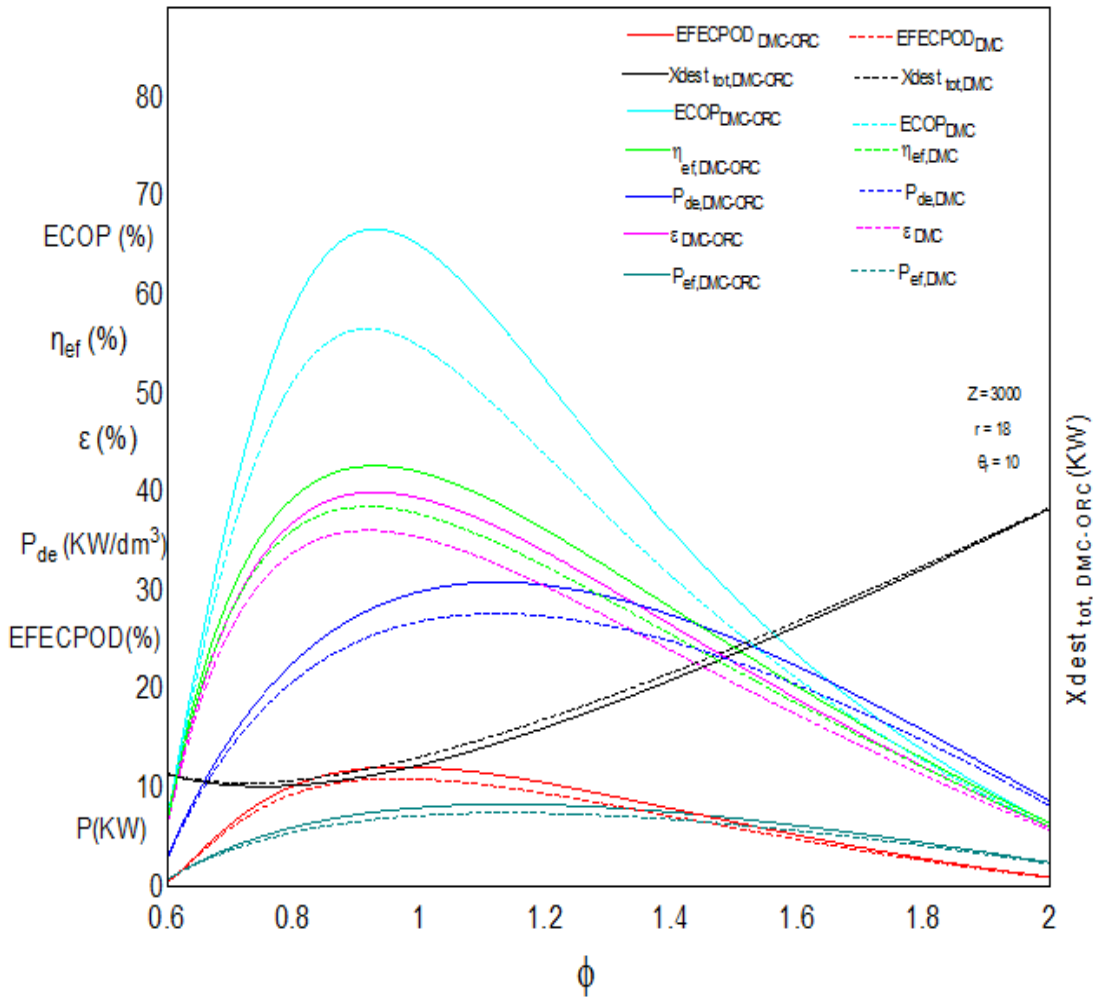


Figure 6.2 Comparison of Dual Miller Cycle versus Dual Miller Cycle – Organic Rankine Cycle parameters performance at variable equivalence ratio (ϕ)

Figure 6.2 demonstrates the engine parameters performance comparison at variable equivalent ratio (0.6-2) but at constant compression ratio (r) and crank angle(θ_r) between DMC and DMC–ORC engines. The medium employed here is steam. In almost all engine parameters comparisons, DMC – ORC engine showed a better and enhanced performance as opposed to DMC. In the DMC–ORC, ECOP reached up to a maximum level of 65% at ϕ=0.93 (which is the optimum equivalence ratio). It shows a boom with a steep slope from a value of around 7% (ϕ=0.6) to a level of 65% (ϕ=0.93). From this point, it falls down with an

average slope to a result of 7% (ϕ=2). For the DMC part it showed a similar fashion of curve, but at a lesser amount for most of the ranges, starting from an ECOP value of 7% at ϕ=0.6. The value enhanced dramatically to a value of 55% at ϕ=0.925, which is the maximum point and drops down at a certain slope until it reaches a value of 7% (ϕ=2). From the graph it is evidently depicted that there is a considerable improvement in ECOP, when an ORC is incorporated with a DMC. The increment is very negligible at start (ϕ=0.6). The gap (variance) , dilates or diverges further as equivalence ratio(ϕ) increases, up to a maximum increment of around 10 %, at optimum value of ϕ=0.93. After this point the variance gets on converged and converged as ϕ increases to 2 and ECOP falls down and merges to about 7% for both lines.

Similarly for $\varepsilon_{DMC-ORC}$ graph emerges out from around 7% at ϕ=0.6 and boosts towards the maximum point 36% at around ϕ=0.925 and then flags down at a considerable slope to a value of approximately 7% (ϕ =2). $\varepsilon_{DMC-ORC}$ starts by merging on the same line with ε_{DMC}, then diverges continually as the slope rises up, up to a maximum value of 40% at the peak level, making a variance of around 5% with ε_{DMC} . From this point it declines down again while converging to a value of 7% at ϕ=2. For the DMC-ORC plant, EFECPOD has a similar trajectory as that of DMC, revealing an enhancement of around 0.6% at optimum level. Similarly P_{de} and η_{ef} first increase and then decrease as is visible from the figure, both of them have value increased with the introduction of ORC (in the DMC-ORC plant).

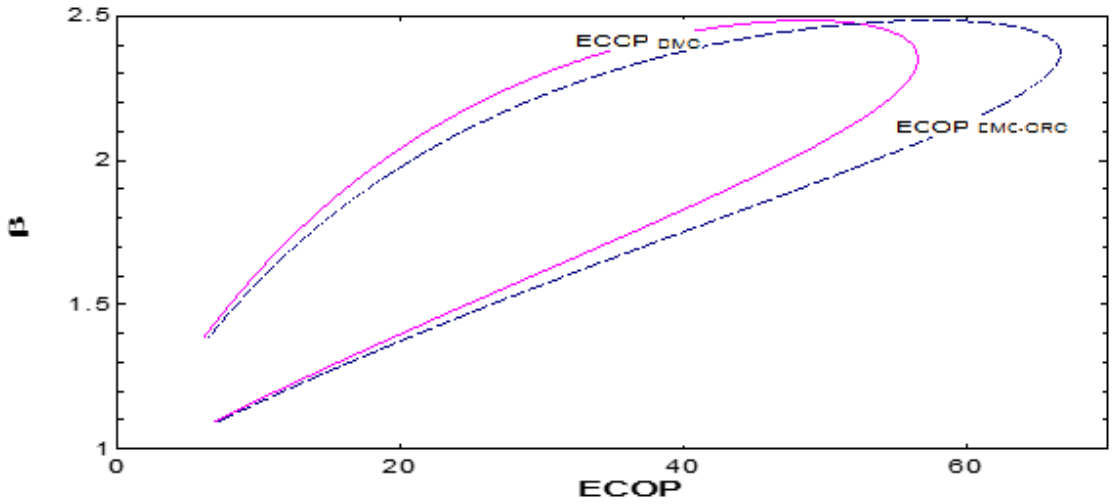


Figure 6.3 Influence of pressure ratio (β) on ecological performance (ECOP)

Fig 6.4 demonstrates the engine parameters performance comparison at variable pressure ratio (β). To start with, ECOP starts from a minimum value of 6.853% at β=1.096 and increases towards a maximum value of 56.55% at β=2.35, which shows clearly the effect of pressure ratio (β) on general and optimal ecological performance. For the combined DMC-ORC part ECOP shows a bit of enhancement from the values recorded at DMC. That is at β=1.096, ECOP is 7.165%, which is 0.312% values more at the minimum stage and then boasts to an optimum value of 66.65% (β=2.372), which is 10.1% value difference from the DMC showing the maximum enhancement at this level. Likewise, P_{de} for the DMC increases from a minimum value of 3 $^{KW}/_{dm^3}$ at β=1.096 to a maximum value of 27.67 $^{KW}/_{dm^3}$ and then drops back to a lowest value of 2.484 $^{KW}/_{dm^3}$ as β increases further. The DMC–ORC in a similar pattern starts from a P_{de} of 3.122 $^{KW}/_{dm^3}$ and boasts to a maximum level of 30.87 $^{KW}/_{dm^3}$ and then bounces back to a minimum value of 2.484 $^{KW}/_{dm^3}$. The EFECPOD for DMC shows an increment to some extent of pressure ratio, and then commences falling with a further increase in pressure ratio, due to the addition of fuel supplied into the cylinder of the ICE. The performance parameters increase as

pressure ratio rises up to a certain extent, after that they decline with further increase in pressure ratio, both in the DMC and DMC-ORC plants.

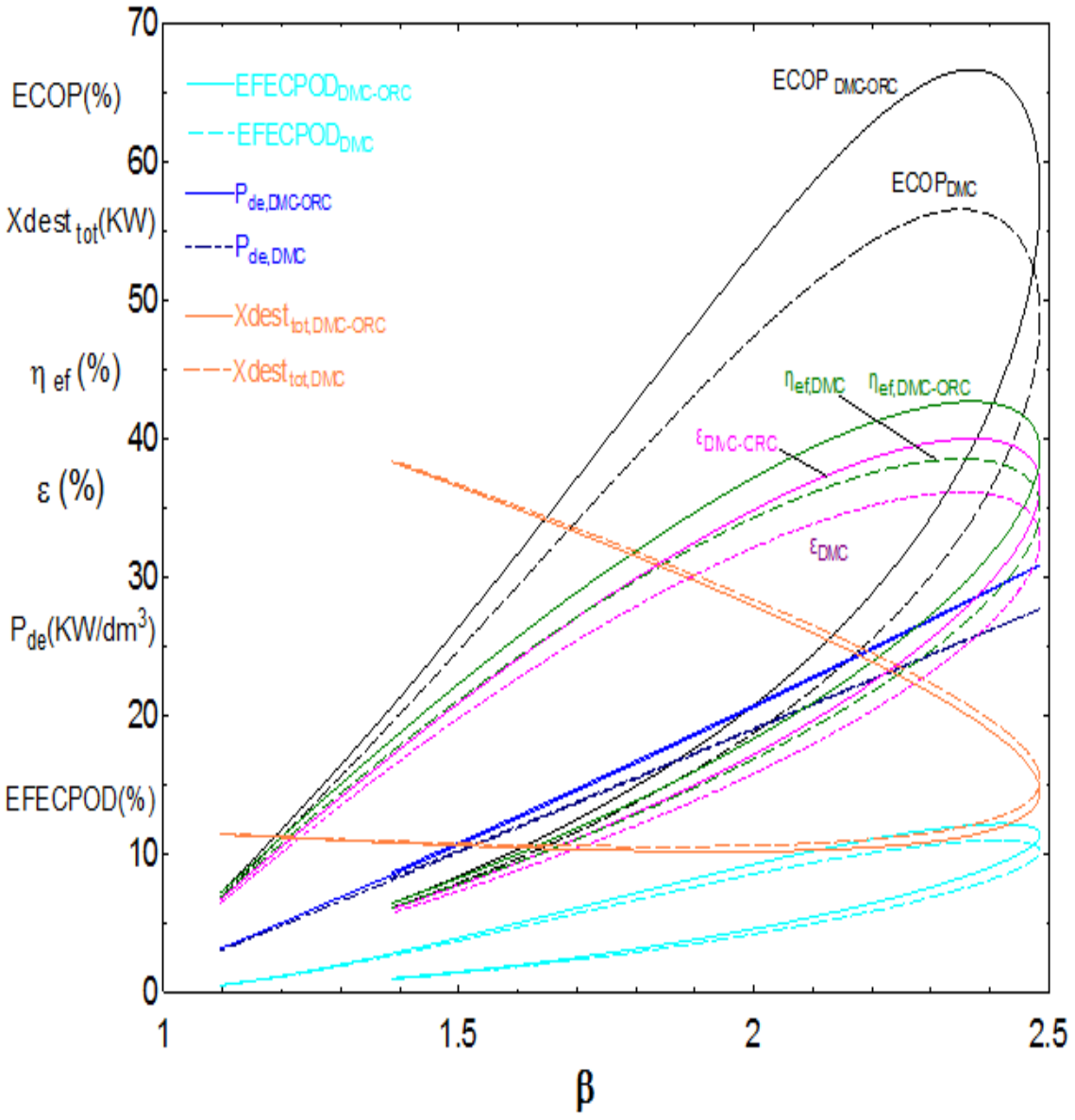


Figure 6.4 Comparison of DMC against DMC- ORC at variable pressure ratio (β).

Figure 6.5 depicts the influence of crank angle (θ_r) over performance parameters at constant starting temperature (T_1) as well as compression ratio(r) with steam as a working fluid. For the DMC part it is evident from the figure that P_{de}, EFECPOD, η_{ef} and $Xdest_{tot}$ decreases uniformly with the increase in θ_r from 0 to 45°. whereas the ε_{DMC} starts by increasing up to a maximum value of 35.41% (θ_r=40°). Then it decreases to a minimum value of 35.05%. ECOP also

increases from 54.7% to a maximum value of 54.83% and then fall back to 53.97% (θ_r= 45°).

For the DMC- ORC part, all performance parameters have portrayed a decline in value as θ_r increases. Moreover, all of them except energy destruction $Xdest_{tot}$ has shown an increment in value when compared with respect to DMC values. They have a maximum increment value at θ_r=0° and the increment level decreases as θ_r approaches 45°. The exergy destruction decreases with the implementation of an ORC into the DMC, because of the utilization of some of the waste heat. Besides the decrement value diminishes as θ_r increases (with ORC), for the constant volume because of power energy utilized from the waste heat. Moreover, it can be seen from parametric table that as θ_r increases the maximum local engine temperature decreases, thus reduces NO_x emissions. It is to be recalled that when local engine temperature increases the production of NO_xemissions increases, while SO_x emission generation increases if temperature is reduced [32]. Therefore in this case SO_x emission also increases.

Figure 6.6 demonstrates the influence of crank angle (θ_r) on the performance parameters like P_{de}(power density), effective efficiency(η_{ef}), ecological performance(ECOP), exergy destruction($Xdest_{tot}$), and effective ecological power density (EFECPOD) at constant starting temperature, compression ratio, equivalence ratio and volume, by taking RC318 as a working fluid. For the DMC part it can be seen from the figure that P_{de}, EFECPOD, η_{ef} and $Xdest_{tot}$ decreases uniformly with the increase in θ_r from 0 to 45°. Whereas the ε_{DMC} starts increasing up to a maximum value of 35.41%, at an optimal value of θ_r=40°. Then it decreases to a minimum value of 35.05%. ECOP also increases from 54.7% to a maximum value of 54.83% (d ECOP=16.9%) and then fall back to 53.97% (θ_r=45°). For the DMC-ORC part, all performance parameters have portrayed a decline in value as θ_r increases. However, all of them except energy destruction ($Xdest_{tot}$), has shown an increment in value when compared with respect to DMC values. They have a maximum increment value at θ_r=0°, and the increment level decreases as θ_r approaches 45°. For example at θ_r=0°,

$\eta_{ef,DMC-ORC}$=44.15%, $\eta_{ef,DMC}$=37.72% and the increment $\Delta\eta_{ef}$= 6.43%. At θ_r =45°, $\Delta\eta_{ef}$ is approximately 4.35%. The exergy destruction decreases with the implementation of an ORC into the DMC, because of the utilization of some of

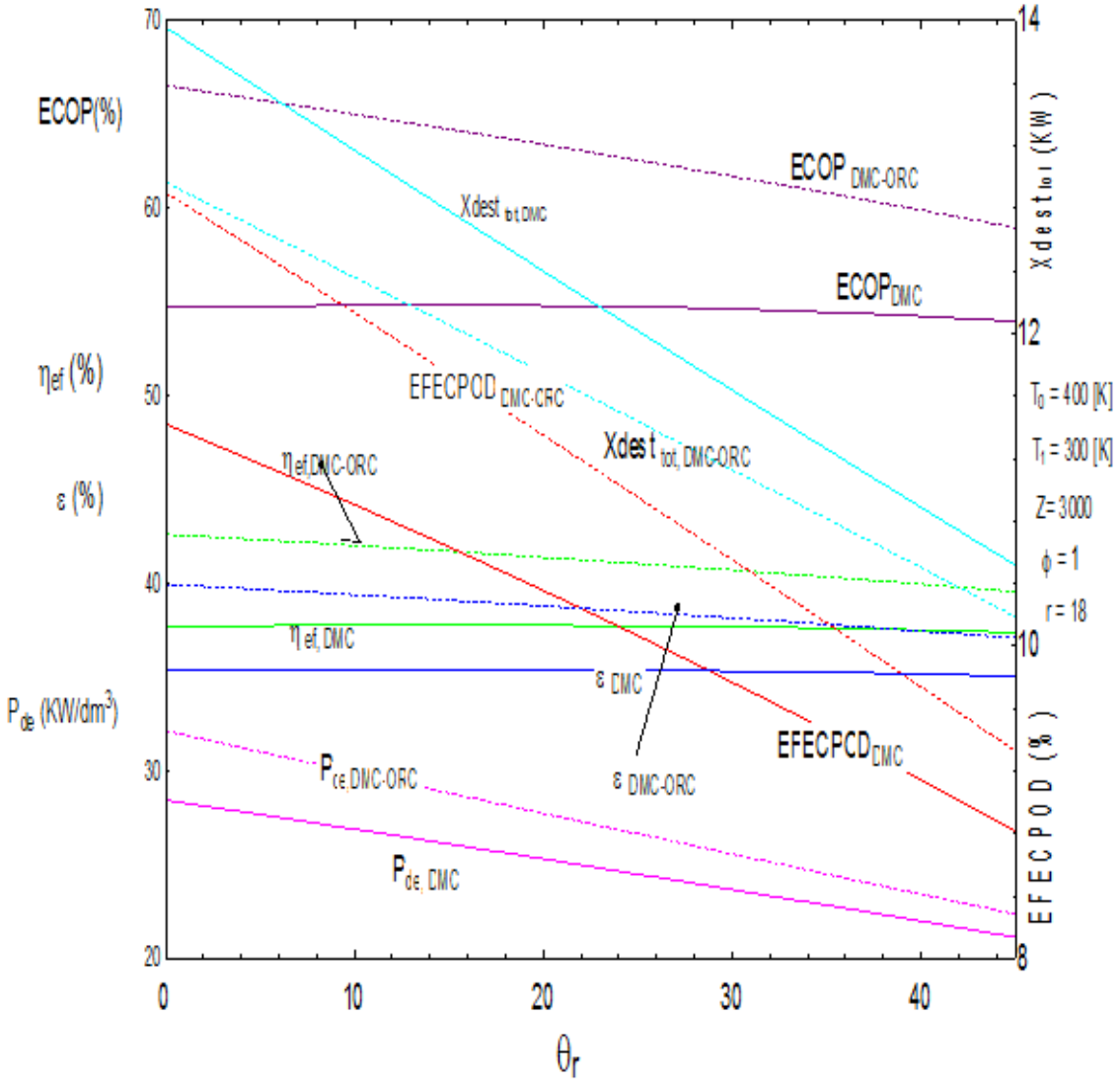


Figure 6.5 Influence of crank angle (θ_r) on performance parameters with Steam as a working fluid

the waste heat. Besides the decrement value diminishes as θ_r increases (with ORC), for the constant volume as energy that would have been lost is being utilized from the waste heat. In this case even when RC318 replaces steam as a working fluid, the trend of NO_x generation remains the same as the engines local temperature isn't that much influenced by the type of WHR or working fluid. However maximum thermal efficiency increases while is using RC318 as a fluid

than steam. This can imply reduction of SFC, so the NO_x emission generation can be reduced to some extent indirectly, considering the same loading conditions.

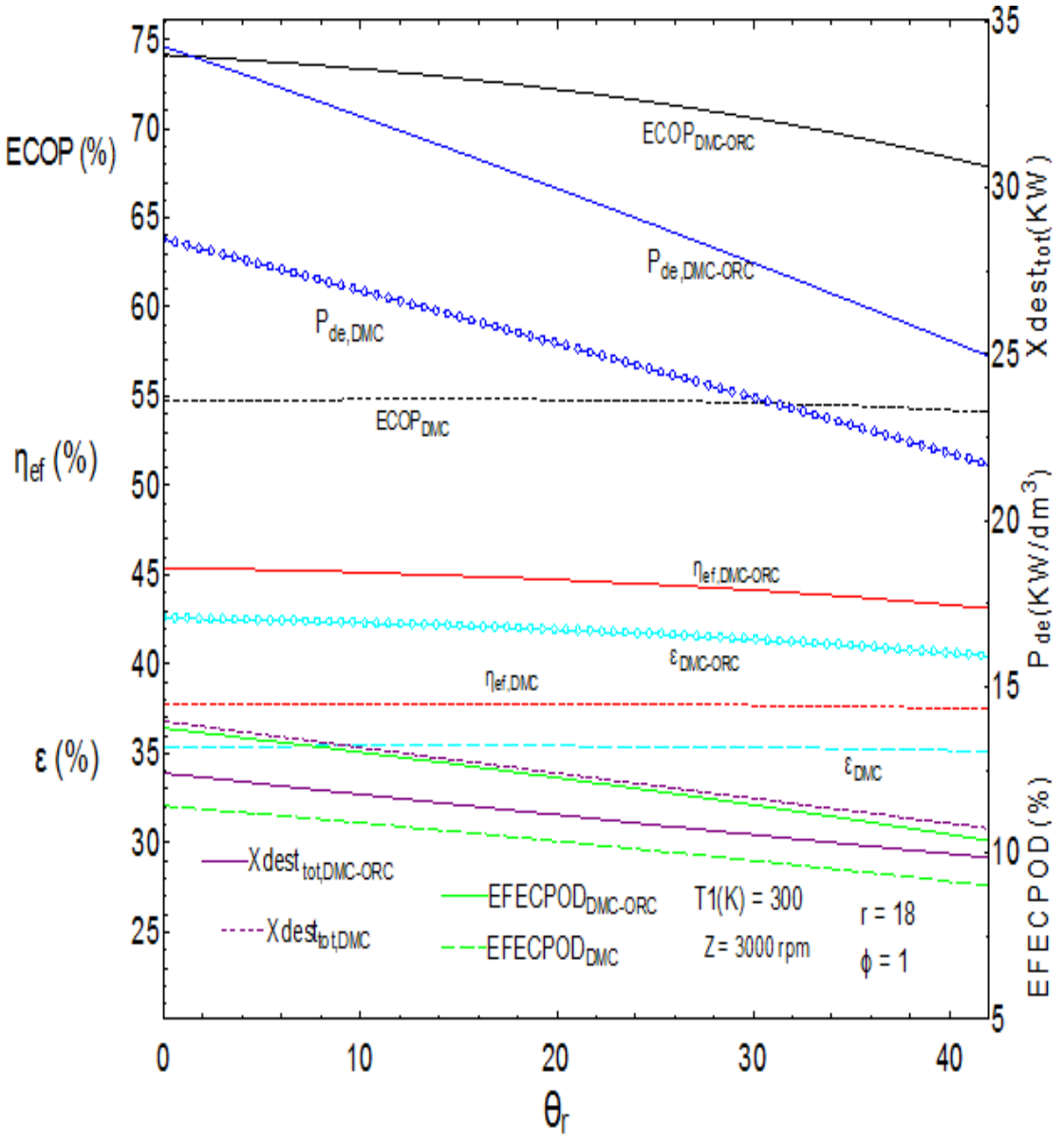


Figure 6.6 Influence of θ_r on performance parameters with RC318 as a working fluid in a DMC and DMC- ORC

Figure 6.7 illustrates the influence of crank angle on the performance parameters like power density, effective efficiency, ecological performance ECOP, exergy destruction($Xdest_{tot}$) and effective ecological power density (EFECPOD) at constant starting temperature, compression ratio, equivalence ratio, volume and so on. For the DMC part it is understood from the figure that

P_{de}, EFECPOD, η_{ef} and $Xdest_{tot}$ decrease uniformly with the increase in crank angle from θ_r=0 to 45°. Whereas the ε_{DMC} starts increasing up

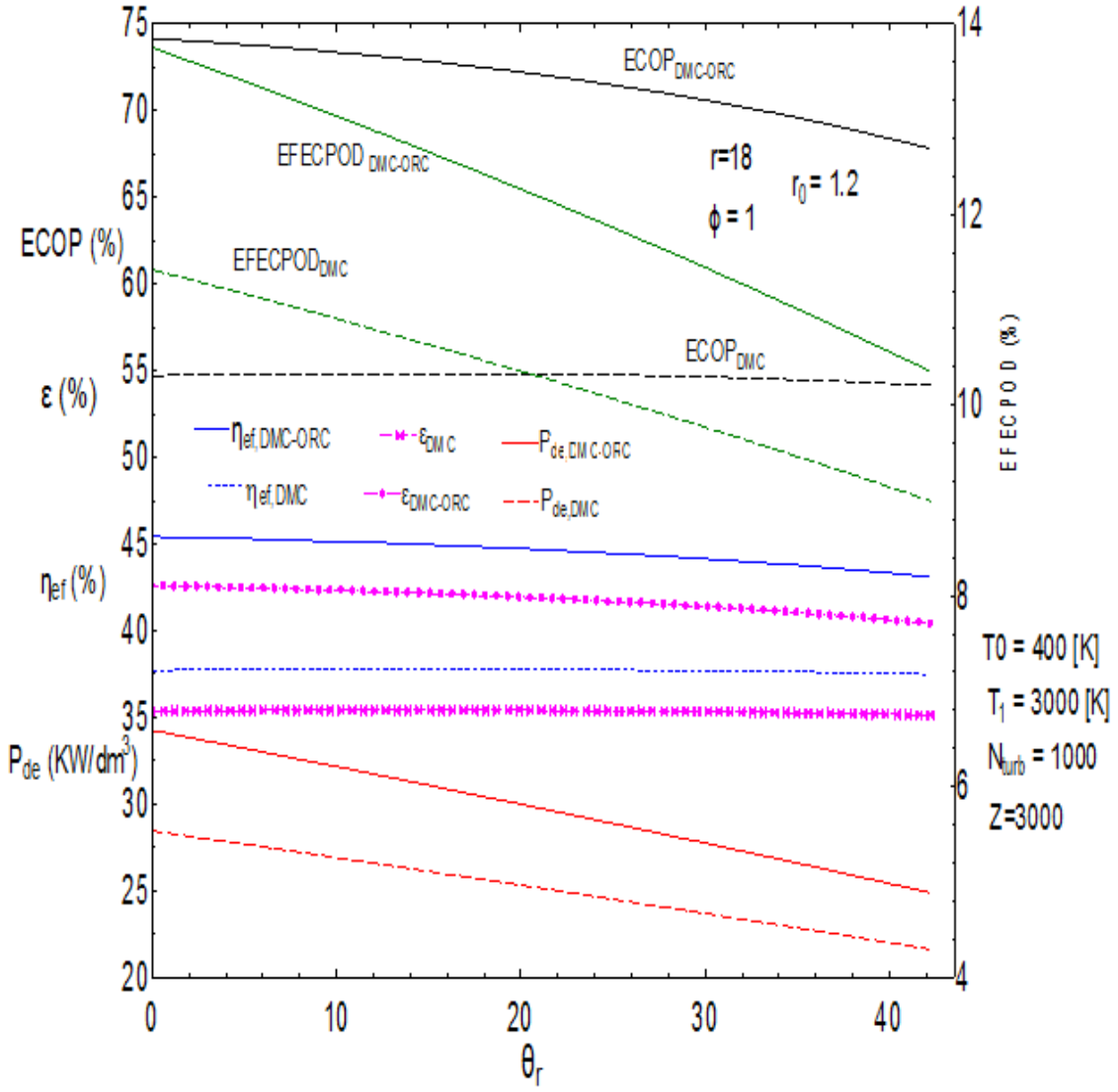


Figure 6.7 Influence of θ_r on performance parameters with R245fa as a working fluid in a DMC and DMC – ORC

to a maximum value of 35.41% at an optimal value of θ_r=40°. Then it decreases to a minimum value of 35.05. ECOP also increases from 54.7% to a maximum value of 54.83% (ΔECOP=0.11%) and then fall back to 53.97% (θ_r=45°).

For the DMC-ORC part, all performance parameters have shown a reduction in value as θ_r increases. Nevertheless all of them apart from energy destruction ($Xdest_{tot}$) has shown an increment in value when compared with respect to DMC values. They have a maximum increment value at θ_r=0°, and the

increment level decreases as θ_r approaches 45 degree. The energy destruction $Xdest_{tot}$ decreases with the implementation of an ORC into the DMC, because of the utilization of some of the waste heat from the exhaust gases. Moreover the decrement value reduces as θ_r enlarges (with ORC), for the constant volume because of power energy utilized from the waste heat.

From figure 6.7 as crank angle increases, temperature reduces. Therefore, NO_x production reduces. With R245fa as a working fluid, the local engine temperature isn't much different than when engines are equipped with ORC's of steam and RC318 as working fluids. So there isn't much NO_x production variance on an account of the change in temperature. On the account overall efficiency however, plant of R245fa medium is shown the most efficient, leading to a reduced SFC for the same power output of the combined plant than the rest plants. Hence, indirectly NO_x generation might be less in a plant of R245fa than pants of RC318 and steam working fluids.

Table 6. 1 Comparison of Maximum Values Achieved in DMC and DMC-ORC

	η_{ef}(%)		$P_{de}\left(KW/dm^3\right)$		ECOP (%)		EFECPOD (%)		$Xdest_{tot}$ (KW)	
Working Fluid	DMC	DMC-ORC	DMC	DMC-ORC	DMC	DMC-ORC	DMC	DMC-ORC	DMC	DMC-ORC
Steam	37.7	42.62	28.45	32.14	54.83	66.54	11.42	12.9	13.96	12.97
RC318	37.7	44.15	28.45	33.29	54.83	70.6	11.42	13.36	13.96	12.66
R245fa	37.7	45.42	28.45	34.25	54.83	74.14	11.42	13.75	13.96	12.4

Figure 6.8 depicts the influence of engine speed in rpm, at constant equivalnce ratio and crank angle. Total intake fuel air mixture boosts with increasing engine speed, which insinuates that generally engine performances improve at a fixed airmass per cycle. The effective efficiency , effective power denstity, ecological performance (ECOP), EFECPOD and exergy destruction increase with increase in enginee speed for the Dual Miller Cycle (DMC) part. This is because of increase in swept volume and combustion temperature due to engine speed increment. For DMC ε increases up to a maximum value at around 3200 rpm engine speed, and as speed increases further, ε value decreases. Similarly effective efficeicy shows an increment up to around 3400 rpm, but from there the effective

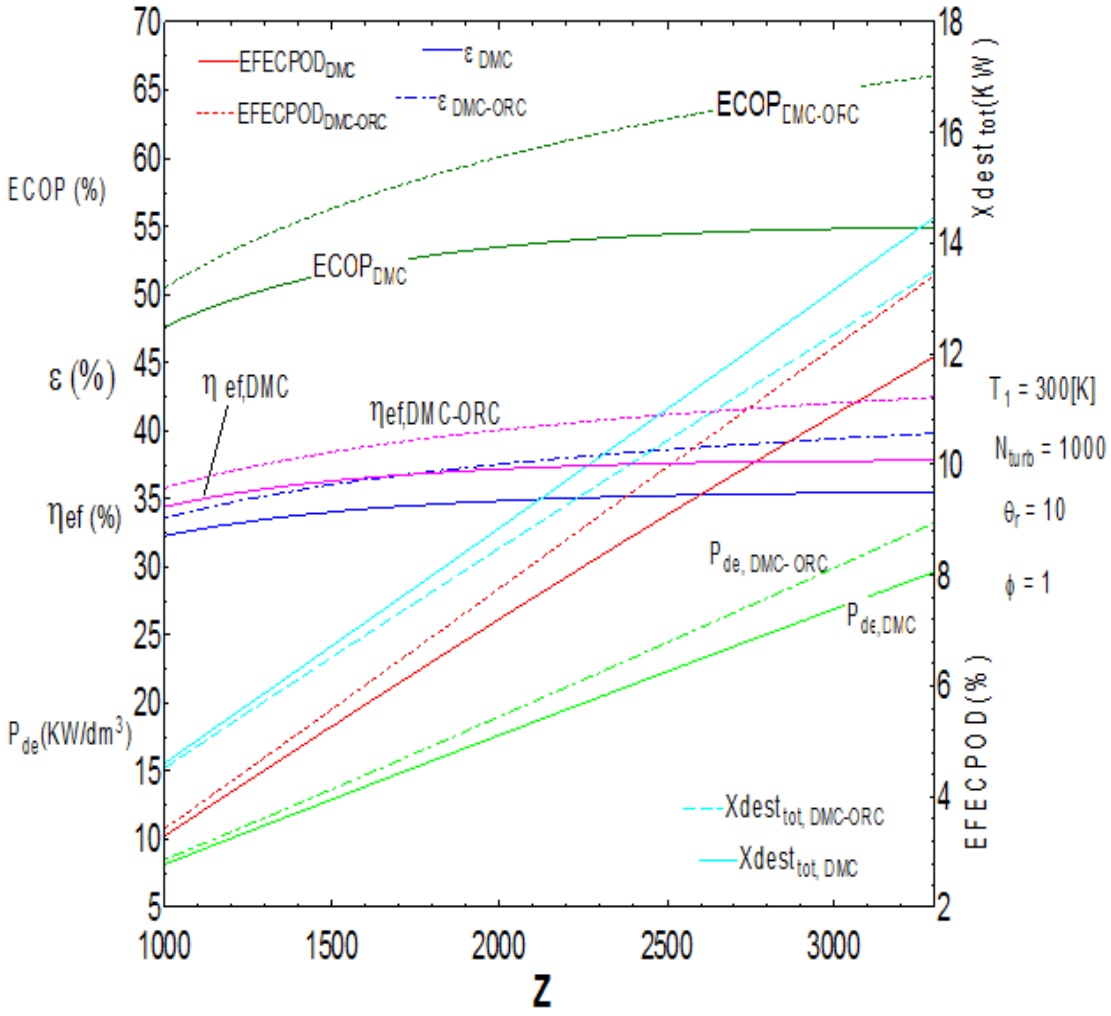


Figure 6.8 Influence of "Z (rpm)" on performance parameters with R245fa as a working fluid

efficiency decreases for both DMC and DMC-ORC. For the DMC–ORC similarly most of the relevant performance parameters considered herein enhances with increase in engine speed, as a result of the combustion temperature increase. On the point of view of comparing the performances of DMC-ORC vurses the performances achieved in DMC, all the parameters considered except exergy destruction ($Xdest_{tot}$), have shown a considerable increment from their corrosponding values obtained at the DMC. For instance implementing ORC into the DMC has increased the effective efficiency by 4.88%, P_{de} by 4.06 KW/dm^3 and the ECOP by 11. 83%, whereas $Xdest_{tot}$ has decreased by 0.09 KW.

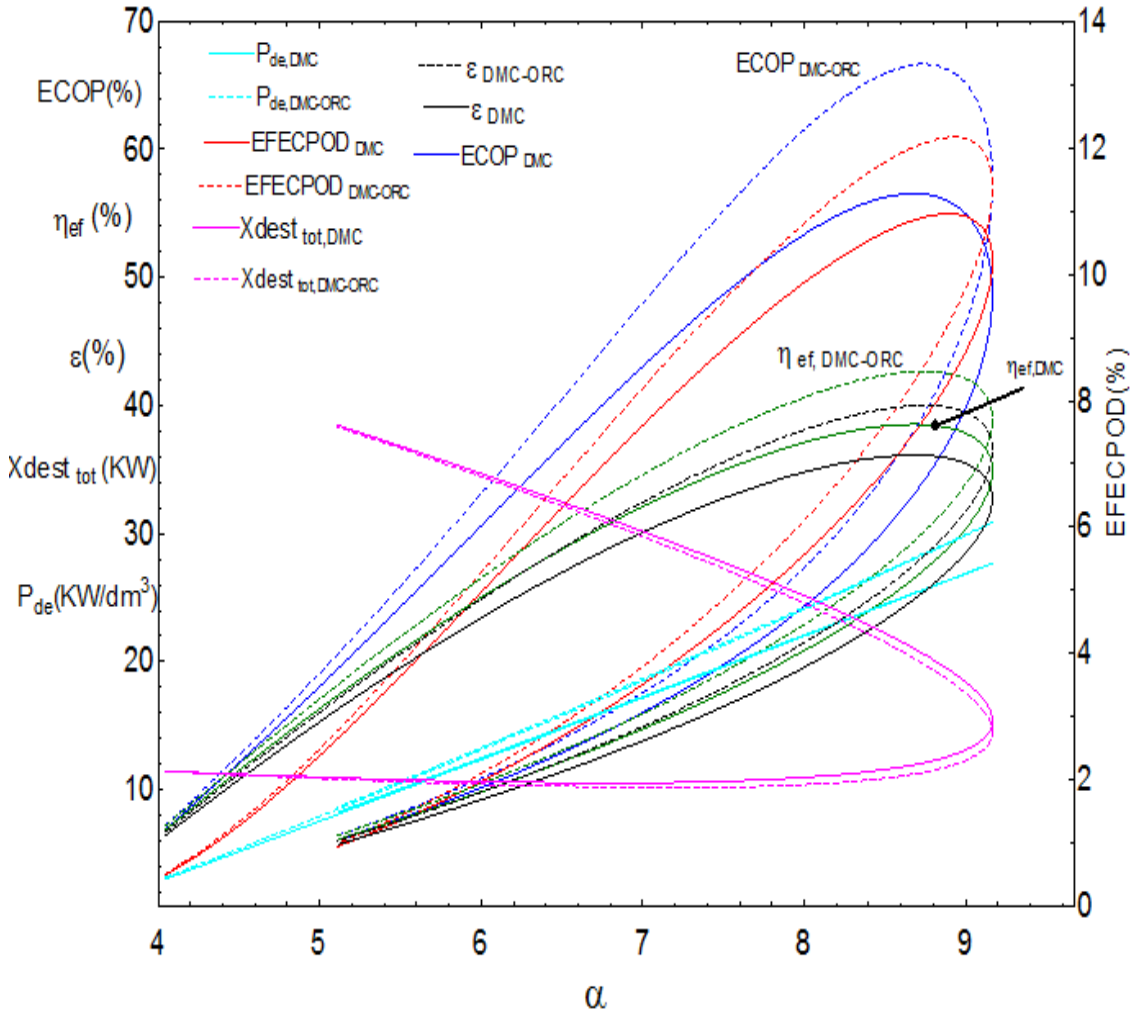


Figure 6. 9 Influence of cycle temperature ratio (α) on engine performance parameters with RC318 as a working fluid

Figure 6.9 demonstrates the analysis of the significance of cycle temperature ratio(α) at various conditions, for the most relevant performance parameters of the engine, using RC318 as a working fluid. To start with the DMC part, ε starts increasing from a point of ε=6.414% (α=4.142) to maximum value of 36.12% (α=8.637). From this point ε decreases down by taking a turn in the form of a loop that's sways back to lower values of ε and α, reaches a minimum ε value of 5.73% (α=5.11). In a similar fashion for the DMC-ORC plant value ascends from an initial ε value of 6.686% (α=4.142) to a maximum value of 39.99% (α= 8.713), a value which is greater by 3.87% from the value achieved from DMC plant. The value then decreases to a minimum amount of ε=6.032 (α=5.11), thereby showing about 3.75% increment at this point of α.

EFECPOD for the DMC starts from an initial value of 0.4901(α=4.142) and increases to a maximum value of EFECPOD=10.95, and from there takes a loop turn descending to a minimum EFECPOD value of 0.9506 by swaying back to a low α value of 5.11. For DMC–ORC, EFECPOD similarly starts from an initial value of 0.5109 %, increasing upwards to a maximum value of 12.17%, then bends down decreasing and swaying back in a loop fashion to a minimum value of 0.9989% (α=5.11).

ECOP for DMC starts from 6.853% increasing in a steep slope way up to a maximum value of 56.55 % (α=8.676) and then descends by swaying back to a minimum value of 6.079% (α=5.11). For DMC–ORC, ECOP progresses from an initial value of 7.165% and increases up to a maximum value of 66.65%. This illustrates the increment achieved in ECOP level by incorporating ORC into DMC is approximately 10.10%, insinuating the ecological performance is greatly enhanced. Then from this point onwards the value declines down to a minimum value of 6.408%.

In contrast to the other performance parameters $\text{Xdest}_{\text{tot}}$ starts by decreasing from a value of 11.45KW, to a minimum value of 10.52KW. However, from this point the value ascends to a maximum value of 38.45KW. Likewise, for DMC-ORC the value decreases from 11.42KW to a minimum value of 10.17KW (α = 7.126), and then takes a loop turn that ascends up to a maximum value of 38.33KW. In this case $\text{Xdest}_{\text{tot}}$ shows a reduction in value with an ORC is installed on the DMC, by a value of around 0.12KW at the maximum point of the two systems.

Power density increases uniformly for both DMC and DMC-ORC plants. For DMC from an initial value of 2.995 $^{KW}/_{dm^3}$ (α=4.142) to a max value of 27.67$^{KW}/_{dm^3}$ (α=8.22). In the same way for DMC-ORC value is increased from a min value of 3.122 to a maximum value of 30.87$^{KW}/_{dm^3}$ (α=8.368). $\eta_{ef,DMC}$ increases from 6.842% to a maximum value of 38.53% (α=8.637), then turns downwards to a minimum value of 6.113% (α=5.11). In a much similar way for DMC-ORC it is from 7.132% to a maximum value of 42.66% (α=8.638), then down to 6%

(α=5.11). The enhancement in efficiency as observed here, due to the installment of ORC type of waste heat recovery is 4.13%. This infers that the power output of the system is increased; specific fuel consumption is also reduced which benefits in lessening the running cost of the system (ship or industry).

The local maximum engine temperature increases as cycle temperature increases, hence raises the NO_x production, whereas the SO_x generation abates. So the emission of the most harmful exhaust gases (NO_x) as a product of the combustion process in the combustion chamber, to the atmosphere increases, that disables a friendly and healthy environment.

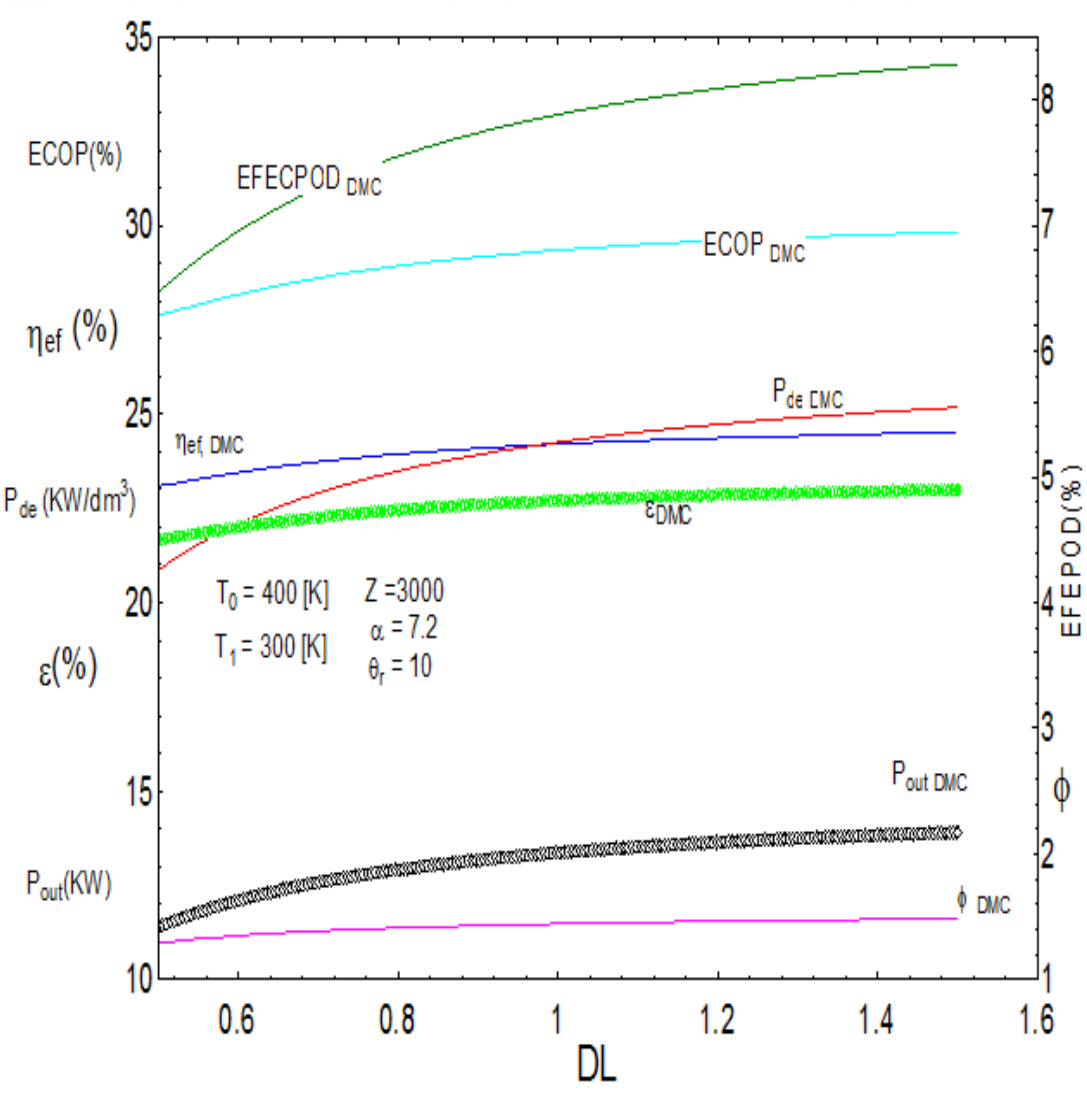


Figure 6.10 Influence of bore to stroke length ratio (DL), on engine performance parameters with R245fa as a working fluid

Figure 6.10 illustrates the influence of bore to stroke length ratio (DL) on engine performance parameters having R245fa as a working fluid. EFECPOD, ECOP, effective efficiency (η_{ef}), P_{de}, ε and P_{out} increase as DL ratio increases. Basically maximum engine temperature appears almost constant even if the DL ratio increases. Therefore NO_x production variance is supposed to be negligible. Nevertheless the increase in efficiency mustn't be overlooked in this case. This may influence the NO_x production indirectly.

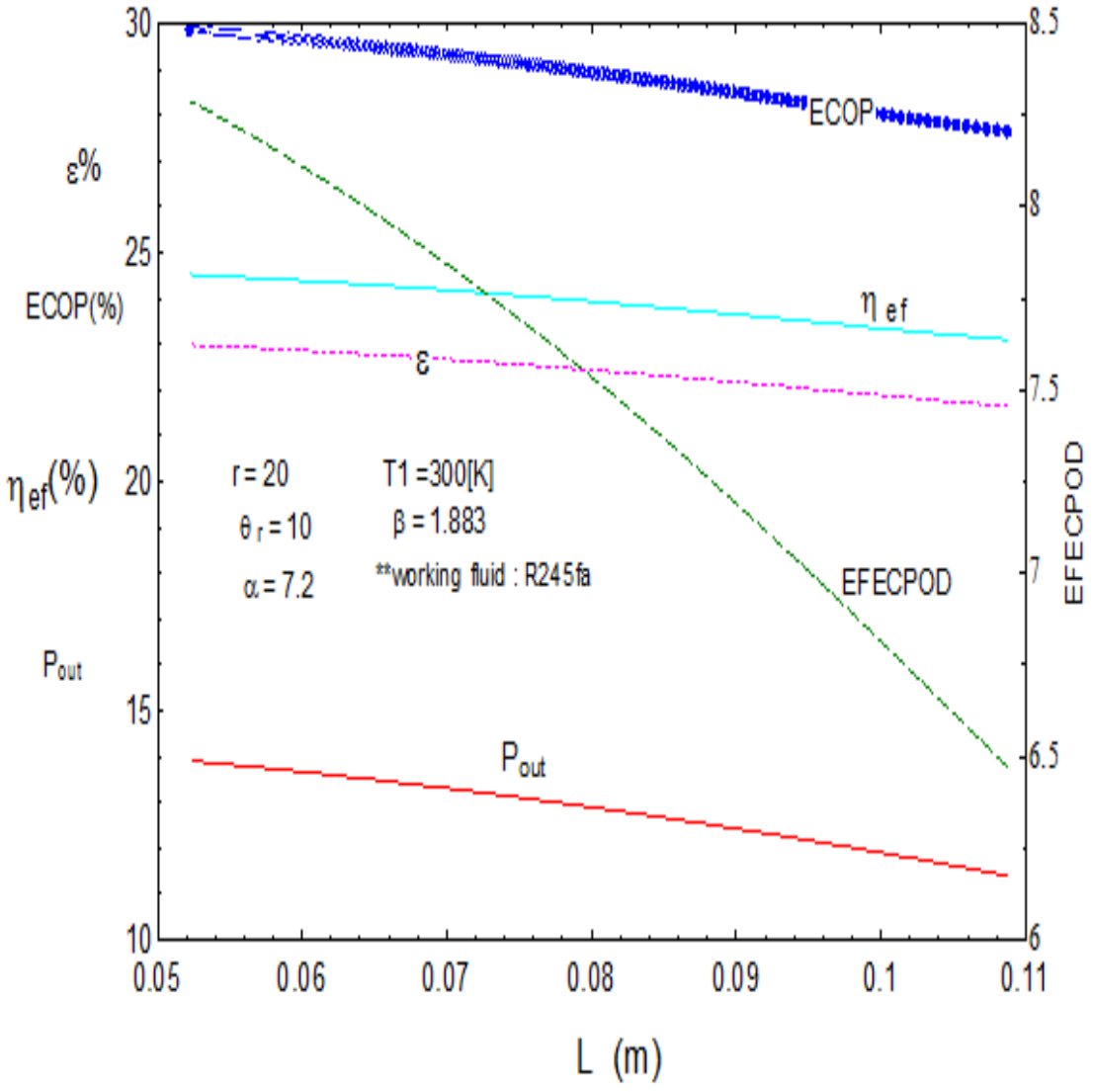


Figure 6.11 Influence of stroke length (l), on engine performance parameters.

From the values obtained as is shown in the graph, all the engine performance parameters considered, has shown a reduction tendency from 0.05 to 0.11m. This is because of heat transfer surface area increment as stroke length increases. Heat transfer surface area increment leads to deterioration of engine performance as large amount of heat is lost to the surrounding from the system. Though the graph depicted above is DMC, the same tendency is true for the DMC – ORC plant. DMC – ORC will show an increase in performance when compared with the DMC.

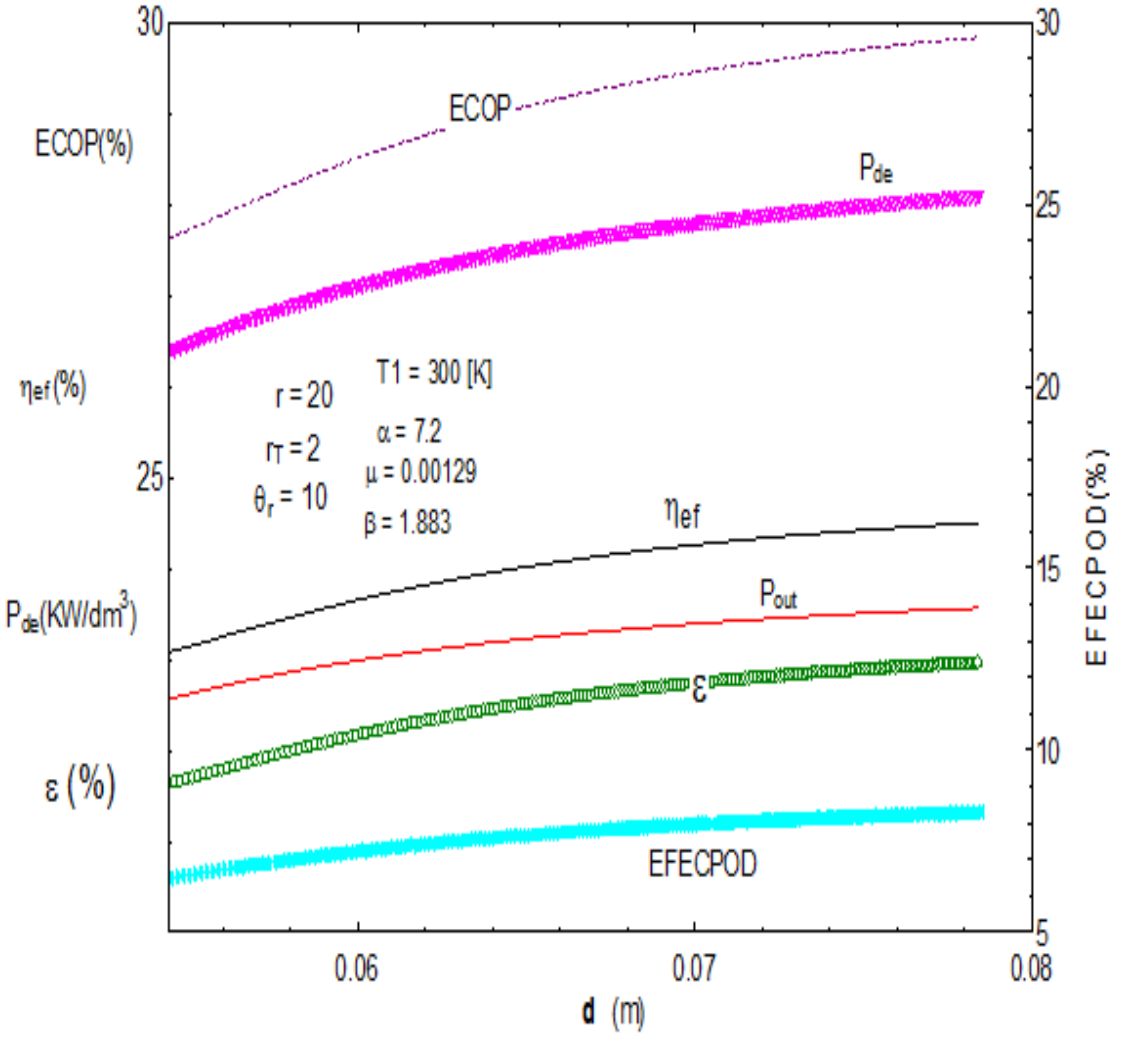


Figure 6.12 Influence of bore diameter (d) of cylinder on engine performance parameters

As is portrayed in figure 6.12, an increase in cylinder bore diameter from 0.054 to 0.08m leads to engine performance enhancement. The heat transfer surface

area decreases if diameter is increased; as a consequence of this the heat loss is decreased leading to a better system performance. So a comparative glance at figures (6.11) and (6.12) shows the effects of bore diameter and stroke length have a reverse result. Increase in bore diameter leads to performance enhancement whereas increase in stroke length tends to deteriorate the engine performance.

7

Conclusion and Recommendations

The outcomes of the analysis and investigations of this work could offer necessary information or guidance for identifying the optimal design and working criteria's of the real combined DMC- ORC that would be sought in the future. The optimal values can be estimated or verified depending on a thermo – ecological optimization investigations by considering the influence of β on engine efficiencies, engine power output and on the other side exhaust gas (SO_x and NO_x) emissions reduction. The influence of cycle temperature ratio (α), crank angle (θ_r), pressure ratio (β), equivalence ratio and engine speed on the optimum effective efficiency (η_{ef}), EFECPOD, ECOP, P_{de}, exergetic efficiency (ε) and $\mathrm{Xdest_{tot}}$ are analyzed as is illustrated in their respective figures.

The temperature ratio (α), equivalence ratio (ε), pressure ratio (β), cut off ratio (r_0) and Miller cycle ratio (r_M) are some of the most significant engine design criteria's. So the identification of the optimal amounts of such necessary criteria's leading to a maximum power outputs, maximum efficiencies, effective ecological power densities, and optimal exergetic efficiencies and so on are very crucial for a sound engine design.

It can be visualized from the figures that DMC – ORC is more efficient and more powerful than when DMC or DDC are inspected alone for the same α, β and ϕ conditions. It can also be proved that DMC-ORC has lower β and α value (figure 6.4) as compared to DMC for the same performances in terms of power density and effective efficiency. These results can take us to foresee that NO_x emissions can be satisfactorily reduced without paying an opportunity cost in the DMC-ORC. It has also shown that as crank angle increases the engine maximum temperature lowers, hence NO_x emission generation reduces. R245fa showed a better performance than RC318 as a working fluid. R245fa has also a safer

environmental impact, with 0 ODP and 960 GWP, while RC318 has got 0 ODP but 10250 GWP. Therefore R245fa is highly recommended than RC318, because of the better thermo dynamical performance and safer global warming potential. However R215fa has also got little concerns about toxicity.

Presented investigative analysis may be a leading approach for the thermo-ecological optimization of real DMC - ORC engines, prioritizing for marine applications. Future studies may include investigating on DMC – ORC including number of stages for the ORC, turbocharging, expanders, compressors, and different mechanisms. This project was only about implementing ORC into DMC and investigating for different performance parameters.

References

[1] H. Wang and N. Lutsey, "Long term Potential for increasing ship efficiency through the adoption of Industry leading practices," *The international council on clean transportation,* Jul. 2003.

[2] JOULES (Joint Operation for Ultra Low Emission Shipping), Project Press release, www.joules-project.eu, 2013 [Accessed September 19, 2018].

[3] S. Suarez and A. Greig, "Making shipping greener: ORC modeling under realistic operative conditions" *Low Carbon Shipping Conference*, London 2013.

[4] MAN Diesel & Turbo, *Waste heat recovery system (WHR) for the reduction of fuel consumption emissions and EEDI,* Technical paper, 2014.

[5] B. Kolsch and J. Radulovic, "Utilization of diesel engine waste heat by Organic Rankine Cycle, " *Applied Thermal Engineering*, 78, pp. 437- 448, Mar. 2015.

[6] C.R. Fergusen, and A.T. Kirkpatrick, *Internal Combustion Engines*, J. Willey & Sons, 2001.

[7] R. Flierl and M. Kluting, "The Third Generation of Valve trains-New Fully Variable Valve trains for Throttle-Free Load Control", *SAE* , Mar. 2000.

[8] H. Drangel, R. Reinmann and E. Olofsson, "The Variable Compression (Svc) and the Combustion Control (Scc) – Two Ways to Improve Fuel Economy and Still Comply With World-Wide Emission Requirements", *Journal of Engines*, 111, pp. 1691-1706, 2002.

[9] R. Ebrahimi "Thermodynamic modeling of performance of a Miller cycle with engine speed and variable specific heat ratio of working fluid" *Computers and Mathematics with Applications*, 62, pp. 2169–2176, Jul. 2011.

[10] R. Ebrahimi, "Performance analysis of an irreversible Miller Cycle with considerations of relative air – fuel ratio and stroke length," *Applied Mathematical Modeling,* 36, pp.4073–4079, Sep. 2012.

[11] S. Bellolio, V.Lemort and P. Rigo, "Organic Rankine Cycle systems for waste heat recovery in marine applications," *2016.*

[12] C. Sprouse III and C. Depcik, "Review of organic Rankine cycles for internal combustion engine, exhaust waste heat recovery," *Applied Thermal Engineering*, 51, pp. 711-722, 2013.

[13] B. Ribeiro and J. Martins, "Direct comparison of engines working under Otto, Miller and Diesel cycles: Thermodynamic analysis and Real Engine Performance," *SAE 2007-01-0261,* 2007.

[14] G. Gonca, “An Optimization Study on an Eco-Friendly Engine Cycle Named as Dual-Miller Cycle (DMC) for Marine Vehicles,” *Polish Maritime Research*, 24, no. 3, pp. 86-98, Sep. 2017.

[15] Y. Ust, A. Parlak, I. Ozsari and F. Arslan, “A theoretical performance investigation of irreversible internal combustion engine named as Dual-Miller Cycle (Performance of Dual-Miller Cycle),” *Department of Naval Architecture and Marine Engineering, Yildiz Technical University, Besiktas, 34349, Istanbul-Turkey*.

[16] H. Mo, Y. Huang, X. Mao & B. Zhuo, “Investigations on the Potential of Miller Cycle for Performance Improvement of Gas Engine,” *Global Journal of Researches in Engineering: Automotive Engineering,* 16, pp. 37-46, 2016,

[17] M. Chunlan , Z. Wen , G. Wei , W. Wei , H. Haozhong and L. Lian, “A Comparative Analysis of Different Cycle Diesel Engine Based on Three-dimensional Simulation,” *Periodical: Advanced Materials Research,* 805-806, Sep. 2013.

[18] J. Song, Y. Song* and C.W. Gu, “Thermodynamic analysis and performance optimization of an Organic Rankine Cycle (ORC) waste heat recovery system for marine diesel engines,” Key Laboratory for Thermal Science and Power Engineering of Ministry of Education, Department of Thermal Engineering, Tsinghua University, Beijing, Mar. 2015.

[19] U. Larsen, L. Pierobon, F. Haglind and C. Gabriel, “Design and optimization of organic Rankine cycles for waste heat recovery in marine applications using the principles of natural selection,” *J. of Energy,* 55, pp. 803-812, Jun. 2013.

[20] P. Linke, A. Papadopoulos, and P. Seferlis ,”Systematic Methods for Working Fluid Selection and the Design, Integration and Control of Organic Rankine Cycles—A Review,” *J. of Energies*, 8, pp. 4755-4801, Jun. 2015.

[21] D.V. Singh and E. Pederson, “A review of waste heat recovery technologies for maritime applications,” Norwegian University of Science and Technology , Jan. 2016.

[22] J. Martins, K. Uzuneanu, B.S. RIBERO and O. Jasansky, “Thermodynamic Analysis of an Over-Expanded Engine” *SAE Technical papers*, Mar. 2004.

[23] Y. Wang, L. Lin and S. Zeng, “Applications of the Miller cycle to reduce NO_x emission from petrol engine,” *J. of Applied energy*, 85, 2008.

[24] S. Shimogata, R. Homma, F.R. Zhang, K. Okamoto and F. Shoji, “Study on Miller Cycle Gas Engine for Co-Gernation Systems - Numerical Analysis for Improvement of Efficiency and Power,” *SAE Technical Paper* 971709, 1997, Tokyo Gas Co. Ltd.

[25] R. Kamo, N.S. Mavinahally, L. Kamo, W. Bryzik and Michael Reid, “Emissions Comparisons of an Insulated Turbocharged Multi-Cylinder

Miller Cycle Diesel Engine", *Adiabatics, Inc., U.S. Army*, TACOM, Mar. 1998.

[26] H. Stebler, G. Weisser, H.U. Hōrler and K. Boulouchos, "Reduction of NOx Emissions of D.I. Diesel Engines by Application of the Miller-System" *An Experimental and Numerical Investigation*; Swiss Federal Institute of Technology, Feb. 1996.

[27] Y. Wang, L. Lin, A.P. Roskilly, S. Zeng, J. Huang, et al., "An analytical study of applying miller cycle to reduce NOx emissions from petrol engine," *Applied Thermal Engineering, Elsevier*, 27 (11-12), pp.1779, 2007.

[28] A.L. Seta , A. Meroni, J.G. Andreasen, L. Pierobon, G. Persico and F. Haglind, "Combined Turbine and Cycle Optimization for Organic Rankine Cycle Power Systems—Part A: Turbine Model," *J. of Energies*, *9*, pp. 313, Apr. 2016.

[29] L. Abramovich, D. Martinović, D. Lenac, "Analysis of variable Inlet Valve Control in two-stage turbocharged marine four-stroke Diesel engines – Miller cycle," *Scientific Journal of Maritime Research,* 31, pp. 67-73, 2017.

[30] G. Gonca and B. Sahin, "Thermo-ecological performance analysis of a Joule-Brayton cycle (JBC) turbine with considerations of heat transfer losses and temperature dependent specific heats," February 2017, Yildiz Technical University, Naval Arch. and Marine Eng. Depart, Besiktas, Istanbul, Turkey.

[31] M.N. Bin Awang, "A Study of 2-Stroke marine diesel engine characteristic based on condition based maintenance," Faculty of Mechanical and Manufacturing Engineering Universiti Tun Hussein Onn Malaysia Jul. 2015.

[32] D. Woodyard, *Pounder's Marine Diesel Engines and Gas Turbines*, Eighth edition. Oxford: Butterworth-Heinemann, 2004.

[33] Martin's Marine Engineering Page, "Marine Diesel Engines," Available: http://www.dieselduck.info.com [Accessed December 15, 2018].

[34] S.S. Hou, "Heat Transfer Effects on the Performance of an Air Standard Dual Cycle," *Journal of Energy Conversion and Management,* 45, pp. 3003–3015, 2004.

[35] Bright Hub Engineering, Marine Engine's Machinery, " *Scavenging in Marine Engines,*" Available: http://www.brighthubengineering.com/marine-engines-machinery/41089-scavenging-in-marine-engines/# Accessed November 4, 2018].

[36] Bright Hub Engineering, Marine Engine's Machinery, "Theoretical-cycles-in-Marine-Diesel-Engines-The-Dual-cycle," Available: http://www.brighthubengineering.com/marine-engines-machinery/9605-theoretical-cycles-in-marine-diesel-engines-the-dual-cycle/ [Accessed January 15, 2019].

[37] V. Maizza and A. Maizza, “Unconventional working fluids in organic Rankine cycles for waste energy recovery systems,” J. of *Applied Thermal Engineering*, 21, no. 3, pp.381–390, 2001.

[38] J. Song, C-w. Gu, “Performance analysis of a dual-loop organic Rankine cycle (ORC) system with wet steam expansion for engine waste heat recovery,” *Applied Energy,* 156, pp. 280–289, 2015.

[39] http://www.imo.org [Accessed February 26, 2019].

[40] International Maritime Organisation. *Revised MARPOL Annex VI: regulations for the prevention of air pollution from ships and NO_x technical code 2008 - 2009*: IMO Publishing.

[41] H. Jääskeläinen, M. K. Khair, *Engine Fundamentals*, DiselNet.com revision Sep. 2018.

[42]http://www.marinediesels.info/2_stroke_engine_parts/Other_info/miller_cycle.htm [Accessed on February 4, 2019].

[43] H. Jääskeläinen, *Miller Cycle Engines*, DieselNet.com. Copyright © Ecopoint Inc. Revision 2017.12

[44] T. Goto, K. Hatamura, S. Takizawa, N. Hayama et. al., “Development of V6 Miller Cycle Gasoline Engine,” *SAE Technical paper*, Mar. 1994.

[45] D. Woodyard, *Pounder’s Marine Diesel Engines and Gas Turbines*, Ninth, edition. Oxford: Butterworth-Heinemann, 2009.

[46] T.N. Akma, “Miller cycle combustion strategy for downsized gasoline engines,” Doctoral Thesis, Loughborough University, Loughborough, 2017.

[47] C. R. Ferguson and A. T. Kirkpatrick, *Internal Combustion Engines: Applied Thermo sciences*, Second Edition, New York: John Wiley & Sons, Inc., 2001.

[48] A. Al-Sarkhi, J. O. Jaber, and S. D. Probert, “Efficiency of a Miller engine,” *Appl. Energy*, 83, pp. 343–351, 2006.

[49] G. Gonca*, B. Sahin and Y. Ust, “Performance maps for an air-standard irreversible Dual-Miller cycle (DMC) with late inlet valve closing (LIVC) version,” J. of Energy, 54, Jun. 2013.

[50] J. Lin, L. Chen, C. Wu and F. Sun, “Finite-time thermodynamic performance of a dual cycle,” *J. of Energy*, 23, no. 9, pp.765-772, 1999

[51] Y. Wang, L. Lin, AP. Roskilly, S. Zeng, J. Huang and Y. He,” An analytic study of applying Miller cycle to reduce NOx emission from petrol engine,” *Applied Thermal Engineering*, 27, pp. 1779-1789, 2007.

[52] V. Chintala and KA. Subramanian, “Assessment of maximum available work of a hydrogen fueled compression ignition engine using exergy analysis,” *Energy,* 67, pp. 162–175, 2014.

[53] R. Saidur, et al., “A review on exergy analysis of bio-mass based fuels,” *Renewable and Sustainable Energy Reviews*, 16, no. 2, pp.1217–1222, 2012.

[54] M.J. Abedin, H.H. Masjuki, M.A. Kalam, A. Sanjid, S.M. Ashrafur Rahman and B.M. Masum, " Energy balance of internal combustion engines using alternative fuels," *Renewable and Sustainable Energy Reviews,* 26, pp. 20–33, 2013.

[55] R. Saidur, M. Rezaei, W.K. Muzammil, M.H. Hassan, S. Paria and M. Hasanuzzaman, "Technologies to recover exhaust heat from internal combustion engines," *Renewable Sustainable Energy Review*, 16, no. 8, pp. 5649–5659, Oct. 2012.

[56] T. Wang, Y. Zhang, Z. Jie, G. Shu1 and Z. Peng, "Analysis of recoverable exhaust energy from a light-duty gasoline engine," *Applied Thermal Engineering,* 53, no. 2, pp. 414–419. 2013.

[57] J. Galindo S. Ruiz, V. Dolz, L. Royo-Pascual, R. Haller, B. Nicolas and Y. Glavatskaya, "Experimental and thermodynamic analysis of a bottoming Organic Rankine Cycle (ORC) of gasoline engine using swash-plate expander," *Energy Conversion Management,* 103, pp. 519–532, 2015.

[58] P. Bombarda, CM. Invernizzi and C. Pietra, "Heat recovery from Diesel engines a thermodynamic comparison between Kalina and ORC cycles," *Applied Thermal Engineering*, 30, pp. 212–219, 2010.

[59] N. Shokati, F. Ranjbar and M. Yari, "Exergoeconomic analysis and optimization of basic, dual-pressure and dual-fluid ORCs and Kalina geothermal power plants: a comparative study," *Renewable Energy*, 83, pp. 527–542. 2017.

[60] M. Ashouri, M. Mehrpooya, A.M Khoshkar Vandi and M.H Ahmadi, "Techno-economic assessment of a Kalina cycle driven by a parabolic Trough solar collector," *Energy Conversion Management*, 105, 1328–1339, Nov. 2015.

[61] M. Yari, A.S Mehr, V. Zare, S.M.S Mahmoudi and M.A. Rosen, "Exergo-economic comparison of TLC (trilateral Rankine cycle), ORC (organic Rankine cycle) and Kalina cycle using a low-grade heat source," *Energy*, 83, pp. 712–722, 2015.

[62] M. Eyidogan, F.C Kilic, D. Kaya, V. Coban and S. Cagman, "Investigation of Organic Rankine Cycle (ORC) technologies in Turkey from the technical and economic point of view," Renewable and Sustainable Energy Reviews, 58, pp. 885–895, 2016.

[63] S. Quoilin, M.V. Den Broek, S. Declaye, P. Dewallef and V. Lemort "Techno-economic survey of Organic Rankine Cycle (ORC) systems," *Renewable and Sustainable Energy Reviews,* 22, pp.168–186, Jun. 2013.

[64] Wang T, et al. "A review of researches on thermal exhaust heat recovery with Rankine cycle," *Renewable and Sustainable Energy Reviews*, 15, no. 6, pp. 2862–2871, 2011.

[65] RV. Padilla, YCS. Too, R. Benito and W. Stein, “Exergetic analysis of supercritical CO2 Brayton cycles integrated with solar central receivers,” *Applied Energy*, 148 pp. 348–365, 2015.

[66] G. Yu, H. Tian, G. Shu and H. Wei, “Multi-approach evaluations of a cascade-Organic Rankine Cycle (CORC) system driven by diesel engine waste heat: part B-techno-economic evaluations,” *Energy Conversion Management,* 108, pp. 596–608, Nov. 2015.

[67] F. Tchanche, M. Pétrissans and G. Papadakis, “Heat resources and organic Rankine cycle machines,” Renewable and Sustainable Energy Reviews, 39, pp. 1185–1199, 2014.

[68] S. Goel, O. Herzag, A. Data, RR. Sond, K. Deshpand, J. Fink and T. Shumacher, “Market Potential Study for Organic Rankine Cycle Technology in India,” Publication on Industrial Energy Efficiency. India: Thermax India Pvt. Ltd.; 2014, [Durr Cyplan Ltd. Germany].

[69] P. Mavrou, A. Papadopoulos, M.Z. Stijepovic, P. Seferlis, P. Linke and S. Voutetakis, “Novel and conventional working fluid mixtures for solar Rankine cycles: performance assessment and multi-criteria selection,” *Applied Thermal Engineering,* 75, pp. 384–396, Nov. 2015.

[70] P. Mavrou, A. Papadopoulos, M.Z. Stijepovic, P. Seferlis, P. Linke and S. Voutetakis, “Selection of working fluid mixtures for flexible Organic Rankine Cycles under operating variability through a systematic nonlinear sensitivity analysis approach,” Applied Thermal Engineering, 89, pp. 1054–1067, 2015.

[71] MAN Diesel & Turbo, *Thermo efficiency system for reduction of fuel consumption and CO2 emission.* 2014a, MAN Diesel, Augsburg, Germany: Kopenhagen, Denmark.

[72] K. Kuiken, *Diesel engines for ship propulsion and power plants-I, vol.1.* Onnen, The Netherlands: Target Global Energy Training; 2008.

[73] G. Shu, Liang, H. Wei, H. Tian, J. Zhao and L. Liu, “A review of waste heat recovery on two-stroke IC engine aboard ships,” *Renewable and Sustainable Energy Reviews,* 19, pp. 385–401, 2013.

[74] BCS Inc. Waste heat recovery: technologies and opportunities in U.S. industry, US Dept. of Energy (DOE); 2008.

[75] JB. Heywood, *Internal combustion engine fundamentals, Vol. 930.* New York: McGraw-Hill, 1988.

[76] Nuclear-power.net, *Rankine cycle, Supercritical Rankine cycle,* Available: https://www.nuclear-power.net/nuclear-engineering/thermodynamics/thermodynamic-cycles/, [Accessed January 6, 2019].

[77] AI Kalina, “Combined cycle and waste heat-recovery power-systems based on a novel thermodynamic energy cycle utilizing low-temperature heat for power-generation,” Mechanical Engineering. 1983; 105, no. 11. 1983.

[78] I. Vlaskos, P. Feulner and C. Michos *Waste Heat Recovery in Marine Propulsion Systems.* SNAME, Athens/Greece, Feb. 2014.

[79] www.orcycle.be [last checked September, 2018].

[80] E. Wali, “Optimum working fluids for solar powered Rankine cycle cooling of buildings,” *Solar Energy*, 25, pp. 235–241, 1980.

[81] B.F. Tchanche, G. Lambrinos, A. Frangoudakis, and G. Papadakis, “Low-grade heat conversion into power using organic Rankine cycles—A review of various applications,” *Renewable and. Sustainable Energy Reviews, 15*, no. 8, pp. 3963–3979, Oct. 2011.

[82] K.J. DiGenova, B.B. Botros and J.G. Brisson, “Method for customizing an organic Rankine cycle to a complex heat source for efficient energy conversion, demonstrated on a Fischer Tropsch plant,” *Applied Energy*, *102*, pp. 746–754. Feb. 2013.

[83] J. Song, Y. Song and C-w. Gu, “Thermodynamic analysis and performance optimization of an Organic Rankine Cycle (ORC) waste heat recovery system for marine diesel Engines,” *Energy,* 82, pp. 976-985, Jan. 2015.

[84] PJ. Mago, LM. Chamra, K. Srinivasan and C. Somayaji, “An examination of regenerative organic Rankine cycles using dry fluids,” *Applied Thermal Engineering*, 28, no. 8-9, pp. 998 – 1007, Jun. 2008.

[85] X. Zhang, M. He, K. Zeng and Y. Zhang, “Selection of working fluid used in vapor power cycle for waste heat recovery of vehicle engine,” *J. of Engineering Thermo physics,* 1, pp. 15–18, 2010.

[86] T. Hung, T. Shai, and A. Wang, “A review of organic Rankine cycles (ORCs) for the recovery of low-grade waste heat,” *Energy,* 22, no. 7, pp. 661–667, Jul. 1997.

[87] H. Chen, D. Goswami and E. Stefanakos, “A review of thermodynamic cycles and working fluids for the conversion of low-grade heat,” *Renewable and Sustainable Energy Reviews,* 14, pp. 3059 – 3067, 2010.

[88] T. Yamamoto, T. Furuhata, N. Arai and K. Mori, “Design and testing of the organic Rankine cycle,” *Energy*, 26, no. 3. pp. 239 – 251, Mar. 2001.

[89] BF. Tchanche , G. Papadakis, G. Lambrinos and A. Frangoudakis, “Fluid selection for a Low temperature solar organic Rankine cycle” *Applied Thermal Engineering*, 29, pp. 2468–2476, 2009.

[90] AI. Papadopoulos, M. Stijepovic and P. Linke, “On the systematic design and selection of optimal working fluids for organic Rankine cycles,” *Applied Thermal Engineering*, 30, pp. 760–769, 2010.

[91] O. Badr, SD. Probert and PW. O'Callaghan, "Selecting a working fluid for a Rankine cycle engine," *Applied Energy,* 21, pp. 1–42, 1985.

[92] H. Chen, DY. Goswami and EK. Stefanakos, "A review of thermodynamic cycles and working fluids for the conversion of low grade heat," *Renewable and Sustainable Energy Reviews,* 14, pp. 3059–67, 2010.

[93] E. Wali, "Working fluids for solar, Rankine cycle cooling systems," *Energy,* 5, pp. 631–639, 1980.

[94] TC. Hung, TY. Shai and SK. Wang, "A review of organic Rankine cycles (ORCs) for the recovery of low grade waste heat," *J. of Energy*, 22, pp. 661–667, 1997.

[95] Wang EH, et al., "Study of working fluid selection of organic Rankine cycle (ORC) for engine waste heat recovery," *Energy*, 36(5), pp. 3406–18. 2011.

[96] https://www.nasa.gov/topics/earth/features/vapor_warming.html [Accessed November 12, 2018].

[97] E. Lemmon, M. Huber, and M. McLinden. NIST reference database 23: reference fluid 824 thermodynamic and transport properties-REFPROP, version 9.1. Standard Reference Data 825 Program. (2013).

[98] Ferguson CR. Internal combustion engines – applied thermo sciences. New York: John Wiley & Sons Inc.; 1986.

[99] EES Academic Professional Edition. V. 9.942-3D, USA, F-Chart Software; 2016.

Publications from the Thesis

Contact Information: samuelmerhawi220@gmail.com

Conference Papers

1. M.S. Zerom, G. Gonca, “Performance Investigation of Dual Miller Cycle – Organic Rankine Cycle Combined Plant for Marine Applications,” ISGRS2018, 1, pp. 86, Oct. 2018.